ANTIOXIDANT EFFECTS OF BASTARD OLEASTER (*ELAEAGNUS LATIFOLIA* L.) WATER EXTRACT AGAINST *TERT*-BUTYL HYDROPEROXIDE-INDUCED HUMAN SUBMANDIBULAR GLAND CELL TOXICITY

KRITSAKORN RAYASILP

Graduate School Srinakharinwirot University

2024

ฤทธิ์ต้านอนุมูลอิสระของสารสกัดน้ำมะหลอดต่อความเป็นพิษของเซลล์เพาะเลี้ยงต่อมน้ำลายของมนุษย์ที่เหนี่ยวนำด้วยเทอร์ท-บิวทิลไฮโดรเพอร์ออกไซด์

กฤษกรณ์ ระย้าศิลป์

ปริญญานิพนธ์นี้เป็นส่วนหนึ่งของการศึกษาตามหลักสูตร
ปรัชญาดุษฎีบัณฑิต สาขาวิชาชีวภาพการแพทย์
คณะแพทยศาสตร์ มหาวิทยาลัยศรีนครินทรวิโรฒ
ปีการศึกษา 2567

ANTIOXIDANT EFFECTS OF BASTARD OLEASTER (*ELAEAGNUS LATIFOLIA* L.) WATER EXTRACT AGAINST *TERT*-BUTYL HYDROPEROXIDE-INDUCED HUMAN SUBMANDIBULAR GLAND CELL TOXICITY

KRITSAKORN RAYASILP

A Dissertation Submitted in Partial Fulfillment of the Requirements

for the Degree of DOCTOR OF PHILOSOPHY

(Biomedical Sciences)

Faculty of Medicine, Srinakharinwirot University

2024

THE DISSERTATION TITLED

ANTIOXIDANT EFFECTS OF BASTARD OLEASTER (*ELAEAGNUS LATIFOLIA* L.) WATER EXTRACT AGAINST *TERT*-BUTYL HYDROPEROXIDE-INDUCED HUMAN SUBMANDIBULAR GLAND CELL TOXICITY

BY

KRITSAKORN RAYASILP

HAS BEEN APPROVED BY THE GRADUATE SCHOOL IN PARTIAL FULFILLMENT OF THE REQUIREMENTS FOR THE DOCTOR OF PHILOSOPHY IN BIOMEDICAL SCIENCES AT SRINAKHARINWIROT UNIVERSITY

(Assoc. Prof. Dr. Chatchai Ekpanyaskul, MD.)

Dean of Graduate School

ORAL DEFENSE COMMITTEE

..... Major-advisor

(Asst. Prof.Yamaratee Jaisin, Ph.D.)

..... Co-advisor

(Asst. Prof.Poommaree Namchaiw, Ph.D.)

..... Chair

(Asst. Prof.Nipapan Malisorn, Ph.D.)

..... Committee

(Asst. Prof.Ruttachuk Rungsiwiwut, D.V.M.,Ph.D.)

..... Committee

(Asst. Prof.Papavee Samatiwat, D.V.M.,Ph.D.)

Title	ANTIOXIDANT EFFECTS OF BASTARD OLEASTER (*ELAEAGNUS LATIFOLIA* L.) WATER EXTRACT AGAINST *TERT*-BUTYL HYDROPEROXIDE-INDUCED HUMAN SUBMANDIBULAR GLAND CELL TOXICITY
Author	KRITSAKORN RAYASILP
Degree	DOCTOR OF PHILOSOPHY
Academic Year	2024
Thesis Advisor	Assistant Professor Yamaratee Jaisin , Ph.D.
Co Advisor	Assistant Professor Poommaree Namchaiw , Ph.D.

Oxidative stress significantly impairs submandibular gland function, adversely affecting saliva production and oral health. *Elaeagnus latifolia* L. (*E. latifolia*) fruit, known as bastard oleaster or Malod in Thailand, is rich in antioxidative polyphenolic compounds. This study focused on the effects of the heated extract against *tert*-butyl hydroperoxide (t-BHP)-induced oxidative stress in human submandibular gland (HSG) cells. The analysis revealed that heated water extraction of *E. latifolia* fruits resulted in the presence of total phenolic (TPC) and total flavonoid contents (TFC), as determined by Folin-Ciocalteu and aluminum chloride colorimetric methods. High-performance liquid chromatography (HPLC) analysis confirmed the presence of bioactive compounds, including malic acid and GABA. Metabolomic profiling using LC-Q-TOF-MS/MS identified a diverse array of secondary metabolites, such as amino acids and organic acid compounds, in this extract. A comprehensive assessment of in *in vitro* antioxidant studies using various assays revealed a significant antioxidant capacity of this extract. Co-treatment between t-BHP and the *E. latifolia* fruit extract enhanced HSG cell viability, as assessed by the resazurin cell viability assay, in parallel with reduced intracellular ROS levels (H_2DCFH-DA assay) and decreased apoptosis, as evidenced by Hoechst and AO/EB staining. Real-time qPCR and Western blot analyses demonstrated that the extract modulates key apoptotic proteins by reducing the Bax/Bcl-2 ratio, cleaved caspase-3, and P-P38 MAPK expression. Additionally, it increased the levels of salivary gland-specific proteins, including AQP5 and α-amylase. Altogether, these findings indicate that the *E. latifolia* fruit extract provides substantial cytoprotective, antioxidant, and anti-apoptotic effects against oxidative stress in HSG cells. This suggests its potential to diminish the harmful effects of oxidative stress on the salivary gland and point out its therapeutic benefits for managing related oral health disorders, with promising applications in the development of oral care products as supportive treatment.

Keyword : Elaeagnus latifolia L. fruits, Oxidative stress, Antioxidants, Human submandibular gland cells, Apoptosis

ACKNOWLEDGEMENTS

I would like to express my heartfelt appreciation to my primary advisor, Assistant Professor Dr. Yamaratee Jaisin, and co-advisor, Assistant Professor Dr. Poommaree Namchaiw, for their unwavering support during my PhD studies and research. Their invaluable guidance and encouragement have been instrumental in my academic journey.

I am grateful to Mrs. Piyanee Ratanachammong for her insights into the in vitro antioxidant aspects of my research and her constructive feedback on my dissertation. My appreciation also extends to the Department of Pharmacology at the Faculty of Science, Mahidol University, for providing essential laboratory equipment, and to Mrs. Cholticha Niwaspragrit from the Thailand Institute of Scientific and Technological Research (TISTR) for supplying the Elaeagnus latifolia fruits used in my study. Special thanks to Dr. Natta Wiriyakun from the National Science and Technology Development Agency (NSTDA), Pathum Thani, Thailand, at the NSTDA Characterization and Testing Service Center for expertly characterizing the bioactive compounds through metabolomic analysis. I am also thankful to the teachers, staff, and lab colleagues in the Department of Pharmacology at Srinakharinwirot University for their support and assistance during my dissertation. My heartfelt gratitude goes to my parents for their love and unwavering support.

Finally, I am thankful to the Faculty of Medicine at Srinakharinwirot University for their financial support through the research grant (number 152-2566) that helped fund my dissertation.

KRITSAKORN RAYASILP

TABLE OF CONTENTS

LIST OF TABLES

Page

LIST OF FIGURES

Page

CHAPTER 1
INTRODUCTION

1.1 Background

Salivary glands are essential for maintaining oral health by regulating oral homeostasis through saliva production. Saliva performs multiple functions essential for protecting the teeth and oral tissues, including lubrication, digestion, antimicrobial activity, and maintenance pH balance. Several factors influence saliva production. External factors include environmental elements such as food intake, exposure to air, and interactions with microorganisms, including bacteria, viruses, and fungi. Internal factors involve lifestyle habits and exposures such as smoking cigarettes, consuming alcohol, using dental restorative materials, and various pharmaceutical agents[1].

These factors can generate reactive oxygen species (ROS), including superoxide ($O_2^{\bullet -}$), hydroxyl ($HO^{\bullet}$), nitric oxide radical ($NO^{\bullet}$), and hydrogen peroxide (H_2O_2). These highly reactive molecules, characterized by unpaired electrons, have the potential to induce oxidative stress in cells and tissues. When antioxidant defenses are inadequate, ROS interact with crucial macromolecules, such as DNA, lipids, and proteins, leading to damage in cells and tissues. In the oral cavity, oxidative stress contributes to cellular dysfunction, inflammation, and oral health problems[2, 3]. Oxidative stress in the oral cavity significantly contributes to cellular dysfunction, inflammation, and a range of oral health complications.

Within the oral cavity, ROS are generated under various physiological and pathological conditions. Key sources of ROS include periodontal inflammation, exposure to xenobiotics such as ethanol, cigarette smoke, and pharmaceuticals, as well as dietary factors like high-fat or high-protein intake. Some dental treatments can also produce ROS, including ozone therapy, ultrasound therapy, non-thermal plasma therapy, and laser therapy [4]. When the production of ROS exceeds the body's antioxidant defenses, oxidative stress occurs, leading to damage in cells and tissues. The consequences of oxidative stress on oral health involve lipid peroxidation, protein oxidation, and DNA damage caused by ROS, which are all quantifiable indicators of oxidative imbalance[5, 6].

Accumulated oxidative stress is a key factor in the dysfunction of salivary glands, directly contributing to disorder conditions such as xerostomia (dry mouth) and hyposalivation (reduced salivary flow). These conditions severely impair oral health by disrupting saliva production, which is essential for maintaining oral homeostasis and defending against infections[4]. Therefore, targeting oxidative stress emerges as a promising therapeutic approach to prevent or reduce salivary gland dysfunction and its associated complications.

A significant consequent oxidative stress is the initiation of apoptosis, a programmed cell death mechanism activated through a cascade of intracellular signaling events. The apoptosis process related to oxidative stress is primarily governed by the activation of the p38 Mitogen-Activated Protein Kinase (MAPK) signaling pathway. This signaling pathway is integral to the regulation of the equilibrium between pro- and anti-apoptotic proteins within the Bcl-2 family. Following phosphorylation of P38 MAPK promotes the translocation of the pro-apoptotic protein Bax from the cytosol to the mitochondria, thereby enabling the release of cytochrome c into the cytosol. This release subsequently triggers the activation of caspase-3, a pivotal effector in the apoptotic pathway[7, 8].

Remarkably, cleaved caspase-3 can further enhance P38 MAPK phosphorylation, establishing a feedback loop that amplifies the apoptotic response. This feedback mechanism highlights the role of oxidative stress in exacerbating cellular damage, particularly in tissues vulnerable to oxidative injury, such as the salivary glands. The complex interactions among P38 MAPK, Bcl-2 proteins, and caspase-3 offer valuable insights into apoptosis molecular mechanisms. By examining the modulation of this apoptotic signaling pathway, potential therapeutic targets can be identified to alleviate oxidative stress-induced cell death, which is essential for preventing or reducing salivary gland dysfunction[7].

Salivary glands produce and secrete saliva, a process regulated by key proteins, including aquaporins. Among these, aquaporin-5 (AQP5), a water channel protein located at the apical membranes of secretory cells, is essential for saliva production and secretion[9, 10]. Additionally, salivary alpha-amylase (α-amylase), encoded by the AMY1 gene, plays a critical role in digestion by hydrolyzing complex carbohydrates into simpler sugars. The expression and activity of both AQP5 and α-amylase must be tightly regulated to ensure optimal salivary gland function[9-12]. Disruptions in the regulation or activity of these proteins can significantly impair salivary secretion, leading to conditions such as xerostomia and hyposalivation, which compromise oral health and increase the risk of oral diseases[10, 13].

In recent years, phytomedicine has gained increasing scientific attention, particularly concerning the antioxidant potential of natural compounds. These compounds have significant applications in both the food and cosmetic industries. *Elaeagnus latifolia* L. (*E. latifolia*), commonly referred to as bastard oleaster or "Malod" in Thailand[14], has attracted attention due to its rich nutritional profile. This encompasses a variety of vitamins, minerals, fatty acids, and a substantial concentration of antioxidant compounds, particularly phenolics and flavonoids. *E. latifolia* has been shown to possess an extensive array of pharmacological actions, encompassing anti-inflammatory, neuroprotective, and antibacterial properties[15]. These diverse bioactive characteristics highlight its potential as a promising candidate for the development of novel therapeutic agents in phytomedicine.

Despite a growing body of research demonstrating the antioxidant and pharmacological properties of *E. latifolia* fruits, the specific effects of these fruits on preventing cytotoxicity and the underlying molecular mechanisms underlying these effects against oxidative stress within submandibular gland (HSG) cells remain largely unexplored.

This study sought to explore the antioxidant and cytoprotective effects of the water extract of *E. latifolia* fruits, as well as its potential to prevent HSG cell dysfunction induced by oxidative damage, utilizing *tert*-butyl hydroperoxide (t-BHP or tBuOOH) as

an inducer of oxidative stress. Additionally, the composition of the extract was analyzed, focusing on key bioactive compounds such as phenolics, flavonoids, and other antioxidant constituents. This investigation was further supplemented by the assessment of the extract's free radical scavenging capacity through *in vitro* assays, including DPPH and ABTS assays, along with an intracellular ROS assay to evaluate its antioxidant capacity.

Beyond its antioxidant properties, this study delved into the molecular mechanisms governing the cytoprotective effects of the extract against t-BHP-induced oxidative stress and apoptosis in HSG cells. The primary focus was on the extract's capacity to modulate apoptotic signaling pathways, particularly through the regulation of P38 MAPK and its downstream signaling cascade. This investigation examined the balance between pro- and anti-apoptotic proteins, specifically Bcl-2 and Bax, in addition to the activation of caspase-3. Furthermore, the study evaluated the extract's influence on AQP-5 and α-amylase expression and activity, which are essential for salivary gland function.

Taken together, these findings demonstrate the substantial pharmacological potential of *E. latifolia* fruits, based on empirical evidence showing their ability to protect HSG cells from oxidative stress. This research highlights the extract's significant role in promoting oral health and its potential application in developing novel therapeutic strategies.

1.2 Objectives

To identify and characterize bioactive compounds in the heated water extract of *E. latifolia* fruits.

To assess the biological effects of this extract, including its antioxidant, cytoprotective, and anti-apoptotic properties.

To investigate the mechanisms by which the extract influences t-BHP-induced damage and dysfunction in HSG cells, focusing on its effects on oxidative stress,

apoptotic signaling pathways, and the expression of α-amylase and AQP5, as well as the activity of α-amylase.

1.3 Research Questions

What bioactive compounds with antioxidant properties are present in the heated water extract of *E. latifolia* fruits?

Does the *E. latifolia* fruit extract exhibit antioxidant activity against t-BHP-induced oxidative stress in HSG cells?

Does the extract protect against t-BHP-induced HSG cell damage?

How does the extract influence apoptosis in HSG cells under oxidative stress, particularly regarding the expression of proteins such as phosphorylated P38, cleaved caspase-3, Bcl-2, and Bax?

What effect does the extract have on the gene expression of AQP5 and α-amylase, as well as on the enzymatic activity of α-amylase in HSG cells under oxidative stress?

1.4 Hypothesis

The heated water extract of *E. latifolia* fruits contains bioactive compounds with antioxidant properties. It demonstrates cytoprotective and anti-apoptotic effects against t-BHP-induced HSG cell damage by downregulating the expression of phosphorylated P38 MAPK, Bax, and cleaved caspase-3, while upregulating Bcl-2. Furthermore, the extract is able to improve HSG cell function by preserving AQP5 expression and maintaining α-amylase activity under oxidative stress conditions.

1.5 Expected Benefits

This study aims to elucidate the bioactive compounds present in the heated water extract of *E. latifolia* fruits and evaluate their antioxidant and cytoprotective effects on HSG cells. The extract's ability to protect against oxidative stress induced by t-BHP will be investigated by analyzing its effects on apoptotic pathways, specifically through the modulation of key proteins such as phosphorylated P38 MAPK, Bcl-2, Bax, and

caspase-3. The study will also explore the effect of the extract on submandibular gland function, focusing on AQP5 expression and α-amylase activity. Beyond the evaluation of its antioxidant properties through DPPH, ABTS, and intracellular ROS assays, the study will utilize high-performance liquid chromatography (HPLC) and metabolomic profiling to identify key bioactive compounds. The results of this investigation may support the potential use of *E. latifolia* fruits as a potential phytomedicine for alleviating oxidative stress-related oral disorders such as xerostomia and salivary hypofunction, thereby offering significant promise for developing phytomedicine-based oral care products for therapeutic applications.

1.6 Scope of study

The scope of this study includes the collection, water extraction, and identification of bioactive compounds with antioxidant properties from *E. latifolia* fruits. Subsequently, the cytoprotective and antioxidant effects of the water extract will be assessed in HSG cells exposed to oxidative stress. A primary objective of the investigation is to uncover the molecular mechanisms that contribute to the cytoprotective and anti-apoptotic effects of the extract, involving an in-depth analysis of gene expression and protein levels related to the apoptosis signaling pathway, including phosphorylated P38 MAPK, cleaved caspase-3, Bcl-2, and Bax.

The expression of AQP5, an essential marker of salivary secretion, will also be evaluated to determine the extract's potential for preserving submandibular gland function. Furthermore, the study will investigate the gene expression and enzymatic activity of α-amylase, a vital enzyme involved in digestion and oral health, particularly under conditions of t-BHP-induced oxidative stress in HSG cells.

Altogether, these findings could offer valuable insights into the pharmacological potential of *E. latifolia* fruits as a phytomedicine for preventing oral disorders, such as xerostomia and salivary hypofunction.

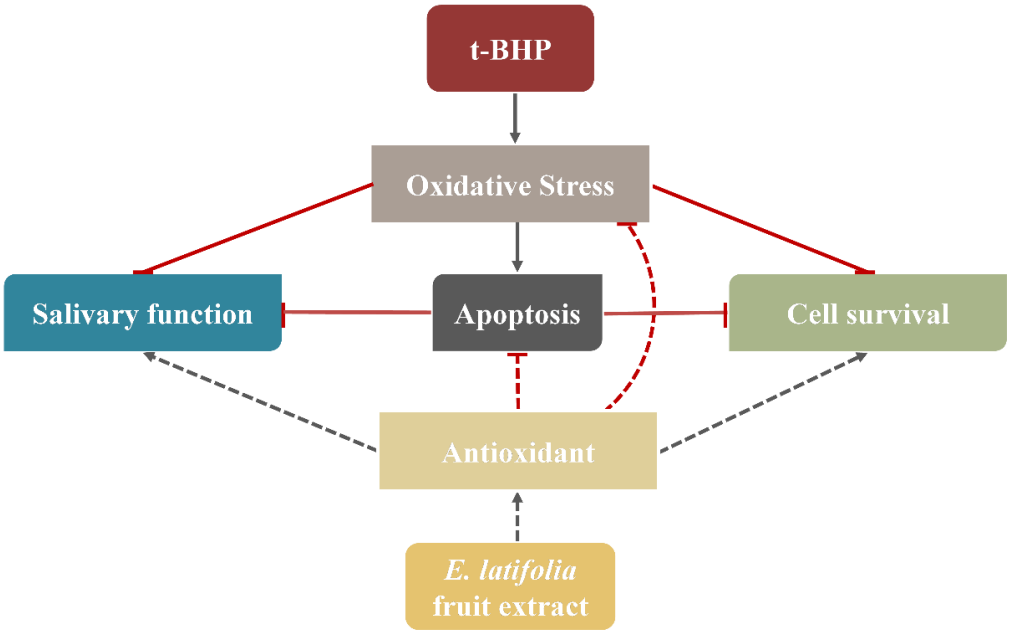

Figure 1 Conceptual framework

CHAPTER 2
LITERATURE REVIEW

2.1 Biology of saliva and oxidative stress in oral health

2.1.1 Overview of the salivary glands

Saliva, a complex biofluid, is produced by the parotid, submandibular, and sublingual glands. Each salivary gland performs a unique function critical to the maintenance of oral health and the initiation of digestion. The parotid gland, the largest of the three, secretes watery, amylase-rich saliva primarily during stimulated conditions, such as eating, which is essential for for carbohydrates breakdown[16]. The submandibular gland, located beneath the mandible, contributes both resting and stimulated saliva. Its secretions are a blend of serous and mucous fluids, providing necessary moisture and lubrication to the oral cavity throughout the day. The sublingual gland, the smallest among them, secretes mucous-rich saliva primarily during unstimulated periods, helping to maintain baseline oral moisture[17].

Saliva is produced by acinar cells, which create the primary saliva, while ductal cells modify its electrolyte composition as it flows through the ducts. Myoepithelial cells, located around the acini and ducts, contract to pump saliva into the oral cavity. The activity of these cells is under the control of the autonomic nervous system (ANS) that aims to regulate saliva production in response to whole-body requirements by balancing the production of saliva[9], as illustrated in Figure 2.

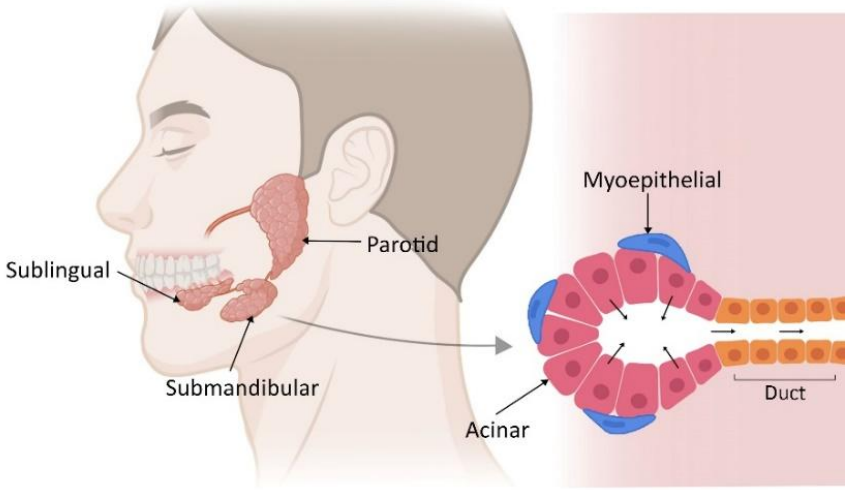

Figure 2 The three main salivary glands and their general structure of saliva [Modified from Piraino et al.,2021][18]

Salivary glands contain aquaporin channels within their membranes, which are vital to saliva production. Aquaporin (AQP) allows water and other small molecules to pass through cellular membranes, maintaining saliva balance and volume. Only three of the thirteen aquaporin types are found in the salivary glands: AQP1, AQP3, and AQP5. AQP5 is localized on the apical membrane of the salivary glands, cornea, and airway epithelium and regulates saliva flow into the mouth. However, dysfunction of AQP5, frequently induced by oxidative stress, can result in dysfunction of the salivary glands and contribute to conditions such as xerostomia (dry mouth). This highlights the importance of protecting AQP5 from oxidative damage in order to preserve normal salivary gland function.[19].

2.1.2 Innervation, autonomics, and salivary secretion

The autonomic nervous system regulates salivary glands, with both sympathetic and parasympathetic systems controlling their function. However, the parasympathetic system has a more potent and longer-lasting effect on salivary gland secretion. Sympathetic nerves arise from postganglionic fibers and activate adrenergic receptors on salivary acinar cells by releasing norepinephrine. Conversely, the parasympathetic system stimulates glands via muscarinic M_3 receptors and elevates substance P, which aids in amylase output, via cranial nerves VII and IX[20]. The parasympathetic system stimulates salivary gland secretion and maintains its function. The parasympathetic supply to the parotid gland is facilitated by the glossopharyngeal nerve, whereas the facial nerve is responsible for the parasympathetic innervation of the submandibular and sublingual glands. Postganglionic fibers reach the glands via the otic, submandibular, and lingual nerves, as shown in Figure 3. The autonomic nerves also play a vital role in the glands' ability to regenerate, avoid atrophy, and maintain their function. This understanding help develop new treatments for chronic oral dryness or salivary gland atrophy[21].

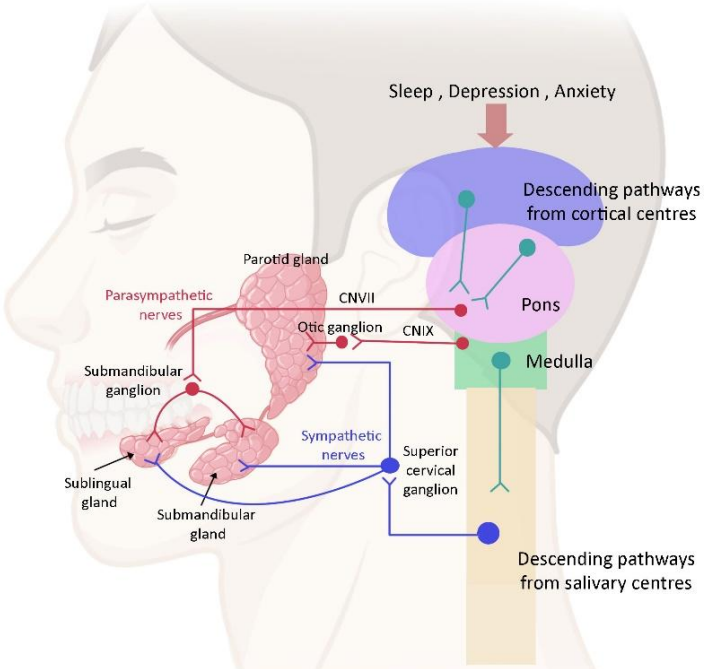

Figure 3 Nerves regulate the secretion of saliva. The central and peripheral nervous systems are involved in the reflex-stimulated secretion of saliva by the major salivary glands [Modified from Proctor et al.,2016][16]

The parasympathetic nervous system controls salivary gland secretion through cholinergic signaling. While neuropeptides such as substance P and adrenergic signaling from the sympathetic nervous system are also involved. The activation of acetylcholine binding to cholinergic receptors allows for the activation of diacylglycerol [22] and inositol triphosphate (IP_3) , subsequently increasing intracellular calcium levels and saliva volume. Substance P activates the neurokinin-1 (NK-1) receptor, leading to a similar increase in intracellular calcium and amylase output. Sympathetic stimulation causes the smooth muscle to contract, ultimately increasing saliva volume and amylase secretion via alpha-receptor activation. Furthermore, norepinephrine stimulates the cAMP cascade through beta receptors, which boosts protein kinase A activity and subsequently enhances both amylase secretion and transient saliva flow[20], as illustrated in Figure 4A.

Two stages characterize the secretion of saliva from the glands. In the first stage, acinar cells secrete isotonic primary saliva that comprises amylase, mucus, and extracellular fluid. Sodium chloride secretion maintains saliva's isotonic nature. In the second stage, the ductal tree modifies primary saliva. This process involves the reabsorption of sodium, secretion of potassium, absorption of chloride, and release of bicarbonate. It is important to note that the ductal epithelium has limited water permeability, resulting in a hypotonic final saliva product. Moreover, muscarinic M_3 receptors, α_1- and β_1-adrenoceptors, and vasoactive intestinal polypeptide receptors are significant in stimulating acinar cells and causing secretion. This process is driven by concentration gradients of electrolytes created by the active transport of Na^+ and K^+ ATPases. Moreover, it is influenced by the distribution of membrane transport proteins[20, 23], as shown in Figure 4B.

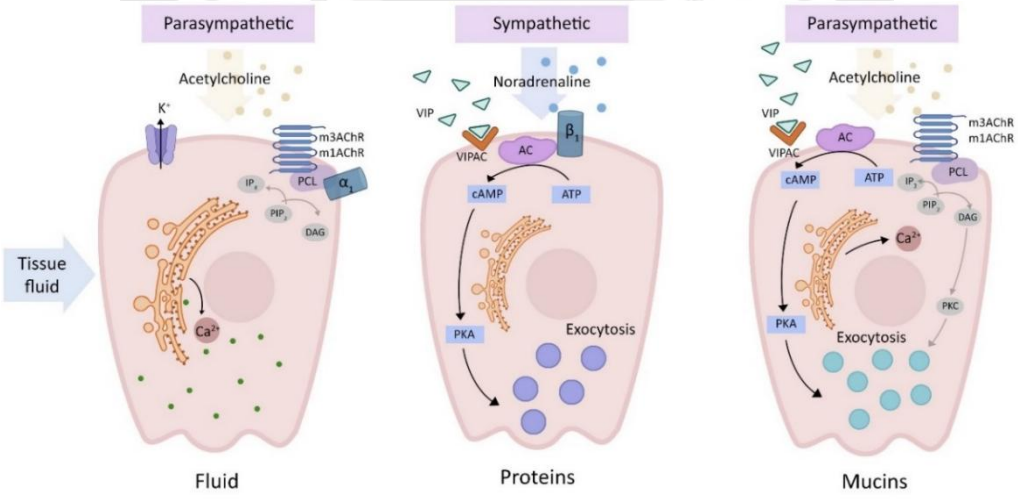

(4A) In response to nerve stimuli, salivary acinar cells secrete fluid and proteins. Acetylcholine and noradrenaline facilitate calcium release and cAMP generation, respectively. This promotes mucous cell exocytosis, unaffected by sympathetic nerves

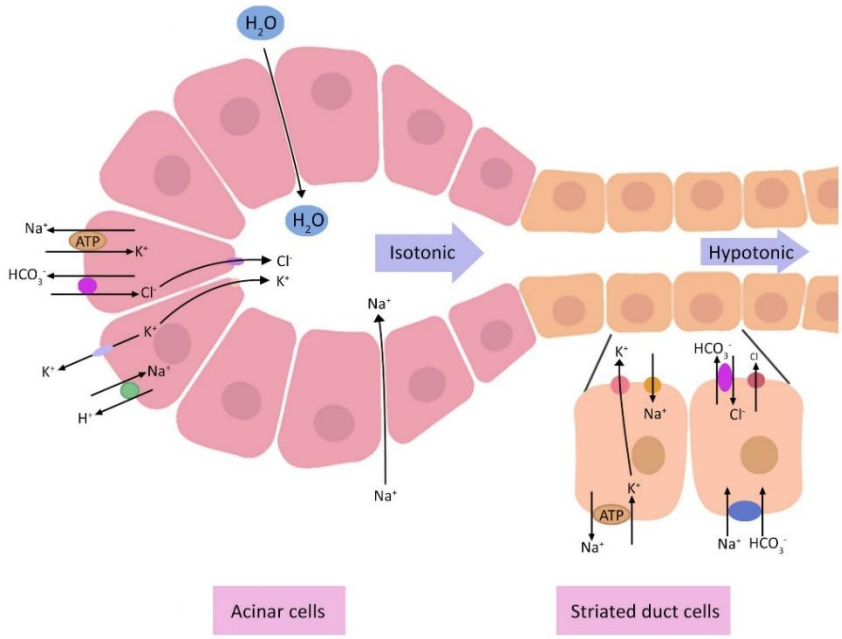

4B) Acinar cells in salivary glands secrete isotonic primary saliva, modified by striated duct cells to a hypotonic product. This process, driven by membrane transporters and Na/K ATPase, involves coordinated action of Na/K and bicarbonate channels, and anti-ports in the ductal cells.

Figure 4 Salivary gland secretion of fluid and protein [Modified From Proctor et al.,2016][16]

2.1.3 Factors influencing stimulant and saliva flow rate of saliva

Both external and internal factors can stimulate salivation. External factors include food, alcohol, smoking, and oral hygiene habits such as gum chewing. These factors activate oral receptors and the parasympathetic nervous system. In addition to internal factors, changes in hormone levels during pregnancy or menopause and the circadian cycle alter the flow rate of salivation. Anxiety and stress increase the sympathetic nervous system, which releases chemicals that stimulate the salivary glands. Moreover, the parasympathetic and sympathetic nervous systems release

neurotransmitters such as acetylcholine and adrenaline/noradrenaline to enhance saliva production. Recognizing these factors is vital for managing disorders that impact salivary secretion, such as chronic mouth dryness[24].

Salivary flow rate refers to the amount of saliva produced at a specific time. Typically, saliva production varies between 0.5 and 1.5 liters per day. There are two types of salivary flow rates: unstimulated and stimulated salivary flow rates. In a state of rest, the overall unstimulated salivary flow is about 0.3–0.4 mL/min, however, this rate can decline to approximately 0.1 mL/min during periods of sleep. The stimulated salivary flow rate averages 1.5–2.0 mL/min, but during activities such as eating and chewing, the rate increases to about 4.0–5.0 mL/min[24]. Factors that affect salivary flow rate include age, sex, biorhythm, oral sugar clearance, and dry mouth sensation. In addition, the secretion of the major salivary glands can be increased by stimulation with citric acid[25].

2.1.4 Saliva composition

As mentioned above, normal saliva production ranges from 0.5 to 1.5 liters per day. Almost all saliva is water, while the remaining 1% comprises different electrolytes like sodium, potassium, calcium, magnesium, phosphate, bicarbonate, and mucus. This 1% also contains carbohydrates, proteins, antimicrobial agents, and digestive enzymes including α-amylase[26].

2.1.4.1 Salivary alpha amylase[27]

The sAA, also known as α-amylase (EC 3.2.1.1; systematic name 4-α-D-glucan glucanohydrolase), is an enzyme found in human saliva that plays a crucial role in starch digestion. It breaks down the internal α -1,4-glucoside bonds of starch into the disaccharide maltose and oligosaccharides[28]. The sAA enzyme encoded by the AMY1 gene is located on chromosome 1p21. Humans have multiple copies of this gene, ranging from 2 to 15 copies per diploid genome, with variations between individuals and populations. For example, people with high-starch diets tend to have higher copy numbers of the AMY1 gene[29].

Advantage of sAA

The sAA has other health benefits beyond improved digestion, such as immunological support, inflammation management, and promoting healthy aging. This can indicate stress and immune biomarkers in children. There is a correlation between its level and their emotional and behavioral adjustment[30].

Dysfunction of sAA

Impairment of sAA, especially the reduction of its secretion levels, can be influenced by oxidative stress, which is defined by a disproportion between ROS and the body's antioxidant capacity. This oxidative stress is associated with numerous pathological conditions that affect the salivary glands. This dysfunction is observed in stroke, obesity, and insulin resistance, wherein oxidative stress is a key factor in the pathogenesis of reduced salivary gland function. Previous studies have shown that stroke patients with reduced saliva production exhibited increased oxidative and nitrosative stress, correlating to decreased salivary flow and amylase activity, suggesting that oxidative stress might impair salivary secretion[31]. Similarly, in obese adolescents, oxidative stress is associated with decreased salivary secretion and altered antioxidant levels, indicating a disruption in salivary gland function[32]. In insulin-resistant rats on a high-fat diet, significant oxidative damage in salivary glands led to reduced salivary flow and protein concentration, implying the impact of oxidative stress on glandular function[33].

Mechanisms of oxidative stress impact on sAA

Hydrogen peroxide interfere with cellular processes, leading to dysfunction in various cell types, including salivary gland cells. This interference can result in reduced sAA enzyme secretion and also altered glandular function[34]. In radiation therapy, oxidative stress is a key factor in salivary gland injury, affecting calcium signaling pathways and leading to cellular damage and reduced gland function[35]. Stress also influences sAA levels, with increased levels observed during

acute psychosocial stress. This sAA enzyme is considered a marker of autonomic nervous system activity, which can be modulated by oxidative stress[36, 37]. However, in conditions like gestational diabetes, although oxidative stress is present, changes in sAA levels are not significant, indicating that other factors may influence enzyme secretion[38].

2.1.5 Salivary functions

Saliva is essential for oral and overall health in various ways. For example, it helps keep the mouth moist and remove food particles, aids in digestion by containing enzymes, and prevents tooth decay by balancing pH levels between 6.2 and 7.6. Saliva also plays a role in taste perception, contains antibacterial substances, and aids wound healing in oral tissues. In addition, it acts as a plentiful source of antioxidants that contribute to the regulation of redox homeostasis in the oral environment and the entire body. Saliva helps prevent oral diseases such as tooth decay, tartar formation, gingivitis, and plaque accumulation and also promotes overall health. Therefore, maintaining healthy mouth hygiene practices such as regular brushing, flossing, and visits to the dentist can ensure optimal saliva production and function. This will promote good oral and overall health[39].

2.1.6 Salivary dysfunction

2.1.6.1 Aberrant Salivary Characteristics

Salivary dysfunction can show up in different ways, such as by producing too much saliva (hypersecretion), which can cause discomfort and symptoms related to acid reflux, or not enough saliva (hyposalivation). Hyposalivation (xerostomia) results in dryness, pain, and swelling in the submandibular gland region. Nocturnal salivary secretion, or excessive saliva produced during sleep, is rare and linked to medical conditions. Thick saliva is caused by reduced salivary fluid production, not excessive talking or inadequate fluid intake[40].

2.1.6.2 Salivary Dysfunction: An Oral Health Concern

Salivary dysfunction can cause various dental and oral health issues, including tooth decay, difficulty swallowing and speaking, dry mouth, bad breath, a

higher risk of infections, malnutrition, thrush, and oral cancer. In addition, the absence of saliva prevents the neutralization of acids produced by bacteria and the washing away of food particles, leading to tooth decay and other dental problems. Dry mouth and bad breath increase infection risk, while difficulty chewing and swallowing food can cause malnutrition. Furthermore, saliva plays a crucial role in repairing damaged DNA in the mouth. A lack of it can increase the risk of DNA damage and mutation, raising the likelihood of oral cancer[39].

In addition, oxidative stress affects oral health, specifically periodontal disease, xerostomia, and salivary gland dysfunction. As aging, the effects of oxidative stress increase throughout the body and specifically in the submandibular gland, which affects the function of the salivary glands and changes saliva composition, properties, and flow rate. The molecular mechanisms of how oxidative stress contributes to oral disease development are not fully understood. Nevertheless, some studies have shown that heightened ROS levels alongside decreased antioxidant capacity may play a significant role. Radiation-induced salivary gland damage was also linked to oxidative stress[34]. In a recent study, an antioxidant gel improved salivary flow rates in xerostomia patients but did not significantly change oxidative stress levels. This finding suggested that antioxidant treatments might benefit these patients[41].

2.2 Free radicals and oxidative stress

2.2.1 Free radicals

Free radicals are defined as atoms or molecules that contain one or more unpaired electrons in their outermost electron shell. These unpaired electrons are represented by a dot on the atom or group where they are primarily located. For example, $H^{\bullet}$ for a hydrogen atom and $HO^{\bullet}$ for a hydroxyl group. Oxygen radicals are a type of free radical with an unpaired electron located mainly on an oxygen atom, such as $O_2^{\bullet -}$, $HO^{\bullet}$, and peroxyl ($ROO^{\bullet}$)[42]. Free radicals are highly reactive due to their unstable and short-lived nature. In their pursuit of stability, free radicals engage in bonding with surrounding atoms, molecules, or isolated electrons. This bonding mechanism initiates

chain reactions, as free radicals either accept or donate electrons from neighboring molecules, functioning as oxidizing or reducing agents[42, 43].

ROS and RNS can exist in radical or non-radical forms[44]. ROS radicals include $O_2^{\bullet -}$ and $HO^{\bullet}$, while non-radical derivatives include H_2O_2, ozone (O_3), and singlet oxygen ($^1O_2$). RNS are radicals based on nitrogen, such as nitric oxide ($NO^{\bullet}$), peroxynitrite ($ONOO^{\bullet}$) and nitrogen dioxide ($NO_2^{\bullet}$). Additionally, non-radical entities, including H_2O_2, nitrous acid (HNO_2) and $ONOO^-$ can also trigger free radical reactions in living organisms, even though they are not free radicals[45], as shown in Figure 5 for more details.

2.2.2 Free radical formation

Free radicals can be produced through homolytic fission and disrupting disulfide bonds. Different cell organelles and enzyme activities can generate these unstable molecules internally during normal metabolisms, such as mitochondria, peroxisomes, and phagocytic cells. Externally, free radicals can come from radiation, chemical reagents, environmental pollutants, microbial infections, and drugs with their metabolites. Exogenous sources of free radicals may include chemical substances such as heavy metals, O_3, and high-temperature cooking, along with environmental pollutants like pesticides and dioxins, in addition to environmental pollutants like pesticides and dioxins[46], as shown in Figure 5.

ROS sources in the mouth can come from many sources, such as gum inflammation, harmful substances (alcohol, smoking, drugs), certain foods (high-fat or high-protein diets, acrolein), dental processes[4].

The following mechanisms can lead to the formation of free radicals:

1. Covalent bond breakage or Imolysis; $A : B \longrightarrow A^{\bullet} + B^{\bullet}$
2. Adding one electron to a neutral atom; $A + e^- \longrightarrow A^{-\bullet}$
3. Loss of one electron from a neutral atom; $A \longrightarrow A^{+\bullet} + e^-$

where A and B are generic symbols representing two different atoms or molecules participating in a chemical reaction, while e^- represents a free electron.

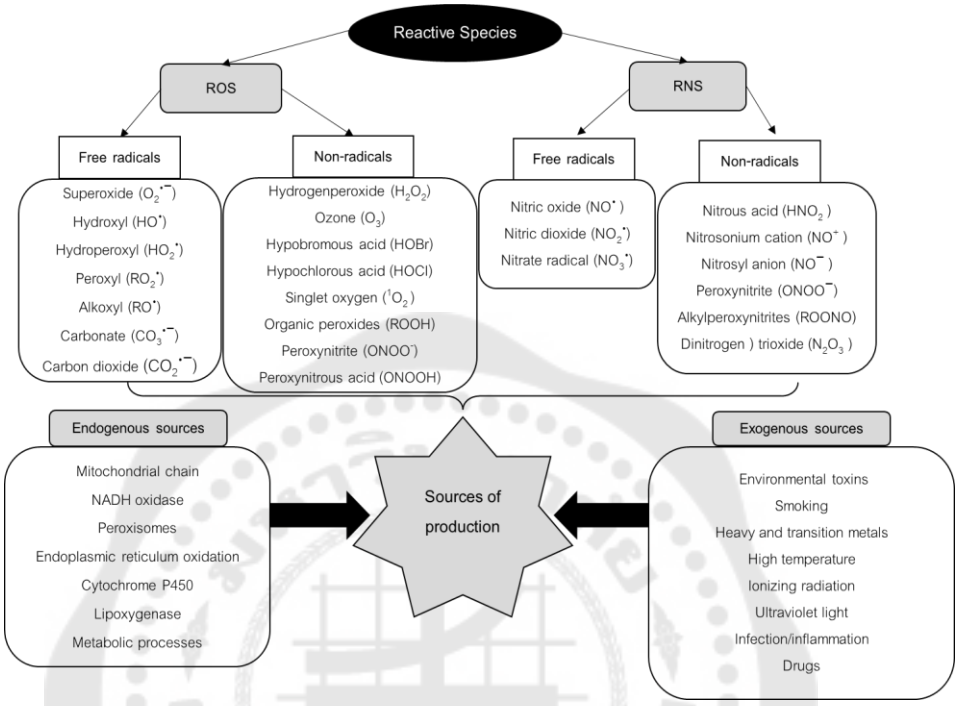

Figure 5 Types of reactive species and their endogenous and exogenous formation sources [Modified from Bisht et al.,2017][47]

Oxidation reaction

In an oxidation reaction, a molecule or atom becomes the electron acceptor by donating its electrons to another molecule. Reducing agents are molecules that facilitate electron donation, whereas oxidizing agents are characterized as molecules that receive electrons. Reactions involving oxidation frequently involve oxygen. It may also refer to a molecule losing hydrogen atoms. Additionally, oxidation reactions produce free radicals, which can interact with other substances to initiate different oxidation reactions[48].

Free radical reaction

Chain reactions involving free radicals have three steps: initiation, propagation, and termination. In the initiation step, free radicals are formed or generated. Then, in the propagation step, free radicals react with other molecules to produce more

free radicals. Finally, in the termination step, free radicals combine to form stable molecules, effectively stopping the reaction. Free radicals form when molecules or atoms with unpaired electrons, including biological molecules, come together under normal conditions. Common free radical reactions in living organisms involve ROS such as $O_2^{\bullet-}$ and H_2O_2[42].

2.2.3 Features of the main free radicals

2.2.3.1 Superoxide radical ($O_2^{\bullet-}$)

$O_2^{\bullet-}$ is a form of oxygen molecule that has gained an electron in a specific orbital, resulting in only one unpaired electron, making it less radical than O_2. When another electron is added, it forms the peroxide ion (O_2^{-}), which lacks unpaired electrons and has a weaker oxygen-oxygen bond. Added two more electrons produces two oxide ions (O_2^{-})[49]. In biological systems, O_2 is reduced to H_2O_2 or water during oxidative phosphorylation in the mitochondrial electron transport chain, generating ATP. Conversely, $O_2^{\bullet-}$ is characterized by its strong reactivity, which can lead to biomolecular damage, and its decomposition may be catalyzed by transitional metal ions, producing the highly reactive $HO^{\bullet}$ via the Fenton reaction. $O_2^{\bullet-}$ can be enzymatically or non-enzymatically produced and is a precursor to highly reactive species[42].

2.2.3.2 Hydroxyl radical ($HO^{\bullet}$)

Among the various free radicals produced in living organisms, the hydroxyl radical, the hydroxyl radical ($HO^{\bullet}$) stands out as the most reactive. It is generated through the Fenton reaction, involving the reaction of free iron (Fe^{2+}) interacts with H_2O_2, and via the Haber-Weiss reaction that occurs when $O_2^{\bullet-}$ interacts with ferric iron (Fe^{3+}), resulting in the formation of Fe^{2+}. The response can also involve ions such as Cu^{2+}, Fe^{3+}, Ti^{4+} and Co^{3+}. $HO^{\bullet}$ is highly reactive and can attack any molecule within a few nanometers[49], potentially causing damage to numerous types of biomolecules, including DNA, proteins, lipids, amino acids, sugars, vitamins, and metal ions. Because of this, $HO^{\bullet}$ impact tissue damage caused by radiation, cardiovascular disease and cancer[42, 45].

2.2.3.3 Hydrogen peroxide (H_2O_2)

H_2O_2 is produced by cells via enzyme reactions or $O_2^{\bullet-}$ dismutation. Due to its lipid solubility, it can cross cell membranes but is not highly reactive and does not quickly oxidize vital biomolecules. However, H_2O_2 can be converted into highly reactive $HO^{\bullet}$ through interaction with UV light or transition metal ions in the Fenton reaction. In living systems, H_2O_2 reacts with other molecules to produce singlet oxygen, which can be damaged. H_2O_2 harms cells directly by attacking heme proteins, which release iron, the inactivation of various enzymes, and the oxidation of critical biomolecules, including lipids, DNA, -SH groups, and keto acids[50].

2.2.3.4 Nitric oxide radical ($NO^{\bullet}$)

$NO^{\bullet}$ is a free radical distinguished by a one unpaired electron, demonstrates reactivity that is less intense than ROS, making it less toxic. However, $NO^{\bullet}$ reacts with $O_2^{\bullet-}$ to produce $ONOO^-$, which sequentially damages proteins, lipids, and DNA. $NO^{\bullet}$ can also generate harmful oxidizing and nitrosative agents by reacting with nitrogen and oxygen. Excessive $NO^{\bullet}$ production can produce neurodegenerative diseases and heart disorders, and $NO^{\bullet}$ is involved in lipid peroxidation and the depletion of ascorbic and uric acid concentrations[45].

2.2.4 Cellular homeostasis

ROS in cells has a dual role in cell physiology, known as the paradox of cellular ROS in redox research as shown in Figure 6. ROS effects on cells become beneficial or harmful depending on their concentration and location in the cells. Antioxidant defense systems consist of ROS scavenging enzymes (superoxide dismutase, catalase, and glutathione peroxidase) and radical scavengers (such as glutathione, thioredoxin, α-tocopherol and ascorbic acid), which tightly regulate ROS concentration within the cell[51]. Under controlled oxidative conditions, ROS stimulates many physiological functions, like signal transduction, gene expression, and cell proliferation. However, the overwhelming accumulation of ROS along with oxidative stress occurs when the antioxidant defense system fails, giving rise to diseases, such as diabetes, cancer, and heart failure. Thus, cellular ROS plays a dual role in the body,

depending on its concentration. At low or moderate levels, ROS functions as essential signaling molecules that regulate normal processes such as cell proliferation, immune response, and tissue repair. At high levels, oxidative stress resulting from ROS is capable of causing damage to cells and contributing to various pathological conditions as previously mentioned[52].

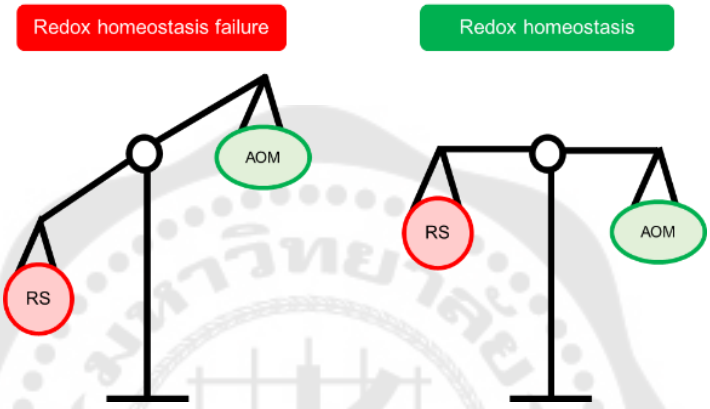

Figure 6 Reactive species (RS) are paradoxical [Modified from Ojha et al., 2018][53]

2.2.5 Oxidative stress

Oxidative damage occurs when the imbalance between free radical generation surpasses the capacity of antioxidant defenses, leading to oxidative stress. The destruction of lipids, proteins, and nucleic acids occurs as a result of this condition[54]. Several factors contribute to short-term oxidative stress, including trauma, infections, heat injuries, toxic substances, and intense exercise. The affected tissues result in elevated levels of enzymes which generate radicals, activate phagocytic activity, or disrupt electron transport chains. This leads to excess ROS, as illustrated in Figure 7 for more details. This imbalance has been linked to cancer progression and development, as well as radiation and chemotherapy side effects of radiation and chemotherapy. Besides, the involvement of ROS in the initiation and progression of common diseases, such as diabetes mellitus, has been documented[3].

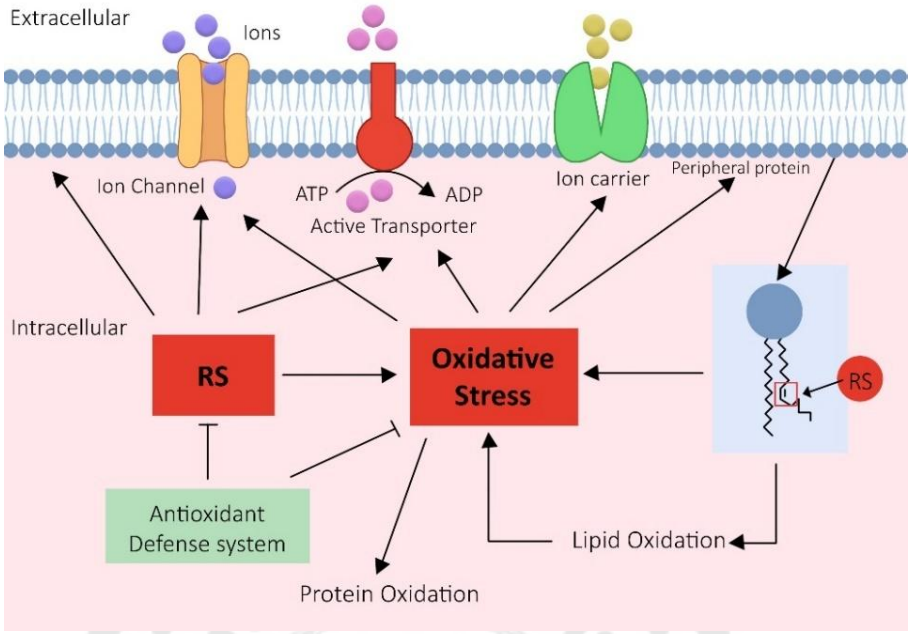

Figure 7 Reactive species can harm cell membranes by modifying proteins [Modified from Ojha et al., 2018][53]

2.2.5.1 Oxidative damage to proteins

Through oxidative damage, proteins can cause modifications in proteins, which may include alterations to amino acids, free radical-induced peptide cleavage, and cross-linking from lipid peroxidation byproducts. Amino acids such as cysteine, arginine, methionine, and histidine are especially prone to oxidative changes[55]. Protein oxidative damage impacts membrane transport, receptor function, and enzyme activity. The oxidative effects of the peroxyl radical on proteins interfere with signal transduction, reduce enzyme efficacy, compromise heat stability, and enhance the susceptibility to proteolysis. It results in amino acid modifications like carbonyls, methionine sulfoxide, and protein peroxide. Reactive groups from overoxidized proteins can also disrupt cellular processes and harm membranes[56].

2.2.5.2 Lipid peroxidation

Oxidative stress has a big impact on physiological and pathological processes, such as aging, inflammation, and carcinogenesis. The most common of

these processes is lipid peroxidation, which provokes a chain reaction involving free radicals, leading to biochemical lesions. This process typically targets polyunsaturated fatty acids in cell membranes[57]. The hydroxyl radical initiates ROS formation, creating a lipid radical ($L^{\bullet}$) and diene conjugates. Eventually, lipid hydroperoxide and other radicals are formed, propagating lipid peroxidation. This process leads to the formation of several compounds, including alkanes, malondialdehyde, and isoprostanes. These compounds are commonly used as markers in lipid peroxidation assays and associated with various diseases[57].

2.2.5.3 Oxidative damage to DNA

Numerous studies have demonstrated that DNA and RNA, particularly DNA, which is a critical target in aging and cancer, are very susceptible to oxidative damage. The production of oxidative nucleotides such as glycol, thymidine glycol (dTG), and 8-hydroxy-2-deoxyguanosine is increased during oxidative damage. These biological metabolites can be used as indicators of oxidative damage[22].

2.2.6 Oxidative stress and oral disorders

The onset of diverse oral disorders and diseases is intricately linked to oxidative stress, including dental caries, periodontitis, pulpitis, oral cancer, xerostomia, and salivary gland dysfunctions. The impact of oxidative stress in the oral cavity leads to lipid peroxidation, protein denaturation, and DNA breakage, resulting in the oral disorders and diseases mentioned above. Identifying the targets of oxidative stress is essential for improving oral health and developing targeted therapeutic strategies. Biomarkers of lipid peroxidation and protein oxidation can be utilized for the diagnosis of oral pathologies. For instance, cancer treatments can cause oral complications such as mucositis, infections, salivary gland dysfunction, taste alterations, and pain. In particular, patients undergoing radiation therapy for head and neck malignancies often experience xerostomia as a result of diminished saliva secretion leading to dental decay and periodontal diseases[4].

2.2.6.1 Mechanisms of oxidative stress in the submandibular gland

Oxidative stress-induced damage to the submandibular gland involves a complex interplay of molecular mechanisms that contribute to cellular dysfunction and tissue injury. This damage is primarily driven by an imbalance between ROS production and the gland's antioxidant defense, leading to significant alterations in glandular structure and function. In the submandibular gland, elevated levels of ROS such as $O_2^{\bullet-}$ and H_2O_2 surpass the capacity of enzymes such as superoxide dismutase, glutathione peroxidase, and catalase. Exposure to radiation and the consumption of high-fat diets enhance the function of pro-oxidant enzymes like NADPH oxidase, contributing to the increased production of ROS and ensuing oxidative damage[58, 59]. A decrease in the activity of antioxidant enzymes exacerbates oxidative stress, as evidenced by studies involving gamma radiation and metronidazole treatment[60, 61].

Oxidative stress results in lipid peroxidation, protein carbonylation, and DNA damage, which are markers of cellular injury in the submandibular gland[33]. High-fat diets and radiation exposure lead to mitochondrial dysfunction, characterized by impaired redox balance and increased apoptosis, indicated by elevated levels of pro-apoptotic proteins such as Bax[58]. Structural changes, including acinar atrophy and ductal degeneration, are common under oxidative stress conditions, leading to impaired salivary secretion and glandular dysfunction[60]. Increased levels of cytokines, such as interleukin-2 (IL-2) and tumor necrosis factor-alpha (TNF-α), are a consequence of oxidative stress-induced inflammatory signaling, which contribute to glandular inflammation and damage[58]. Apoptosis is a significant consequence of oxidative stress, with heightened expression of pro-apoptotic markers and reduced cell viability in the submandibular gland[33].

2.2.6.2 Oxidative stress-induced xerostomia

Excess ROS production has been implicated in radiation-induced damage to the oral cell cavity, characterized by oxidative stress and xerostomia, the therapeutic potential of antioxidants in addressing salivary gland dysfunction merits

further investigation. Likewise, some salivary oxidative stress parameters and disorders of redox homeostasis may be valuable diagnostic biomarkers for xerostomia[62].

As aforementioned, oxidative stress caused by many factors or diseases plays a major role in oral disease pathogenesis. Specifically, xerostomia is a consequential oral health disorder resulting from oxidative damage. The imbalance between free radicals and antioxidant systems in the oral cavity is crucial for maintaining the salivary gland hypofunction, resulting in low saliva production and dry mouth. Hence, preventing oxidative stress and searching for antioxidants may alleviate oxidative stress-related xerostomia. Oxidative stress also causes cell death and cell membrane damage. A previous study reported that one of the main symptoms of xerostomia in menopausal women was dysfunctional salivary glands bringing on oxidative stress-induced salivary gland deterioration. Resveratrol could alleviate this condition[63]. By lowering ROS, cordycepin could also diminish oxidative stress, attenuating salivary hypofunction[13].

A growing body of evidence suggests that it is still unclear how oxidative stress results in xerostomia. However, it is presumed that excess ROS could damage cell membranes and result in necrosis or apoptosis, leading to cell death. Hyposalivation can occur due to this damage, affecting the salivary glands[64].

2.2. 7 Cell death pathway

Cell death is a natural process that affects how living tissues respond to foreign substances. It consists of two characteristics: necrosis and apoptosis, each with distinct biochemical and histological features.

2.2.7.1 Necrosis

Necrosis is a hazardous state that results in death due to the unregulated degradation of cells. This condition causes swelling of the nucleus and mitochondria, membrane disintegration and chromatin condensation. The inflammatory response is triggered by the subsequent secretion of pro-inflammatory cytokines such as IL-4 and TNF[65].

2.2.7.2 Apoptosis

The mechanism of apoptosis, a controlled form of cell death, is characterized by the absence of inflammation. It involves a biochemical cascade that activates proteases and results in cell shrinkage, chromatin and cytoplasmic condensation, DNA fragmentation, and apoptotic bodies. The process occurs in three distinct phases: cell detachment, DNA fragmentation, vesicle encapsulation, and finally, generating an apoptotic body, which is phagocytosed by macrophages. The process takes about 15 to 20 minutes and the cell membrane becomes permeable to dyes like Trypan blue in the final phase.

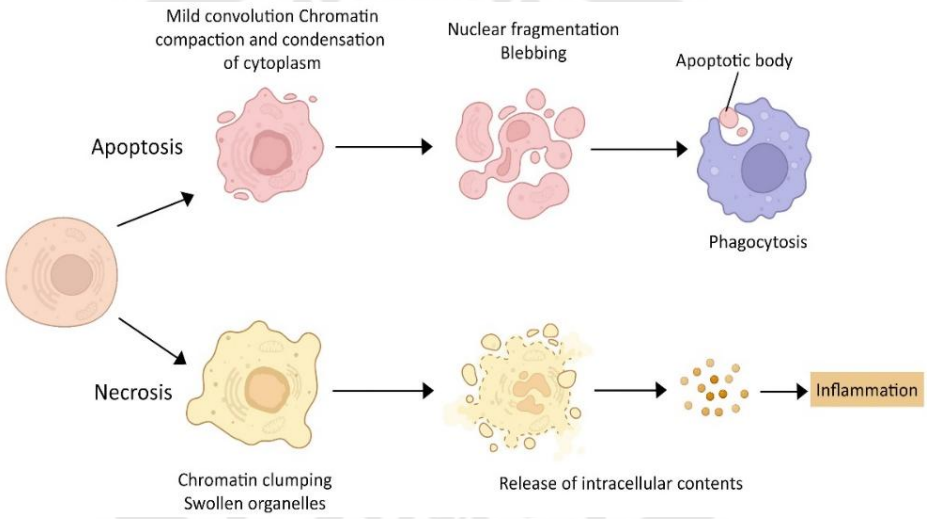

Figure 8 Comparison of necrotic and apoptotic cells, highlighting the distinct cellular modifications induced by each process [Modified from Asensi et al, 2017][66].

2.2.7.3 Apoptosis mechanisms

Apoptosis is an essential process in our bodies that maintains balance and fights diseases. Two main intrinsic and extrinsic pathways activate caspases, like small scissors that break down abnormal cells. However, if apoptosis is not controlled correctly, it can cause health problems like Parkinson's, cancer, and other disorders[67].

2.2.7.3.1 Extrinsic pathway

The activation of intracellular pathways in the extrinsic signaling pathway occurs through the interaction of death ligands with death receptors on the surface of the cell, forming a death-inducing signaling complex (DISC), and activating caspases that cause cell death. The process can be stopped by a protein called c-FLIP, which inhibits caspase activation. Overall, this pathway is crucial for cells undergoing apoptosis.

2.2.7.3.2 Intrinsic pathway

Different kinds of damage, such as physical, chemical, and genetic damage, can trigger the intrinsic apoptotic pathway. Once these stimuli alter the inner mitochondrial membrane, two protein groups that support apoptosis are released. This initial group activates the mitochondrial pathway that is dependent on caspases through the binding and activation of procaspase-9and Apaf-1.The second group, released later, induces caspase-independent DNA fragmentation and chromatin condensation. Apoptosis is regulated by the Bcl-2 protein family, which affects the permeability of the mitochondrial membrane. In addition, the Bcl-2 family is controlled by the tumor suppressor protein p53, which promotes cell death[67], as shown in Figure 9 for more details.

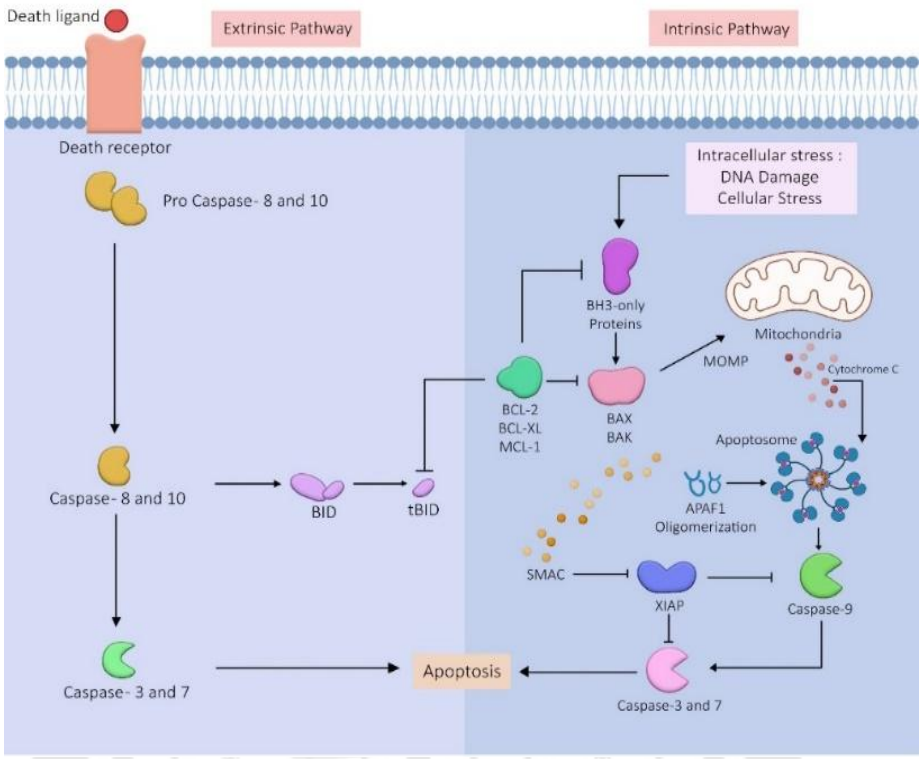

Figure 9 Apoptosis, activated via intrinsic or extrinsic pathways. [Modified from Wanner et al.,2021][68]

2.2.7.4 Regulation of Apoptosis Signaling Pathway

2.2.7.4.1 p38 Mitogen-Activated Protein Kinase (MAPK)

Cellular stress response pathways critically depend on p38 mitogen-activated protein kinase (MAPK), playing a vital role in regulating apoptosis, cell cycle arrest, and other cellular processes. Phosphorylation of p38 MAPK, particularly the p38γ isoform modulates apoptotic pathways. In oral squamous cell carcinoma (OSCC), elevated levels of phosphorylated p38 (p-p38) significantly influence cell survival and apoptotic mechanisms[69]. Oxidative stress profoundly impacts p38 MAPK phosphorylation in oral cells. ROS serve as primary activators of p38 MAPK, initiating signaling cascades that lead to apoptosis, inflammation, and alterations in cell cycle progression[70, 71]. In OSCC, oxidative stress-induced activation of p38 MAPK has been associated with increased tumor aggressiveness and treatment resistance, indicating that modulation of this pathway influences cancer progression[72, 73].

Antioxidants like N-acetyl-l-cysteine (NAC) can inhibit p38 MAPK phosphorylation, reinforcing the critical role of ROS in activating this pathway[74, 75]. In addition to its independent activity, the p38 MAPK pathway integrates with other signaling networks, such as those involving ERK and JNK, to regulate cellular responses to oxidative stress. Inhibition of p38 MAPK disrupts the balance among these pathways, affecting cell survival and apoptosis[76]. In oral cancer cells, oxidative stress-induced activation of p38 MAPK is linked to both autophagy and apoptosis, processes vital for cancer cell survival and resistance to chemotherapy[74]. Modulating p38 MAPK activity in response to oxidative stress can influence cancer treatments efficacy, as different OSCC cell lines exhibit varying responses to ROS-modulating agents[73].

Regulation of oxidative stress responses across diverse tissues is a ubiquitous function of p38 MAPK, including gastric mucosal injury and intestinal epithelial cell apoptosis[70, 71]. Its involvement in oxidative stress responses underscores its potential as a therapeutic target for conditions characterized by excessive oxidative stress, such as cancer and inflammatory diseases[77, 78]. Oxidative stress significantly influences the phosphorylation and activation of p38 MAPK in oral cells, impacting apoptosis and other cellular processes. Development of effective treatments for oxidative stress-associated pathologies, including oral cancers, necessitates a thorough understanding of ROS-mediated p38 MAPK activation and its impact on cell survival and apoptosis.

2.2.7.4.2 Caspases

Caspases are essential protease enzymes involved in programmed cell death, present in most cells in an inactive procaspase form. Once activated, caspases initiate a cascade of protease activity, amplifying apoptotic signaling pathways that eventually result in cell death. Some caspases have specific functions: for instance, caspase-11 regulates apoptosis and cytokine maturation during septic shock; caspase-12 mediates apoptosis related to endoplasmic reticulum stress and amyloid-β cytotoxicity; and caspase-14 is predominantly expressed in embryonic tissues. They activate executioner caspases, including caspase-3, triggered by any initiator caspases

(caspase-8, 9, or 10). In the extrinsic pathway, the interaction between death ligands and death receptors recruits pro-caspase-8, which is eventually converted to active caspase-8, leading to the execution of the apoptotic pathway.

In the intrinsic pathway, cytochrome c release from mitochondria induces apoptosome formation. This sequentially activates effector caspases through the interaction between active caspase-9 and Apaf-1. Initiator caspases auto-activate during the apoptosome at the initial stages of apoptosis, stimulating executioner caspases such as caspase-3. For the extrinsic pathway, apoptosis is activated via death receptor-mediated caspase-8 stimulation by death ligands. Finally, in the intrinsic pathway, cytochrome c release from mitochondria induces apoptosome formation, activating effector caspases through the interaction between caspase-9 and Apaf-1[79]. Overexpression of cleaved caspase-3, a hallmark of apoptosis, is often associated with oxidative stress, a condition that is linked to various oral diseases. This phenomenon constitutes a key etiological factor in the development of oral conditions such as OSCC, mucosal diseases, and periodontal disease.

In OSCC, oxidative stress contributes to carcinogenesis through mechanisms involving ROS-induced DNA damage and inflammation[80, 81]. These studies identified differentially expressed genes related to oxidative stress in OSCC, suggesting potential biomarkers for diagnosis and prognosis. The involvement of oxidative and nitrosative stress in OSCC is further evidenced by increased markers like pAKT and NOS1, indicating their role in tumor progression[72]. Similarly, conditions like oral lichen planus, pemphigus, and leukoplakia are linked to oxidative stress, which exacerbates inflammation and tissue damage[82, 83]. Moreover, overexpression of cleaved caspase-3 is often observed in cells undergoing oxidative stress-induced apoptosis[84]. In various oral diseases, the presence of cleaved caspase-3 may indicate ongoing cellular apoptosis due to oxidative damage, suggesting its potential as a biomarker for assessing disease severity and progression[85].

2.2.7.4.3 Bcl-2 family

Control of apoptosis by the Bcl-2 family is mediated by its effects on mitochondrial membrane integrity and the subsequent activation of caspases. Single-domain and multi-domain pro-apoptotic proteins, such as Bax, Bak, and Bok, are unified by their possession of a BH3 domain. This activates Bax and Bak, which form an oligomeric pore in the outer mitochondrial membrane and release cytochrome c. However, after a death stimulus, BH3-only proteins induce the pro-apoptotic protein. As a result, a conformational alteration occurs in Bax, prompting its relocation to the mitochondria, where it generates an oligomeric pore that releases proteins situated in the intermembrane space. Bak is already resident in the mitochondrial membrane. Once released, cytochrome c activates caspase-9. This initiates caspase-3 and caspase-7, ultimately leading to cell death. Puma overexpression increases Bax expression, which triggers mitochondrial translocation, cytochrome c release, and reduced mitochondrial membrane potential. Among the Bcl-2 family, Bcl-2, Bcl-xL, and Bcl-w function as inhibitors of apoptosis through their interaction with pro-apoptotic proteins like Bax and Bak, inhibiting their activity. However, Bax and Bak can form toxic homodimers if an imbalance occurs, resulting in cytochrome c release and cell death. Maintaining the equilibrium between these proteins is crucial for cell survival, and any disruption can trigger cell death via the apoptosome complex[86].

Elevated ROS levels lead to overexpression of Bax and downregulation of Bcl-2, promoting apoptosis. This phenomenon is evident in oral squamous cell carcinoma (OSCC), where oxidative stress-related genes are differentially expressed, contributing to carcinogenesis[81]. High Bax expression has also been observed in periodontally compromised patients, suggesting its role as a biomarker for oral diseases initiated by periodontal bacteria[87]. Moreover, Bax upregulation is associated with increased apoptosis in oral lesions and cancers, indicating its involvement in early carcinogenic events[88].

The downregulation of Bcl-2 in response to oxidative stress facilitates apoptosis by reducing the cell's ability to counteract pro-apoptotic signals. ROS can

degrade Bcl-2 through the ubiquitin-proteasomal pathway, diminishing its anti-apoptotic function[89]. In OSCC, reduced Bcl-2 expression correlates with increased Bax expression and apoptosis, particularly in well-differentiated tumors[90]. Similarly, decreased Bcl-2 levels are observed in oral precancerous lesions, contributing to the progression of benign and malignant oral tumors[91]. Cellular fate during oxidative stress is largely determined by the balance between Bax and Bcl-2 activity. A higher Bax/Bcl-2 ratio is associated with increased apoptosis and, in the context of oral cancers, may lead to better therapeutic outcomes[92]. Modulation of these proteins by oxidative stress is a key mechanism in in anticancer activity. For instance, 4-O-methylhonokiol induces apoptosis in OSCC cells by altering Bax and Bcl-2 expression[93].

2.2.8 Antioxidant

Antioxidants are molecules that neutralize free radicals, stopping cell damage. The human body synthesizes certain antioxidants (e.g., glutathione, uric acid), while others, including the crucial dietary antioxidants vitamin E, vitamin C and beta-carotene, must be acquired through nutrition, even though the body has some mechanisms to combat free radicals.

2.2.8.1 Antioxidant defense system

Antioxidants eliminate harmful ROS overproduction in the body. These actions are achieved by scavenging free radicals, donating electrons or hydrogen atoms, breaking down peroxides, neutralizing singlet oxygen, inhibiting certain enzymes, acting synergistically, and chelating metal ions. Both enzymatic and non-enzymatic antioxidants work within and outside cells to neutralize excess ROS and protect against oxidative damage.

2.2.8.2 Mechanism of action of antioxidants

Antioxidants have two main mechanisms. The first is chain-breaking, where they donate an electron to free radicals and break the chain reaction of oxidative damage. The second involves their effect on biological systems, such as donating electrons, binding to metal ions, acting as co-antioxidants, or regulating gene expression[94].

2.2.8.3 Endogenous antioxidants

Harmful ROS are counteracted by the body's production of endogenous antioxidant enzymes such as superoxide dismutase [95], catalase (CAT), and glutathione peroxidase (GPX)[95]. The enzymatic detoxification of ROS involves several enzymes, such as glutathione reductase (GR), glutathione-S-transferase, and glucose-6-phosphate dehydrogenase. Endogenous antioxidants include water-soluble antioxidants (ascorbate, glutathione, and uric acid) and lipid-soluble antioxidants (tocopherols, ubiquinols, and carotenoids) and are divided into enzymatic and non-enzymatic types.

2.2.8.3.1 Enzymatic antioxidants

A core element of the antioxidant defense system consists of the key enzymes SOD, CAT, and GPX, are all present in saliva.

2.2.8.3.1.1 Superoxide dismutase (SOD)

SOD (EC 1.15.1.1) is an enzyme found in most aerobic cells and extracellular fluids, categorized into three families based on their metal cofactors: Cu/Zn, Fe, Mn and Ni types. SOD is responsible for scavenging free radicals produced during cellular metabolism, making it a vital antioxidant by converting them into H_2O_2, as illustrated by the equation[94]:

$$2O_2^{\bullet-} + H^+ \rightarrow H_2O_2 + O_2$$

After that, the CAT converts H_2O_2 into water and O_2, making it harmless. SOD is vital for free radical conversion into non-toxic substances. Studies have demonstrated a correlation between reduced SOD levels and the presence of both type 2 diabetes and oral pathology, indicating antioxidant depletion[96].

2.2.8.3.1.2 Catalase (CAT)

CAT (EC 1.11.1.6) is a very important enzyme found in all living things. It breaks down H_2O_2, which is a harmful waste product of cell metabolism, into less dangerous oxygen and water molecules, as in the following equation:

$$2H_2O_2 \longrightarrow 2H_2O + O_2$$

In addition, CAT can break down harmful substances, such as phenols, formaldehyde, formic acid, and ethanol, by reacting with H_2O_2 to produce non-

toxic substances and two water molecules. The following equation represents this process[94]:

$$H_2O_2 + H_2R \longrightarrow 2H_2O + R$$

CAT deficiency does not cause mortality, implying that other enzymes like peroxiredoxin may also break down H_2O_2. CAT further reduces H_2O_2 conversion to $HO^{\bullet}$ by detoxifying phenols and alcohols and inhibiting the Fenton reaction. Nogueira et al. observed decreased catalase levels in the salivary glands of xerostomia patients, specifically in the submandibular glands[97].

2.2.8.3.1.3 Glutathione peroxidase (GPx)

GPx (EC 1.11.1.9) is an antioxidant enzyme that converts H_2O_2 to H_2O using glutathione as a reducing agent, as shown in this equation:

$$2\text{glutathione} + H_2O_2 \longrightarrow \text{oxidized glutathione (GSSG)} + 2H_2O$$

The study demonstrated that GPx was able to neutralize the harmful effects of H_2O_2 and safeguard cells from lipid peroxidation by facilitating the transformation of organic peroxides (R-O-O-H) into alcohols (R-O-H). This process involves glutathione, as illustrated in the following equation:

$$2\text{glutathione} + \text{R-O-O-H} \longrightarrow \text{R-O-H} + \text{GSSG} + 2H_2O$$

Glutathione is a non-enzyme antioxidant composed of three amino acids linked by sulfur bonds. It exists primarily in its reduced form and functions as a co-enzyme for GPx to break down free radicals. GSH also controls lipid peroxidation reactions that damage cell membranes and reduces chain reactions of lipid peroxidation within cells.

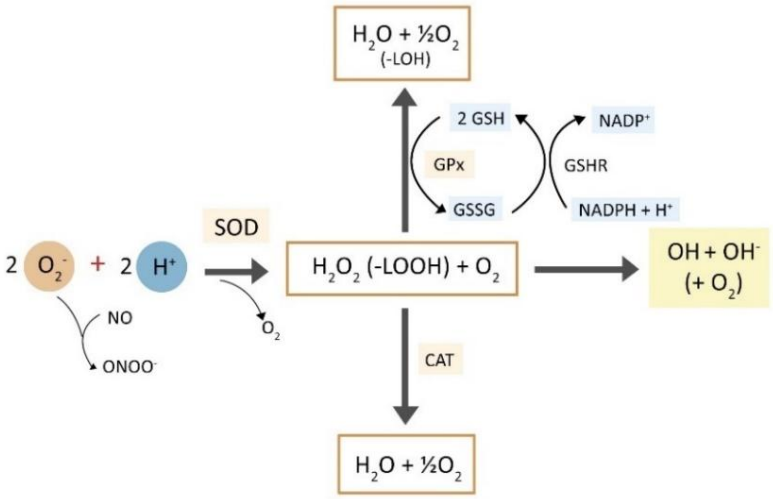

Figure 10 SOD, GPx, and CAT Enzymatic Defense Against Free Radicals [Modified from Pandey et al.,2010][98]

2.2.8.3.2 non-enzymatic antioxidants

Among the non-enzymatic antioxidants are compounds such as GSH, alpha-lipoic acid (ALA), uric acid, NADPH, coenzyme Q, albumin, ferritin, metallothionein, melatonin, bilirubin, and L-carnitine, function by scavenging ROS and RNS[99].

2.2.8.4 Exogenous antioxidants

Exogenous antioxidants are from sources outside the body, like supplements and diets. Natural sources include fruits, vegetables, herbs, spices, and vitamins. Phytochemicals, a type of exogenous antioxidant, are compounds such as flavones, flavonoids, isoflavones, catechins, coumarins, lignans, and gallic acid. These compounds are phenolic and polyphenolic. Exogenous antioxidants include dietary, synthetic, and protein hydrolysate antioxidants.

2.2.8.4.1 Dietary antioxidants

There are three main types of dietary antioxidants: polyphenols, carotenoids, and specific nutrients.

Polyphenols are plant antioxidants composed of flavonoids and non-flavonoid polyphenolic compounds. These compounds contain an aromatic benzene ring neutralizes free radicals by donating hydrogen or an electron without forming another one. Polyphenols can also bind with prooxidant transition metal ions like Fe^{2+} to generate free radicals. Besides, they can scavenge lipid alkoxyl, $LO^{\bullet}$ and $LOO^{\bullet}$ radicals that damage lipids. Examples of foods with polyphenols are leafy vegetables, potatoes, whole grain products, plums, and coffee[100].

Carotenoids, except water-soluble crocin, are pigments found in plants, fungi, and bacteria. They function as lipid-soluble antioxidants and are categorized into oxygen-containing and non-oxygen-containing carotenoids. They scavenge radicals and quench singlet oxygen triplet states. Oxygenated carotenoids encompass alpha- and beta-cryptoxanthin, lutein, and zeaxanthin, whereas non-oxygenated carotenoids consist of alpha, beta, and gamma-carotene, as well as lycopene. These compounds are found in brightly colored fruits and vegetables, algae, and some nutrients such as vitamins C and E.[101]

Vitamin C is a water-soluble antioxidant in the form of ascorbate anions in the human body. Ascorbate anions convert to monodehydroascorbate and dehydroascorbate, which are relatively stable radicals. Vitamin C is crucial for proline hydroxylation to hydroxyproline and preventing scurvy. It protects against oxidative damage in the cytosol and mitochondria by scavenging radicals such as H_2O_2, $OH^{\bullet}$ and $RO_2^{\bullet}$. Vitamin C also enhances vitamin E's antioxidant activity by converting alpha-tocopherol radical ($TO^{\bullet}$) to alpha-tocopherol (TOH). This indirectly limits lipid peroxidation in cell membranes. Foods such as citrus fruits and bell peppers are effective sources of vitamin C[102].

Vitamin E is an antioxidant that dissolves in fats and oils. Its structure has an aromatic ring, giving it phenolic antioxidant properties. Vitamin E is crucial as a

primary membrane-bound antioxidant that prevents lipid peroxidation. It does this by quenching $^1O_2$ or directly intercepting free radical intermediates such as $OH^{\bullet}$, $L^{\bullet}$, $LO^{\bullet}$, and $LOO^{\bullet}$ by donating hydrogen to stop the chain reaction of peroxidation[103].

Gamma-aminobutyric acid is a neurotransmitter in the brain that regulates mood, reduces muscle spasms, and treats conditions like high blood pressure and diabetes. It is naturally produced in the human body and can be obtained from foods, supplements, and medicines designed to boost GABA levels[104]. Some studies have demonstrated that GABA can turn on antioxidant enzymes, lower oxidative stress, and maintain redox homeostasis simultaneously[105]. GABA plays a protective role against salinity and heat stress in plants by influencing nitrogen metabolism, increasing polyphenol levels, and supporting the antioxidant system [106]. Also, GABA can enhance the antioxidant and free radical scavenging abilities in soybean sprouts exposed to NaCl stress. Studies have also shown that taurine and GABA can eliminate free radicals and protect tissues from oxidative damage[107].

2.3 *Elaeagnus latifolia* L.

Elaeagnus latifolia L. (*E. latifolia*) or bastard oleaster is an edible fruit tree that grows in many parts of the world, particularly in tropical or subtropical areas of North America, Asia, and Europe. This plant is in the family Elaeagnaceae and genus *Elaeagnus* L. In Thailand, this fruit is mainly found in the upper northern, northeastern, and southern regions. It is known by several local names such as Ma Lod, Salot Thao, Bek Lod, Ba Lod, and Ba Lod in the North, or Som Lod in the South[108].

2.3.1 Biological and morphological aspects of *E. latifolia*

E. latifolia fruit has three fruits per cluster. After ten weeks, the major axis diameter of this medium-sized, egg-shaped, fleshy drupe is 26.40 millimeters, and its length is 36.72 millimeters. The fruit consists of three layers: a soft, white, slightly spread outer layer (exocarp); a thick, juicy, light green to reddish-orange middle layer (mesocarp); and a relatively rigid inner layer (endocarp), divided into eight sections and

attached to a green seed. The fruit's endocarp turns from green to dark red as it ripens[109]

A report revealed the highest vitamin C concentration in the fruit was found around five weeks, while the highest acidity and tannin concentrations were present at 7 and 9 weeks, respectively. At 10 weeks, the fruit's total soluble solid content was 14 brix. The fruit's taste was 80% sour and 20% sweet. The sour variety had more sugar, polyphenols, and antioxidants than the sweet variety, but both contained high levels of vitamin A and E. The implications of these findings extend to both the improvement of agricultural techniques and the refined classification of this economically and nutritionally valuable plant species [110].

2.3.2 Taxonomical Classification[15]

Kingdom	Plantae
Phylum	Tracheophyta
Class	Magnoliopsida
Order	Rosales
Family	Elaeagnaceae
Genus	*Elaeagnus* L.
Species	Elaeagnus latifolia L.

2.3.3 Phytochemical Composition

Flower: *E. latifolia* flowers contain phytosterols, glycosides, and saponins. These compounds had medicinal properties, suggesting that this plant's flowers could be used in traditional medicine[15].

Seed and Bark: The seeds contain fatty acids abundant in palmitic acid and linoleic acid, as well as other bioactive compounds and essential fatty acids. In addition, palmitic acid was found in the bark[111].

Fruit: *E. latifolia* fruits contain carbohydrates, ascorbic acid, tannins, phenolics, flavonoids, and purpurin. In addition, carotenoids, terpenoids, organic acids, coumarins, alkaloids, steroids, lycopene, polyphenols, and GABA have also been

discovered in the fruit according to phytochemical and biological evaluation studies[14, 15, 108]. Niwaspragrit et al. found that early ripening of *E. latifolia* fruit results in high malic acid levels. Besides, the fruit has antioxidant properties, indicating its potential health benefits [112].

2.3.4 Malic acid

Malic acid is a natural food preservative and flavor enhancer in many fruits and vegetables that has a sour taste due to its two carboxylic groups. Plants use malic acid in the Calvin cycle to fix carbon and in the Krebs cycle to convert it to pyruvic acid, which promotes muscle growth. Malic acid also stimulates salivary secretion, gastric juice, and intestinal peristalsis. In low dosages, it is prebiotic, but in high dosages, it inhibits growth and act as a bactericide. Topical application of a 1% malic acid solution has demonstrated efficacy in alleviating xerostomia associated with antihypertensive medication and chronic graft-versus-host disease (GVHD). Two groups of 45 patients were established for this study; one group received a malic acid spray, while the other received a placebo as a control. The spray improved antihypertensive-induced xerostomia and stimulated saliva production[113]. Another study found the same spray effective in treating GVHD-induced xerostomia. Additionally, the spray has been effective when combined with xylitol and fluoride, increasing the unstimulated salivary flow rate and improving dry mouth questionnaire scores[114].

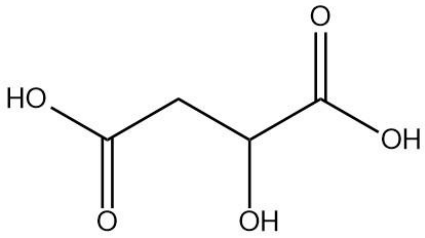

Figure 11 Malic acid structure [Modified from Rachmaniah et al.,2019][115]

2.3.5 Pharmacological activity

2.3.5.1 Antioxidant activity

Flower and Leaf: A comparative analysis of total phenolic and flavonoid content was conducted on methanol extracts derived from the flowers and leaves of *E. latifolia*. A marked difference in total phenolic and flavonoid content was observed, with leaf extracts exhibiting significantly higher levels than flower extracts. (61.15 ± 1.23 and 15 ± 0.125 µg/ml, respectively). However, the methanol extract from *E. latifolia* flower inhibited DPPH radical at an IC_{50} equal to 144.64 ± 0.25 µg/mL. In contrast, the methanol extract from *E. latifolia* leaves could inhibit H_2O_2 at IC_{50} equal to 444.59 ± 3.77 µg/ml[116].

Fruit: The 70% methanol extract from *E. latifolia* fruits was analyzed using HPLC, revealing the presence of purpurin, tannic acid, quercetin, catechin, reserpine, rutin, carbohydrates, ascorbic acid, tannins, phenolics, and flavonoids. Furthermore, the methanol extract from the fruits exerted the inhibition of DPPH radical, superoxide radical, hydroxyl radical, and Fe^{2+} chelation, with IC_{50} equal to 134.31 ± 8.39, 150.78 ± 4.20, 238.09 ± 11.63, and 993.68 ± 50.74 µg/mL, respectively [14]. Moreover, the 50% methanol extract from *E. latifolia* fruits had total phenolic contents equal to 24.2±1.9 mg GAE/g which had antioxidant capability (total antioxidant activity) equal to 32.1±1.7%, and inhibited the DPPH radical at an IC_{50} equal to 0.06 mg/mL[117].

The researchers studied *E. latifolia* fruit in Chiang Mai Province, Thailand, at various stages, such as early ripe, moderately ripe, and lately ripe. They found that the amount of citric acid and malic acid in the *E. latifolia* fruit was decreased when the fruit was ripe, while the amount of tartaric acid was increased when the *E. latifolia* was at a more mature stage. In addition, the total phenolic contents were 51.40, 40.23, and 39.92 mg GAE/g extract, respectively. The total antioxidant activity was 54.88, 37.45, and 37.37 g/mL, respectively[118].

In agreement with a study conducted in northeastern India, they analyzed the composition of *E. latifolia* fruits and found that it contained high levels of potassium, with the extract containing 610.13 mg/100g, as well as several vitamins and minerals such as phosphorate, sodium, calcium, magnesium, iron, zinc, vitamin C, lycopene, and beta-carotene. In addition, HPLC analysis revealed organic acids,

including tartaric, pyruvic, and oxalic acids. In addition, it revealed polyphenols, polyphenols, such as gallic, p-coumaric, ferulic acids, and catechins. Furthermore, the juice extract from *E. latifolia* fruits exhibited inhibition of the DPPH radical at IC_{50} = 2394.06 µg/mL and had an ABTS elimination effect at 58.41 µg/mL[119].

In Thailand's provinces of Loei and Nong Khai, a study was conducted to examine extracts from *E. latifolia* fruits. The fruit's organic acid profile included tartaric, malic, and citric acids; however, malic acid was found to be especially prevalent in the early ripening phase (357.4±79.5 mg/g of extract). During the fruit ripening stage, the glucose content was 154.6 mg/g of extract, the fructose content was 234.3 mg/g of extract, and the sucrose content was 180.2 mg/g of extract, all of which were higher than before the fruit ripening stage. The fruit extracts also had a total polyphenol content of 647.26 mg/mL and an inhibitory effect on the DPPH radical, with IC_{50}= 15.82 mg/mL in the pre-ripening stage compared to the fruit maturation stage[112].

A previous study analyzed *E. latifolia* fruit pulp water extract using HPLC. It found that the red, yellow, and dark red fruits contained GABA contents of 0.1301±0.0054, 0.1640±0.0032, and 0.0913±0.0080 mg/g of extract, respectively. Additionally, fruit extracts inhibit tyrosinase enzymes and exhibit antioxidant activity[108].

2.3.5.2 Anti-inflammatory effect

Leaf: The methanol extract from *E. latifolia* leaf inhibits cyclooxygenase-2 (COX-2) and lipoxygenase-15 (LOX-15) associated with the inflammatory process[120].

Fruit: When injecting crude extract from dried *E. latifolia* fruits at different doses (10, 20, 30, 40, and 50 mg/kg) into the stomachs of mice for 30 minutes before injecting formalin into the right hind paw of the mice to induce inflammation, the results showed that extracts with doses higher than 30 mg/kg were effective in reducing pain, compared to the positive control drugs dexamethasone and indomethacin. The extract's anti-inflammatory mechanism was attributed to its ability to inhibit COX-1 and COX-2[121]. Khodakarm-Tafti et al. found that when raw extract powder containing 300 and 600 mg/kg of the dried *E. latifolia* fruit was administered to mice with ulcerative colitis by

inducing inflammation in the colon with 3% acetic acid through the rectum, it was found that the extract was able to restore and maintain the mucosal tissue of the colon, reduce erosion and ulceration of the colon, and also reduce the infiltration of inflammatory cells when studied using histopathology methods[122].

In addition, another study found that when the water extract of *E. latifolia* fruit at a concentration of 500 mg/mL was applied to the wounds of mice, it was able to increase the wound healing rate on days 5, 10, and 15 faster than the application of 2% mupirocin ointment used as a positive control and quicker than the group that only applied ointment. The mechanism underlying this effect may involve the extract's antioxidant properties and its capacity to modulate TGF-β1 and TNF-α expression[123].

2.3.5.3 Brain protection

Leaf: There is no study specifically on *E. latifolia*'s protective effects against H_2O_2-induced oxidative damage. However, other close Elaeagnus species were studied, such as *E. umbellata* (Thunb.) had shown protective effects against oxidative stress and could reduce the death of apoptotic neurons and the level of free radicals in induced Schwann neurons with H_2O_2 compared to untreated neurons. Moreover, the water extract of *Elaegnus* could increase the expression of specific proteins such as Bcl-2, PI3K, and p-Akt, while decreasing the expression of the Bax protein, indicating that the leaf extract can protect neurons[124].

2.3.5.4 DNA protection

Fruit: The study assessed the phytochemicals, antioxidants, and DNA protective potential of the *E. latifolia* fruits. The 70% methanol extract from the fruits exhibited free radical scavenging activity and protected pUC18 DNA with P_{50} = 695.91 ± 15.84 µg/ml; P_{50} signifies the concentration for 50% protection. In addition, the fruit is also reported to be a rich source of vitamins, minerals, essential fatty acids, and other bioactive compounds[14].

2.3.5.5 Antibacterial effect

Leaf: The study investigated the antibacterial activity of methanol extract from various plant species, including *E. latifolia*, which was examined against pathogenic bacteria. The findings indicated that methanol extract from *E. latifolia* leaves exhibited significant antibacterial activity against pathogenic *Salmonella typhi*, *Shigella flexneri*, and *Bacillus subtilis*[125].

Fruit: The methanol extract from *E. latifolia* fruits and leaves exhibited antibacterial properties compared to the antibiotic ofloxacin[116].

2.3.5.6 Clinical study

Fruit: Taheri et al. determined the efficacy of a wound gel containing 19% *E. latifolia* fruit extract in treating oral lichen planus. This causes discomfort and burning mouth pain. The results indicated a 75% reduction in pain and a 50% reduction in wound size[126]. Another study investigated the potential of *E. latifolia* extract as a remedy for gag reflex in dental patients. The participants were given candy containing fruit extract before and after the dental procedure. These findings demonstrated that consuming candy with *E. latifolia* extract significantly reduced regurgitation reactions, particularly in the soft palate and pharyngeal tonsils. These results suggested that *E. latifolia* extract might hold promise as an effective therapeutic intervention for gag reflexes in dental patients[127].

2.3.6 Toxicological effects

There is limited information available on the toxicological effects of *E. latifolia*

Leaf: The investigation of the 70% methanol extract from *E. latifolia* leaves demonstrated a cytotoxic effect on Vero cell lines in rats, with an IC_{50} of 248.5 ± 3.12 µg/mL [120].

Seed: The methanol extract from *E. latifolia* seeds was administered to rats at a dose of 2000 mg/kg and determined to be non-toxic compared to the control group of mice, suggesting that the extract was safe for application[128].

Fruit: The study of *E. angustifolia* fruit extract had no favorable effects on chondrificat

CHAPTER 3
MATERIALS AND METHOD

3.1 Chemicals

Sodium carbonate (Na_2CO_3) and ethylenediaminetetraacetic acid (EDTA) were purchased from HiMedia Laboratories (St. Louis, Missouri, U.S.A.). Hydrochloric Acid (HCl) was purchased from J.K. Baker (Shanghai, China). Sodium chloride (NaCl) was purchased from Calbiochem (Darmstadt, Germany). Potassium Chloride (KCl) was purchased from Univar (Illinois, U.S.A.). Sodium phosphate ($NaHPO_4$), dipotassium phosphate (K_2HPO_4), sodium carbonate (Na_2CO_3), ethanol (C_2H_5OH), methanol (CH_3OH), potassium phosphate (K_2HPO_4), potassium dihydrogen phosphate (KH_2PO_4), Dimethyl sulfoxide, Folin-Ciocalteu's reagent, quercetin ($C_{15}H_{10}O_7$), aluminium chloride ($AlCl_3$), potassium acetate (CH_3COOK), ethylene-diaminetetraacetic acid disodium salt dihydrate ($C_{10}H_{14}N_2Na_2O_8 \cdot 2H_2O$), and ferrous sulfate heptahydrate were purchased from Sigma Chemical Company (St. Louis, Missouri, U.S.A.). Methanol (MeOH) was purchased from RCI Labscan (Bangkok, Thailand). Gallic acid monohydrate ($C_7H_6O_5 \cdot H_2O$) was purchased from Riedel-de Haën (Seelze, Germany). 2,2-Diphenyl-1-picryl hydrazyl ($C_{18}H_{12}N_5O_6$) and (±)-6-Hydroxy-2,5,7,8-tetra-methylchromance-2-carboxylic acid were purchased from Fluka (Seelze, Germany). Sodium nitroprusside was purchased from HiMedia Laboratories (St. Louis, Missouri, U.S.A.). N-(1-Naphthyl) ethylenediamine dihydrochloride ($C_{10}H_7NHCH_2CH_2NH_2 \cdot 2HCl$) was purchased from AppliChem GmbH (Darmstadt, Germany). Sulfanilamide ($C_6H_8N_2O_2S$) was purchased from Kemaus (Cherrybrook, Australia). Phosphoric acid (H_3PO_4) was purchased from Carlo Erba Reagents (Chaussée du Vexin, France). 2',7'-Dichlorodihydrofluorescein diacetate was purchased from Invitrogen™ Molecular Probes™ (Eugene, Oregon, U.S.A.).

3.2 Apparatus

Water purification system (Milli-Q, ROs): Millipore

Freeze dryer: Alpha 1-2 LD, Sigma, Germany

Spectrophotometer: Bio-Tek Instruments, Winooski, VT, USA

Vortex mixer: Genie 2

Laminar hood air flow: Telstar

CO_2 water-jacketed incubator: NuAire

Water bath: Heto

Inverted microscope: Olympus DP20

Cell B imaging software for Life science microscopy: Olympus

Nanodrop: Thermo Fisher, USA

High-Performance Liquid Chromatography: Waters®2695 Separations Module, USA

Confocal laser scanning microscope: Zeiss LSM 900, Zeiss, Oberkochen, Germany

StepOnePlus: Applied Biosystems, Waltham, MA, USA

Nanodrop: Thermo scientific

Gel documentation

3.3 Plant extraction and preparation

Pre-ripening (orange-stage) fruits of *E. latifolia* were harvested in March 2022 from the Lamtakhong Research Station, which is located in the Pak Chong District of Nakhon Ratchasima Province in Thailand. To ensure consistency in the experimental material, only fruits measuring approximately 3–4 cm was selected. The extraction protocol was adapted from Niwaspragrit et al.,2020[112], with modifications aimed at optimizing compounds.

Initially, the fruits were thoroughly washed to remove surface impurities. The cleaned fruits were homogenized into a uniform paste and combined with sterile distilled water at a ratio of 1:5 (100 g of fruit to 500 mL of water). This mixture was gently heated

at 50°C for 5 minutes to facilitate the extraction of phenolic and other water-soluble compounds. Rapid cooling in an ice-water bath, immediately following filtration (Whatman No. 1 filter paper), ensured the stability of heat-sensitive components within the heated mixture.

The filtrate was frozen and subsequently lyophilized under vacuum conditions at a temperature of -52°C. A concentrated powdered extract was produced and maintained at -20°C until required for further experimentation. For subsequent analyses, the lyophilized powder was reconstituted in sterile distilled water and centrifuged to remove insoluble materials. To prevent degradation of light-sensitive compounds, the supernatant was collected and stored at -20°C in the absence of light. The experimental work was carried out in the Department of Pharmacology and the Central Laboratory of the Faculty of Medicine, Srinakharinwirot University, in collaboration with the Faculty of Science, Mahidol University, Thailand.

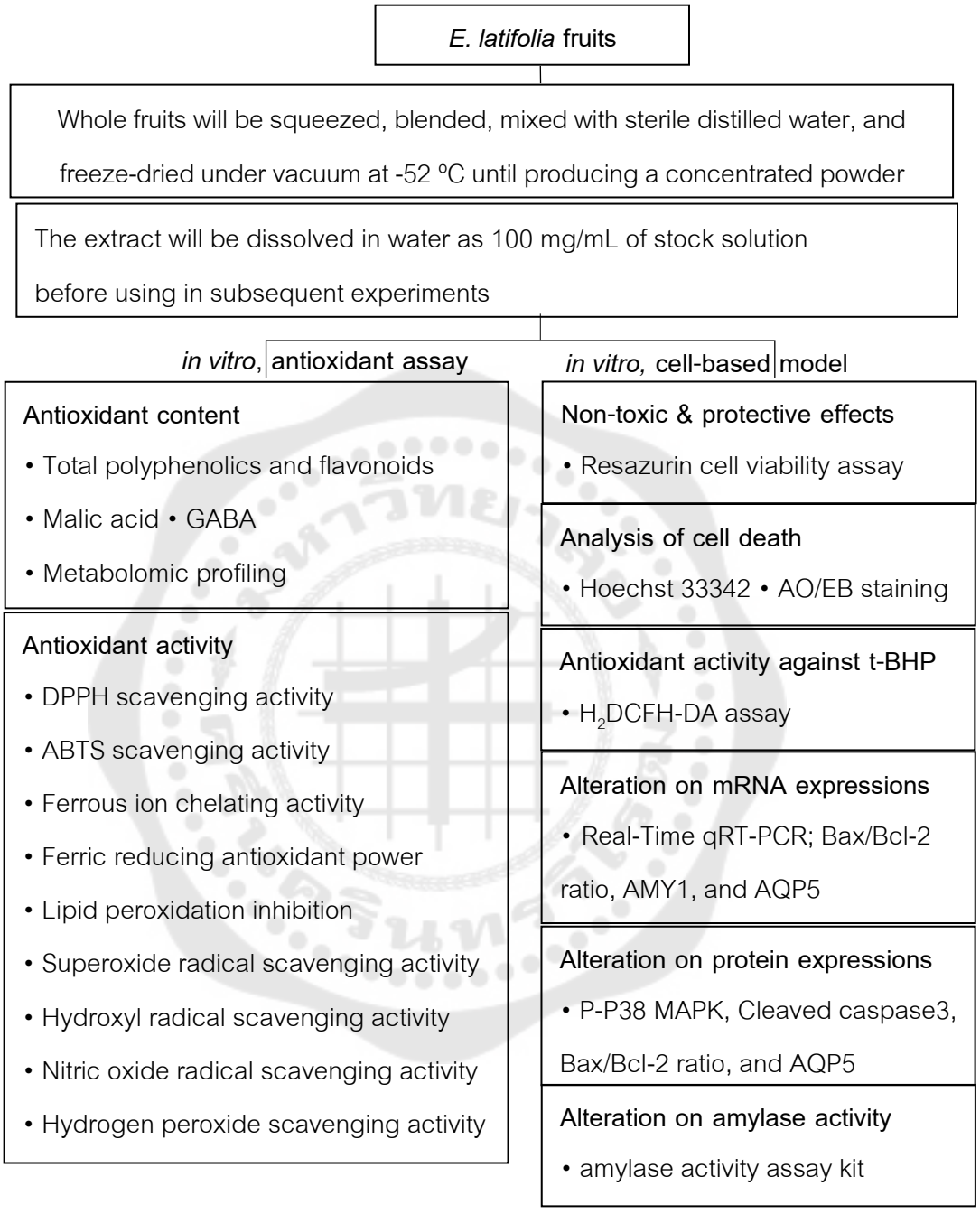

Figure 12 Research framework

3.4 Determination of antioxidant contents in heated water extract of *E. latifolia* fruits

3.4.1 Determination of the total phenolic content

Total phenolic content of the *E. latifolia* fruit extract was determined using the Folin-Ciocalteu method, which quantifies phenolic compounds based on their ability to reduce a phosphomolybdate-phosphowolframate complex in an alkaline medium, as described by Kupina et al.,2018[129]. Gallic acid standards (0.1-0.5 µg/mL) were used to create a calibration curve, and the extract was analyzed at a concentration of 20 µg/mL.

Briefly, 30 µL of either the gallic acid standard or the extract was mixed with 770 µL of distilled water. This mixture was then combined with 50 µL of Folin-Ciocalteu reagent to initiate the colorimetric reaction. After 1 minute, 150 µL of saturated sodium carbonate (Na_2CO_3) solution was incorporated. A 25 g of Na_2CO_3 was dissolved in 100 mL of deionized water was then allowed to equilibrate for 24 hours, and filtered using Whatman No. 1 filter paper, and volume adjustment to 125 mL.

Ambient temperature incubation in the dark for a period of 50 min to allow maximum color development. Total phenolic content was determined using a gallic acid standard curve and expressed as milligrams of gallic acid equivalents per gram of extract (mg GAE/g extract); absorbance measurements were taken at 750 nm with a UV-Vis spectrophotometer (Bio-Tek Instruments, Winooski, VT, USA). Each sample was analyzed in triplicate to ensure reliability and reproducibility.

3.4.2 Determination of the total flavonoid content

Quantification of flavonoids in the extract was achieved through a colorimetric method that leverages the formation of complexes between flavonoids and aluminum chloride, as described by Shraim et al., 2021[130]. This technique exploits the interaction between aluminum chloride ($AlCl_3$) and flavonoids, which generates acid-resistant complexes at the C-4 keto and C-3/C-5 hydroxyl functionalities, as well as acid-labile complexes with ortho-dihydroxyl groups in the A or B-ring of flavonoids.

For the assay, 100 µL of quercetin standard solutions (0.02 to 0.1 mg/mL), a blank, or the extract (50 mg/mL) was mixed with 550 µL of distilled water. The mixture was supplemented with 30 µL of 1M potassium acetate (CH_3COOK) and 20 µL of 10%

$AlCl_3$. After the addition of 300 µL of 95% ethanol, the samples underwent incubation at ambient temperature for 30 min in the absence of light. Measurements of absorbance at 415 nm were performed using a (Bio-Tek Instruments, Winooski, VT, USA). Based on the quercetin calibration curve, the total flavonoid content was determined and reported as milligrams of quercetin equivalents per gram of extract (mg QE/g extract).

3.4.3 Determination of malic acid content

Malic acid, a dicarboxylic organic compound contributing to the fruits' sour taste, was quantified in the water extract using high-performance liquid chromatography (HPLC), using a modified version of the method described by Shui et al.,2002 [131]. A Grace Davison Discovery Sciences™ Prevail Organic Acid column (4.6 × 250 mm, 5 µm particle size) within a Waters® 2695 HPLC system (USA) was used to analyze a 20 µL sample of the extract, which had been previously filtered (0.45 µm nylon syringe filter) and transferred to a 1.5 mL vial. A flow rate of 0.6 mL/min of a 25 mM potassium dihydrogen phosphate buffer (pH 2.5) was used as the mobile phase for isocratic elution. The detection was carried out using a UV/VIS Detector 2489 at 210 nm. Chromatographic data were acquired and processed using Empower® Chromatography Data Software. A standard curve enabled the calculation of malic acid content, which was reported as milligrams of malic acid per gram of extract (mg/g). Sample analysis was conducted in triplicate to ensure accuracy and reproducibility.

3.4.4 Determination of GABA content

The GABA content in the *E. latifolia* extract as determined using an adapted HPLC method with *o*-phthaldialdehyde derivatization (Meeploy et al.,2019) [108]. The experimental procedure involved preparing a solution of OPA and 2-mercaptoethanol in 0.4 M borate buffer (pH 10), which was then filtered through a 0.45 µm nylon membrane. Chromatographic separation utilized a C18 column (150 mm × 4.6 mm, 5 µm particle size), with gradient elution employing acetonitrile and 5 mM citrate buffer as the mobile phase: 0–20 minutes with ACN: citrate buffer at a ratio of 15:85, then adjusted to

16.5:83.5, 30:70, and back to 15:85, respectively, at 15–35, 35–40, and 40–50 minutes, respectively. Detection was achieved through a fluorescence detector, and data were analyzed with Empower® Chromatography Data Software. The extract's GABA content was evaluated by referencing a calibration standard, with the final results presented as micrograms of GABA per milligram of extract.

3.4.5 Characterization of bioactive compounds using metabolomic techniques

To comprehensively characterize the bioactive compounds, present in the water extract of *E. latifolia* fruit, metabolomic analysis was conducted in collaboration with the National Omics Center, National Science and Technology Development Agency (NSTDA), Thailand. The lyophilized extract underwent examination via an advanced analytical method combining liquid chromatography and quadrupole time-of-flight tandem mass spectrometry (LC-Q-TOF-MS/MS) for metabolite profiling. Data obtained were analyzed to identify compounds associated with the extract's antioxidant and cytoprotective effects

3.5 Determination of the heated water extract of *E. latifolia* fruits for antioxidant activity

3.5.1 DPPH scavenging activity

The extract's capacity to neutralize free radicals was assessed through the application of the DPPH assay, as outlined by Chedea et al.,2019[132], with ascorbic acid serving as a standard. The quantification of antioxidant properties often relies on DPPH, which free radical stability stems from its unique electron configuration. This arrangement, featuring a delocalized unpaired electron, precludes dimerization. The characteristic gives DPPH its deep purple color, with a distinct absorption peak around 515 nm in ethanol solution. Upon reduction or electron acceptance, the DPPH solution transitions to pale yellow, as illustrated in Figure 13.

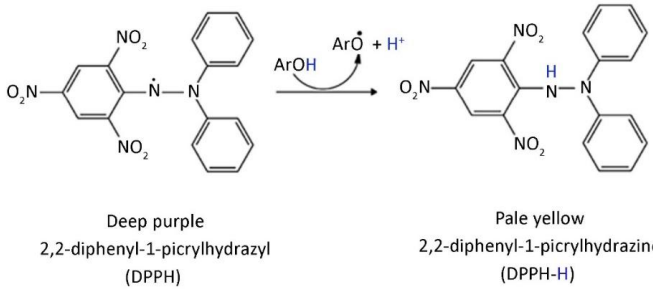

Figure 13 DPPH reaction mechanism [Modified from Bibi Sadeer et al.,2020][133]

The analytical procedure entailed the addition of 20 µL of sample (either standard ascorbic acid, blank, or extract) to 180 µL of newly prepared DPPH solution within a 96-well microplate. After a 15-minute dark incubation at ambient conditions, spectrophotometric analysis was performed at 515 nm using a UV-Vis spectrophotometer (Bio-Tek Instruments, Winooski, VT, USA). The DPPH scavenging activity was calculated using the equation:

$$\%\text{DPPH radical scavenging activity} = [(A_{control} - A_{sample})/ A_{control}] \times 100$$

Where: $A_{control}$ is the absorbance of the control (blank without extract),

A_{sample} is the absorbance of the standard or extract sample.

The mean inhibitory concentration (IC_{50}) value was determined by plotting the concentration of the standard or extract sample against the percentage of DPPH scavenging activity. Each experiment was performed in triplicate for each tested concentration to ensure reliability and reproducibility of the results.

3.5.2 ABTS radical scavenging activity

The antioxidant potential of the extract was evaluated using the ABTS assay. This technique, based on the protocol described by Won et al.,2021[134], quantifies the electron-donating ability of antioxidant compounds to $ABTS^{\bullet+}$, reducing its reactivity and preventing oxidative damage. $ABTS^{\bullet+}$ is generated by oxidizing ABTS with a potent oxidizing agent, resulting in a blue-green chromophore that quickly reacts with electron-donating compounds such as antioxidants. The ABTS radical scavenging capacity was measured spectrophotometrically at 734 nm. A decrease in absorbance indicates the scavenging capacity of antioxidants, as shown in Figure 14.

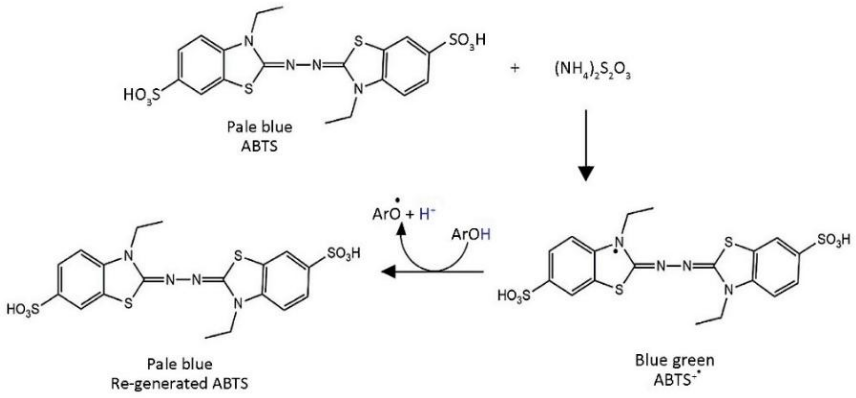

Figure 14 ABTS reaction mechanism [Modified from Bibi Sadeer et al.,2020][133]

Preparation of the $ABTS^{\bullet+}$ radical involved combining a 7 mM ABTS solution with 2.45 mM potassium persulfate at a 2:1 ratio. The resulting mixture was left to incubate in dark conditions at ambient temperature for 12-16 hours. Subsequently, ethanol was used to dilute the solution to attain an absorbance of 0.8 ± 0.02 when measured at 734 nm. To perform the assay, 20 µL of the test sample (extract or Trolox standard) was added to 180 µL of the ABTS solution. The mixture was allowed to incubate for 6 min at room temperature, followed by absorbance determination at 734 nm. The ABTS scavenging ability was subsequently calculated using the equation;

$$\%\text{ABTS radical scavenging activity} = [(A_{control} - A_{sample})/ A_{control}] \times 100$$

Where: $A_{control}$ is the absorbance of the control,

A_{sample} is the absorbance of the standard or extract sample.

The IC_{50} value is determined by plotting the concentration of the standard and extract sample against the percentage of ABTS radical scavenging capacity. All measurements were performed in triplicate.

3.5.3 Ferrous ion (Fe^{2+}) chelating activity

The Fe^{2+} chelation activity assay measures the ability of a substance to bind with Fe^{2+} ions and prevent free radical generation, using the method described by Adjimani et al.,2015[135]. Fe^{2+} ions serve as major catalysts for producing various free radicals, including superoxide radicals. The assay involves adding the test substance to a solution containing Fe^{2+} ions and ferrozine, which reacts to form a stable ferrozine-Fe^{2+} complex. The tested sample competes with ferrozine for Fe^{2+} ions, leading to a decrease in the formation of the ferrozine-Fe^{2+} complex, as shown in the following equation:

$$3\text{ferrozine} + Fe(H_2)_6^{2+} \longrightarrow Fe(\text{ferrozine})_3^{4-} + 6H_2$$

The reduction in absorbance was monitored at a wavelength of 562 nm. A significant reduction in absorbance indicates a stronger Fe^{2+} chelation activity of the tested substance, as illustrated in Figure 15

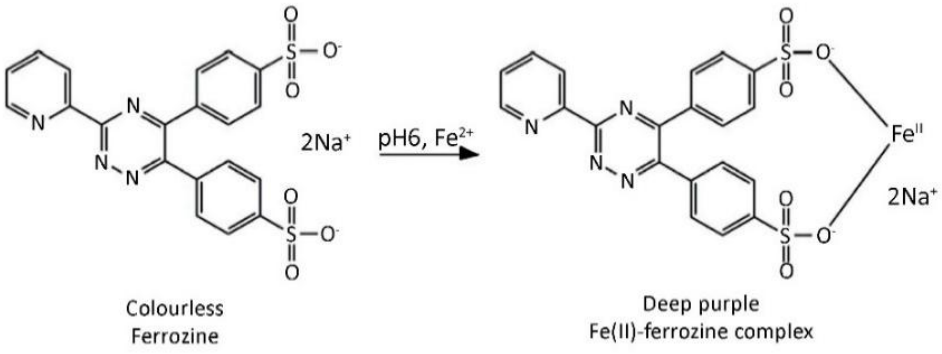

Figure 15 Metal chelating reaction mechanism [Modified from Bibi Sadeer et al.,2020][133]

This study assessed different concentrations of the extract and the standard iron chelator EDTA. The assay procedure entailed mixing 55 µL of the test substance with 814 µL of deionized water and 22 µL of 2 mM ferrous sulfate ($FeSO_4$). Following the addition of 44 µL of 5 mM ferrozine, the mixture was incubated for 10 minutes in darkness

at room temperature. Absorbance was then measured at 562 nm using a UV-Vis spectrophotometer. The Fe^{2+} chelating activity was calculated using the equation:

$$\%Fe^{2+} \text{ chelating activity} = [(A_{control} - A_{sample})/ A_{control}] \times 100$$

Where: $A_{control}$ is absorbance of control,

A_{sample} is absorbance of the standard or extract sample.

The IC_{50} value was determined by plotting the concentration of the standard and extract concentration against the percentage of Fe^{2+} chelating activity. Experiments were conducted in triplicate.

3.5.4 Ferric reducing antioxidant power (FRAP)

Determination of the extract's antioxidant capacity was carried out using the FRAP assay, which measures the sample's efficacy in reducing ferric (Fe^{3+}) to ferrous ions (Fe^{2+}). Ferric ions can induce oxidative damage to biological molecules, making their reduction a significant indicator of antioxidant activity, as described by Benzie et al.,2014[136], as shown in Figure 16.

To prepare the FRAP working solution, $FeCl_3 \times 6H_2O$, acetate buffer, and 2,4,6-tripyridyl-s-triazine (TPTZ) were blended in a 10:1:1 ratio and warmed to 37°C. Different extract concentrations were then added to the FRAP solution and incubated at 37°C for 30 minutes in the absence of light. Spectrophotometric analysis at 593 nm was conducted to quantify the reduction of Fe^{3+} to Fe^{2+}, resulting in the formation of a ferrous-tripyridyltriazine complex. Antioxidant capacity was calculated using a standard curve of ascorbic acid. Results of the reducing power assays are expressed as Trolox equivalents (mgTE/g extract). All samples were analyzed in triplicate.

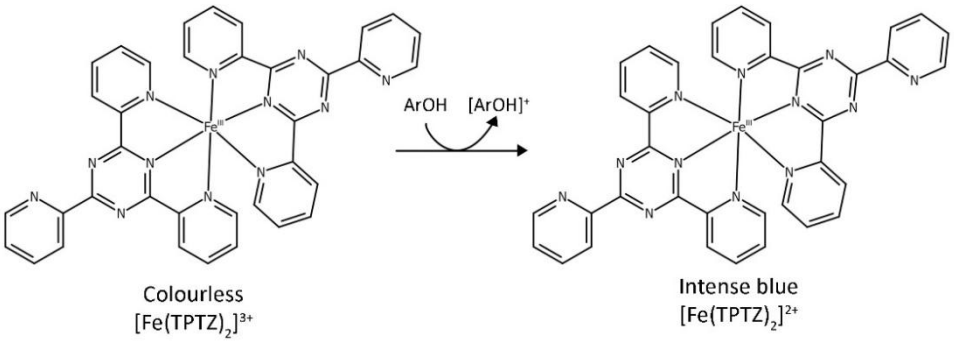

Figure 16 FRAP reaction mechanism [Modified from Bibi Sadeer et al.,2020][133]

3.5.5 Lipid peroxidation inhibition

The inhibition of lipid peroxidation was evaluated using low-density lipoproteins (LDL) oxidation induced by copper sulfate ($CuSO_4$), as modified from Osorio et al.,2013[137]. Cu^{2+} ions oxidize the unsaturated fatty acids present in LDL, resulting in the formation of lipid peroxides. These lipid peroxides react with thiobarbituric acid (TBA) to create malondialdehyde-TBA_2 adducts, commonly known as thiobarbituric acid-reactive substances (TBARS). The TBARS assay is a reliable method for detecting and quantifying lipid peroxidation in biological systems, including LDL. The extent of lipid peroxidation is indicated by the absorbance of the red-pink color developed, measured at 532 nm using a microplate reader, as shown in **Figure 17**.

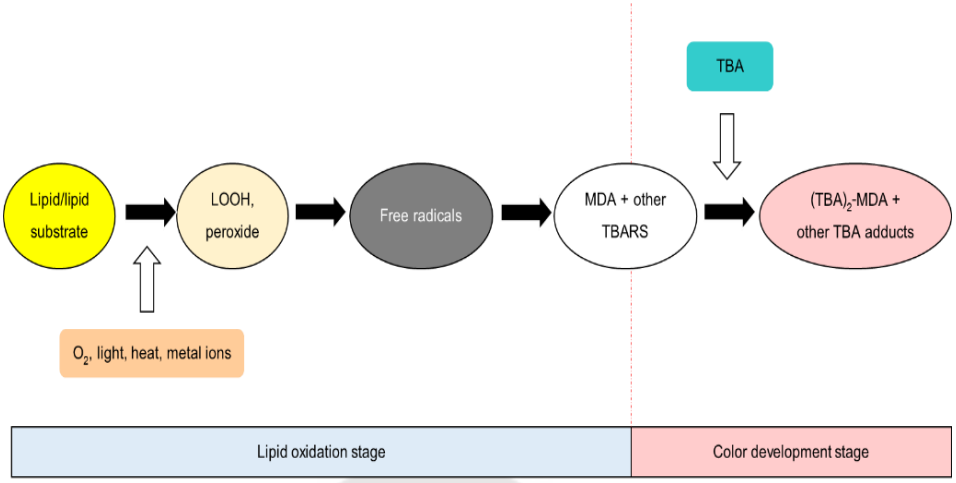

Figure 17 Lipid peroxidation mechanism [Modified from Bibi Sadeer et al.,2020][133]

A 50 µL aliquot of LDL (300 µg/mL protein concentration) was mixed with 10 µL of Trolox or varying concentrations of the extract. Lipid peroxidation was initiated by adding 5 µL of 55 µM $CuSO_4$ which was then incubated at 37°C for 6 h. The reaction was stopped by the addition of 25 µL of 1% EDTA. After cooling, 880 µL of a trichloroacetic acid (TCA) and TBA stock solution (20% w/v TCA; TBA at a 1:1 ratio) was combined with the sample. The mixture was heated to 95°C for 30 min and allowed to cool at room temperature. Absorbance was recorded at 532 nm, and lipid peroxidation inhibition was calculated using the equation:

$$\text{\% lipid peroxidation inhibition} = [(A_{control} - A_{sample})/ A_{control}] \times 100$$

Where: $A_{control}$ is absorbance of control,

A_{sample} is absorbance of the standard or extract sample.

The IC_{50} value was determined by plotting the concentrations against the percentage inhibition. All tests were performed in triplicate.

3.5.6 Superoxide radical ($O_2^{\bullet-}$) scavenging activity

The superoxide radical scavenging activity was evaluated using the xanthine oxidase (XO) method, which can lead to significant cellular and tissue damage, as reported by Azmi et al.,2012[138]. Inhibiting XO activity is an effective strategy to reduce $O_2^{\bullet-}$ production. This assay measures the extract's ability to prevent lipid oxidation by

superoxide radicals. In this assay, the extract is added to a solution containing xanthine, and XO generates $O_2^{\bullet-}$, which is measured spectrophotometrically at 295 nm, as illustrated in Figure 18.

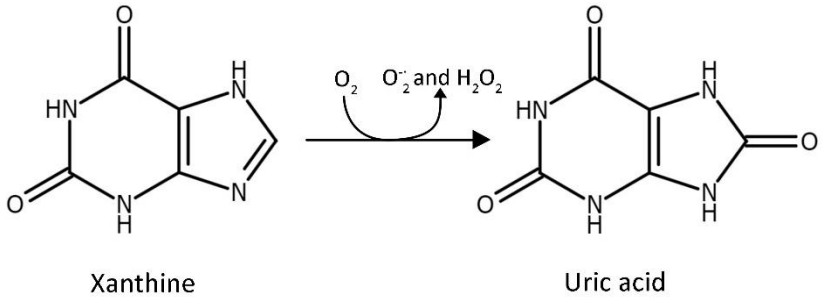

Figure 18 Conversion of xanthine to uric acid by xanthine oxidase [Modified from Özyürek et al.,2009][(139)]

The composition of the reaction mixture included 300 µL of 50 mM sodium phosphate buffer (pH 7.5), 100 µL of either the sample solution or Trolox as a positive control, and 100 µL of a freshly prepared solution of xanthine oxidase at a concentration of 0.2 units/mL in phosphate buffer, and 100 µL of deionized water. After a 15-min incubation at 37 °C, 200 µL of 0.15 mM xanthine was incorporated, and the sample was incubated for another 30 min. The reaction was halted by adding 200 µL of 0.5 M HCl, and the absorbance was assessed at 295 nm using a UV-VIS spectrophotometer (Bio-Tek Instruments, Winooski, VT, USA). Superoxide scavenging capacity was determined using the formula:

$$\textbf{\% superoxide radical scavenging activity} = [(A_{control} - A_{sample})/ A_{control}] \times 100$$

Where: $A_{control}$ is absorbance of control,

A_{sample} is absorbance of the standard or extract sample.

The IC_{50} value was obtained by plotting concentration versus scavenging activity. Each assay was conducted in triplicate.

3.5.7 Hydroxyl radical ($OH^{\bullet}$) scavenging activity

The ability of hydroxyl radicals ($OH^{\bullet}$) to be scavenged was measured through the deoxyribose method, as reported by Li 2013[140]. This assay quantifies the

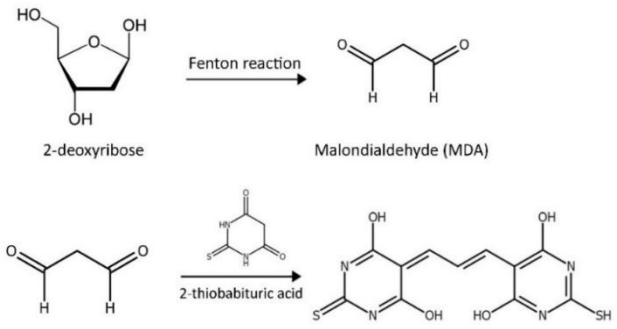

extract's ability to inhibit deoxyribose degradation caused by $OH^{\bullet}$ radicals, which are generated through the Fenton reaction involving Fe^{2+} and H_2O_2. The reaction leads to $OH^{\bullet}$ attack on deoxyribose, resulting in its degradation. The extent of degradation was measured by the formation of TBARS at 523 nm, as illustrated in Figure 19.

Figure 19 Reaction scheme from 2-deoxyribose to the pink chromogen $(TBA)_2$-MDA [Modified from Brizzolari et al.,2017][141]

The Fenton reaction was utilized to generate $OH^{\bullet}$ by combining 10 mM 2-deoxyribose, 0.41 mL of phosphate buffer (pH 7.4), 0.01 mL of ferric chloride (10 mM), 0.1 mL of H_2O_2 (10 mM), and 0.1 mL of EDTA (1 mM), Following this, 0.25 mL of the sample solution and 0.1 mL of ascorbic acid (1 mM) were mixed to the reaction. The mixture was incubated for 12 h at 37°C. In the blank control, 0.25 mL of the sample solution was added with 1 mL of the reaction mixture that excluded ferric chloride. Following incubation, 0.75 mL of TCA (2.8% w/v) and 0.75 mL of TBA (1% w/v in 50 mM NaOH) were introduced, followed by heating the mixture at 100 °C for 1 h. Absorbance reading were taken at 523 nm using a UV-VIS spectrophotometer, with Trolox acting as the positive control. The formula used to calculate hydroxyl radical scavenging activity is as follows:

$$\% \text{ Hydroxyl radical scavenging activity} = [(A_{control} - A_{sample})/ A_{control}] \times 100$$

Where: $A_{control}$ is absorbance of control,

A_{sample} is absorbance of the standard or extract sample.

The IC_{50} value was determined by plotting concentration against scavenging activity. Each test was performed in triplicate.

3.5.8 Nitric oxide radical ($NO^{\bullet}$) scavenging activity

The scavenging activity of the extract against nitric oxide ($NO^{\bullet}$) was evaluated using the technique established by Parul et al. 2013[142]. This method is predicated on the reduction of nitric oxide by antioxidant compounds present in plant extracts. Nitric oxide was generated from sodium nitroprusside through the Griess reaction. Its levels was quantified spectrophotometrically at 546 nm, as shown in Figure 20.

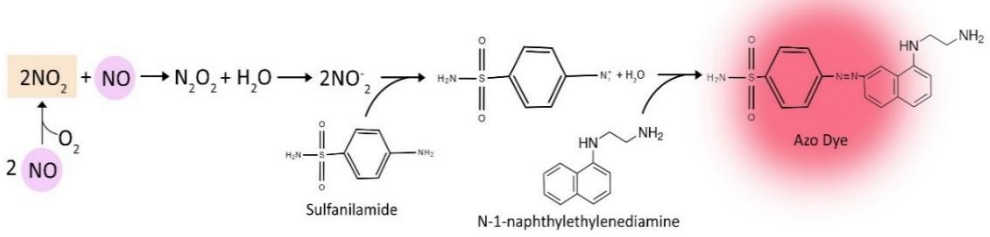

Figure 20 Reaction of Griess assay reagent NO_2^- for measures NO indirectly [Modified from Coneski et al.,2012][143]

For the assay, a mixture was created by combining 200 µL of 1 mM sodium nitroprusside dissolved in phosphate buffer (pH 7.4) was mixed with 100 µL of several concentrations of the extract and incubated under UV light at room temperature for 10 minutes. An equivalent reaction mixture without the tested extract served as a control. After incubation, 500 µL of Griess reagent (composed of 1% sulfanilamide, 2% H_3PO_4, and 0.1% N-(1-naphthyl)ethylenediamine dihydrochloride) was incorporated into the mixture. Gallic acid was applied as a positive control. The absorbance was measured at 546 nm utilizing a UV-VIS spectrophotometer, and the $NO^{\bullet}$ scavenging capacity was calculated using the formula:

$$\% \text{ nitric oxide radical scavenging activity} = [(A_{control} - A_{sample})/ A_{control}] \times 100$$

Where: $A_{control}$ is absorbance of control,

A_{sample} is absorbance of the standard or extract sample.

The IC_{50} was obtained by plotting concentration versus scavenging activity. Experiments were conducted in triplicate.

3.5.9 Hydrogen peroxide (H_2O_2) scavenging activity

The H_2O_2 scavenging activity assay was determined using horseradish peroxidase (HRP) to catalyze the breakdown of H_2O_2 into water and oxygen, following the method of Sroka et al.,2003[144]. This activity was quantified using a colorimetric assay with phenol red as the substrate. The formation of a colored complex was proportional to the amount of H_2O_2 in the sample, as illustrated in **Figure 21**.

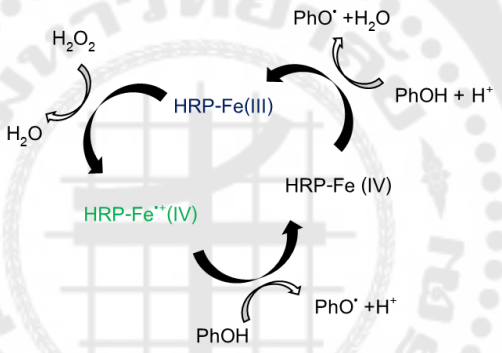

Figure 21 H_2O_2 scavenging activity mechanism [Modified from Grosu et al.,2018][145]

To assess the activity, various concentrations of the extract or ascorbic acid (as the positive control) were incorporated into a mixture comprising 50 µL of a 0.002% H_2O_2 solution and 400 µL of 0.1 M phosphate buffer. After 10-min incubation at 37ºC, 500 µL of a phenol red (0.2 mg/mL) and HRP (0.1 mg/mL) was mixed. The resulting mixture was incubated at 37ºC for an additional 15 min, followed by the introduction of 25 µL of 1 M NaOH to terminate the reaction. Absorbance readings were obtained at 610 nm using a UV-VIS spectrophotometer. The scavenging activity of H_2O_2 was determined using the formula:

$$\%\ H_2O_2\ \text{scavenging activity} = [(A_{control} - A_{sample})/ A_{control}] \times 100$$

Where: $A_{control}$ is absorbance of control,

A_{sample} is absorbance of the standard or extract sample.

The IC_{50} value was determined by plotting concentration against scavenging activity. All experiments were performed in triplicate.

3.6 Cell culture

The human submandibular gland (HSG) cell line acquired from the American Type Culture Collection (ATCC®HTB-41™, Manassas, VA, USA). The cells were maintained in Dulbecco's modified Eagle medium (DMEM) enriched with high glucose (GIBCO, CA, USA), supplemented with 10% (v/v) fetal bovine serum, 1% (v/v) non-essential amino acids, 1% (v/v) L-glutamine, and 1% (v/v) and 1% (v/v) penicillin–streptomycin. Cultures were maintained at 37 °C in a humidified atmosphere containing 5% CO_2. The culture medium was replaced three times a week.

3.7 Assessment of the non-toxic concentration of water extract on HSG cells and its protective effects against t-BHP

A resazurin cell viability assay kit (Sigma-Aldrich, St. Louis, MO, USA) was employed to evaluate cell viability. Resazurin is a blue fluorescent dye that is reduced to resorufin in viable cells due to intracellular diaphorase enzyme activity, resulting in a strong pink fluorescence signal[146]. To determine the non-toxic concentration of the extract, HSG cells were plated at a density of 5×10^4 cells/well and treated with various concentrations of the extract, between 12.5 to 200 µg/ml, then incubated for 24 h at 37°C. To analyze the cytoprotective effects, the cells were exposed to 400 µM t-BHP for 30 min, followed by treatment with the extract, and incubated for 6 h. After treatment, a resazurin solution was added, and fluorescence intensities were recorded using a microplate reader with excitation and emission wavelengths set at 530 and 590 nm, respectively. The viability of the cells was then determined using the equation below:

$$\% \text{ Cell viability} = (A/B) \times 100$$

Where A is the absorbance of the treated group, and B is the absorbance of the untreated control group.

3.8 Assessment of the antioxidant activity of the water extract on HSG cells against t-BHP-induced oxidative stress

To measure intracellular reactive oxygen species (ROS) levels, the fluorescent probe 2',7'-dichlorofluorescein diacetate (DCFH-DA) was utilized, which is oxidized to the highly fluorescent 2',7'-dichlorofluorescein (DCF) under oxidative stress[147]. HSG cells were exposed to 400 μM t-BHP to induce oxidative stress, followed by treatment with water extract for 6 h. Upon completion of the treatment, the cells were incubated with 20 μM DCFH-DA in darkness at 37°C for 30 min. The cells were then washed with PBS and subsequently incubated for an additional 30 min. Fluorescence intensity was measured immediately using a microplate reader set at excitation and emission wavelengths of 485 nm and 535 nm, respectively. ROS levels were directly proportional to fluorescence intensity.

3.9 Analysis of cell death

3.9.1 Hoechst 33342 Staining

Apoptotic cells were identified using Hoechst 33342 staining, following the method described by Atale et al.,2014[148]. HSG cells were cultured in 8-well chambered cover glass dishes at a density of 7×10^5 cells per dish. After exposure to 400 μM t-BHP and subsequent treatment with the extract. Following treatment, the cells were rinsed with PBS and then incubated in phenol red-free DMEM for 30 min in the dark. Subsequently, the medium was replaced with DMEM without phenol red. Following this, Hoechst 33342 staining was performed for 5 minutes at room temperature, also in the dark in the dark. Morphological changes and nuclear fragmentation indicative of apoptosis were visualized using a phase-contrast microscope and a Zeiss LSM 900 confocal laser scanning microscope (Zeiss, Oberkochen, Germany).

3.9.2 Acridine orange/Ethidium bromide staining (AO/EB)

To assess apoptosis through fluorometric changes, acridine orange/ethidium bromide (AO/EB) double staining was performed as described by Chen et al.,2024[149]. Cells were stained with 10 μL of AO/EB stain solution, consisting of a 1:1 mixture of

100 µg/mL acridine orange and 100 µg/mL ethidium bromide in PBS. The stained cells were immediately observed and photographed using a Zeiss LSM 900 confocal laser scanning microscope. Viable cell nuclei displayed green fluorescence, whereas apoptotic cell nuclei exhibited orange-red fluorescence.

3.10 Assessment of protein expression of the extract on HSG cells against t-BHP-induced oxidative stress using western blot analysis

The HSG cells were grown in 100 mm dishes with a density of 10×10^6 cells/dish. As a result of the treatment with the reagents, the cells were harvested, and total protein was extracted using RIPA buffer supplemented with 1% protease and phosphatase inhibitor cocktails. The determination of protein concentrations was conducted with a commercial kit. Equal amounts of protein were separated by SDS-PAGE, including 14% gels for phosphorylated p38 MAPK, AQP5, and Bcl-2, and 15% gels for cleaved caspase-3 and Bax. Next, the proteins were transferred onto nitrocellulose membranes, which were subsequently blocked with a 5% skim milk in TBS-T buffer for 1 hour, followed by overnight incubation at 4°C with primary antibodies against Bax, Bcl-2, Phosphorylated p38 MAPK, cleaved caspase-3, and AQP5. GADPH was used as an internal control. After extensive washing, the membranes were incubated with with secondary antibodies conjugated to horseradish peroxidase. The resulting protein bands were visualized using a chemiluminescence imaging system. (Alliance Q9 Advanced Chemiluminescence Imager).

3.11 Assessment of mRNA expression by using Real-time quantitative reverse transcription PCR (Real-time qRT-PCR)

HSG cells were cultured in dishes at a density of $2.5\text{x}10^6$ cells/dish and exposed to different reagents and exposure times according to the experimental plan. After treatment, RNA will be extracted from the cells using the RNA extraction kit. The conversion of RNA to cDNA will be carried out using a reverse transcription-PCR (RT-PCR) kit. The protocol specified by the manufacturer will be followed with slight modification. Afterward, the cDNA amplification will be upregulated using the SentiFast

SYBR® Hi-ROX mix (Bioline, TN, USA), in accordance with StepOnePlus (Applied Biosystems, Waltham, MA, USA). Moreover, the real-time relative gene expression will also be analyzed using QuantStudio™ Real-Time PCR System (Applied Biosystems, Waltham, MA, USA). The relative gene expression was calculated using the $2^{-\Delta\Delta CT}$ method, normalizing to GAPDH expression. Primers used in the experiment are listed in Table 1

Table 1 The primer sequences used for real-time PCR

Gene	Forward Primer	Reverse Primer
Bax	5'-CCCGAGAGGTCTTTTTCCGAG-3'	5'-CCAGCCCATGATGGTTCTGAT-3'
BCl-2	5'-GGTGGGTCATGTGTGTGG-3'	5'-CGGTTCAGGTACTCAGTCATCC-3'
AMY1	5'-GTAATGGCCGGGTGACAGAA-3'	5'-CCCAACCTTCTCCCCAGTTC-3'
AQP5	5'-CGGGCTTTCTTCTACGTGG-3'	5'-GCTGGAAGGTCAGAATCAGCTC-3'
GAPDH	5'-ACAACTTTGGTATCGTGGAAGG-3'	5'-GCCATCACGCCACAGTTTC-3'

3.12 Assessment of amylase activity of the extract on HSG cells against t-BHP-induced oxidative stress

The amylase activity was determined using a spectrophotometric method in accordance with the protocol provided in the Amylase Activity Assay Kit (Sigma-Aldrich, St. Louis, MO, USA). Homogenized HSG cells (4×10^6) in 0.5 mL of Amylase Assay Buffer were centrifuged at 13,000 g for 10 min to remove insoluble material. Samples (1–50 µL) or 5 µL of Amylase Positive Control were added to the wells of a 96-well plate and adjusted to 50 µL with Amylase Assay Buffer. Nitrophenol standards (0–20 nmol/well) were prepared by adding 0–10 µL of a 2 mM Nitrophenol Standard solution and bringing the volume to 50 µL with water. A Master Reaction Mix (50 µL of Amylase Assay Buffer and 50 µL of Amylase Substrate Mix) was prepared, and 100 µL was added to each

well. The plate was incubated at 25 °C, and absorbance readings at 405 nm ($A_{405\ initial}$) were taken every 5 min until the most active sample approached the highest standard (20 nmol/well). The final absorbance ($A_{405\ final}$) used for calculating enzyme activity was taken just before this point. Amylase activity was calculated using this formula:

Amylase activity (nmol/min/mL) = B × Sample Dilution Factor/ Reaction Time × V

Where: B is the amount (nmol) of nitrophenol generated ($\Delta A_{405} = A_{405\ final} - A_{405\ initial}$), Reaction Time is $T_{final} - T_{initial}$ in minutes, V is the sample volume in mL

One unit of amylase activity was indicated as the amount of enzyme that produces 1 µmol of p-nitrophenol per minute at 25°C. Experiments were performed in duplicate for accuracy.

3.13 Statistical analysis

To ensure experiment reproducibility, all assays were performed in triplicate. Results from the *in vitro* determination of phenolic and flavonoid contents, and antioxidant capacities, are presented as mean ± standard deviation (SD) from independent experiments, while other results are indicated as mean ± standard error of the mean (SEM) from three independent experiments. Statistical analysis was conducted using one-way ANOVA followed by Tukey's post-hoc test in GraphPad Prism version 8 to discern significant differences across groups ($p < 0.05$, $p<0.01$ and $p<0.001$).

CHAPTER 4
RESULTS

4.1 *E. latifolia* extraction yield measurement

Water is considered a highly efficient solvent for extracting antioxidants from herbal medicines, including the heated water extract of *E. latifolia* fruits, due to its ability to dissolve a diverse range of phytochemical constituents, particularly phenolic compounds and flavonoids. The heated extraction yielded 29.7 g of dry extract from 100 g of fresh *E. latifolia* fruit, resulting in an extraction yield of 29.7%.

4.2 Total phenolic and flavonoid contents

The quantification of total phenolic content in the *E. latifolia* fruit extract was performed using a calibration curve for standard gallic acid, constructed with solutions ranging from 0.1 to 0.5 mg/mL. This calibration curve was defined by the linear equation $y=0.9115x + 0.0256$ ($R^2 = 0.9947$), as illustrated in Figure 22A. A calibration curve based on standard quercetin, with concentrations from 0.02 to 0.10 mg/mL, was used to measure the total flavonoid content ($y=3.194x + 0.0217$, $R^2 = 0.9918$), as shown in Figure 22B. Utilizing these calibration curves, the total polyphenolic and flavonoid contents of the extract were quantified and conveyed as mg GAE/g extract and mg QE/g extract, respectively, as presented in Table 2.

A

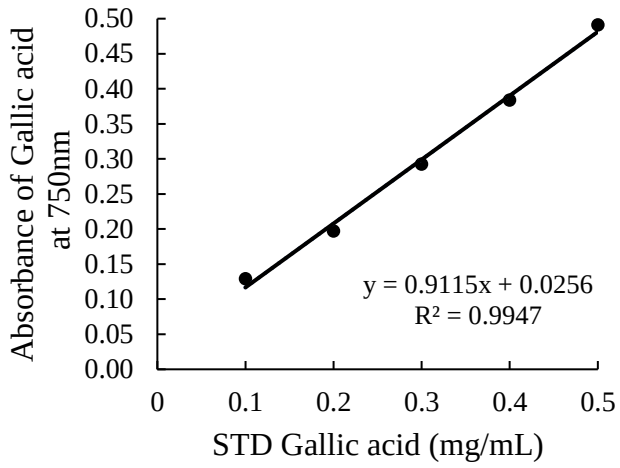

B

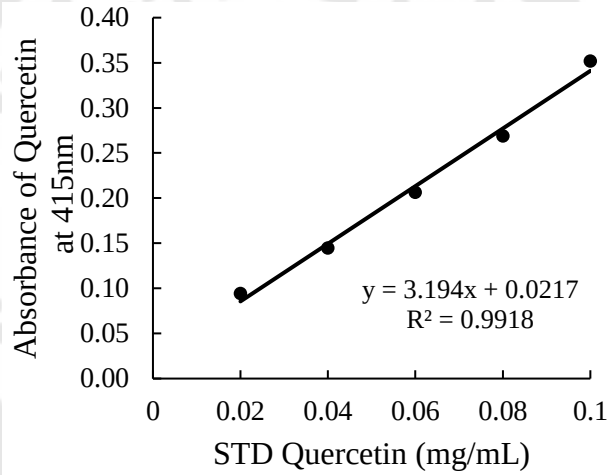

Figure 22 Calibration curves for the quantification of (A) total phenolic and (B) flavonoid contents, with gallic acid and quercetin standards, respectively.

The analysis determined the levels of phenolic and flavonoid compounds in the *E. latifolia* fruit extract, with results demonstrating a presence of 24.38 ± 0.40 mg GAE/g extract for phenolic compounds and 0.13 ± 0.06 mg QE/g extract for flavonoid compounds, respectively (Table 2). These values demonstrate the substantial presence of bioactive compounds in the extract, which are known for their antioxidant properties and potential health benefits.

Table 2 The contents of total phenolic and flavonoid the heated water extract of *E. latifolia* fruits.

E. latifolia	Phenolic contents (mg GAE/g extract)	Flavonoid contents (mg QE/g extract)
Fruit extract	24.38±0.40	0.13±0.06

4.3. HPLC analysis

4.3.1 Malic acid

The malic acid contents of the *E. latifolia* fruit extract was quantified using HPLC analysis, with the results detailed in Table 3. The HPLC chromatogram, using standard malic acid ($Y=2.48e^{0.02}X + 1.26e^{002}$, $R^2 = 0.99941$) with a retention time of 7.324 min, confirmed the presence of malic acid in the extract, with a retention time of 7.280 min, respectively (Figure 23).

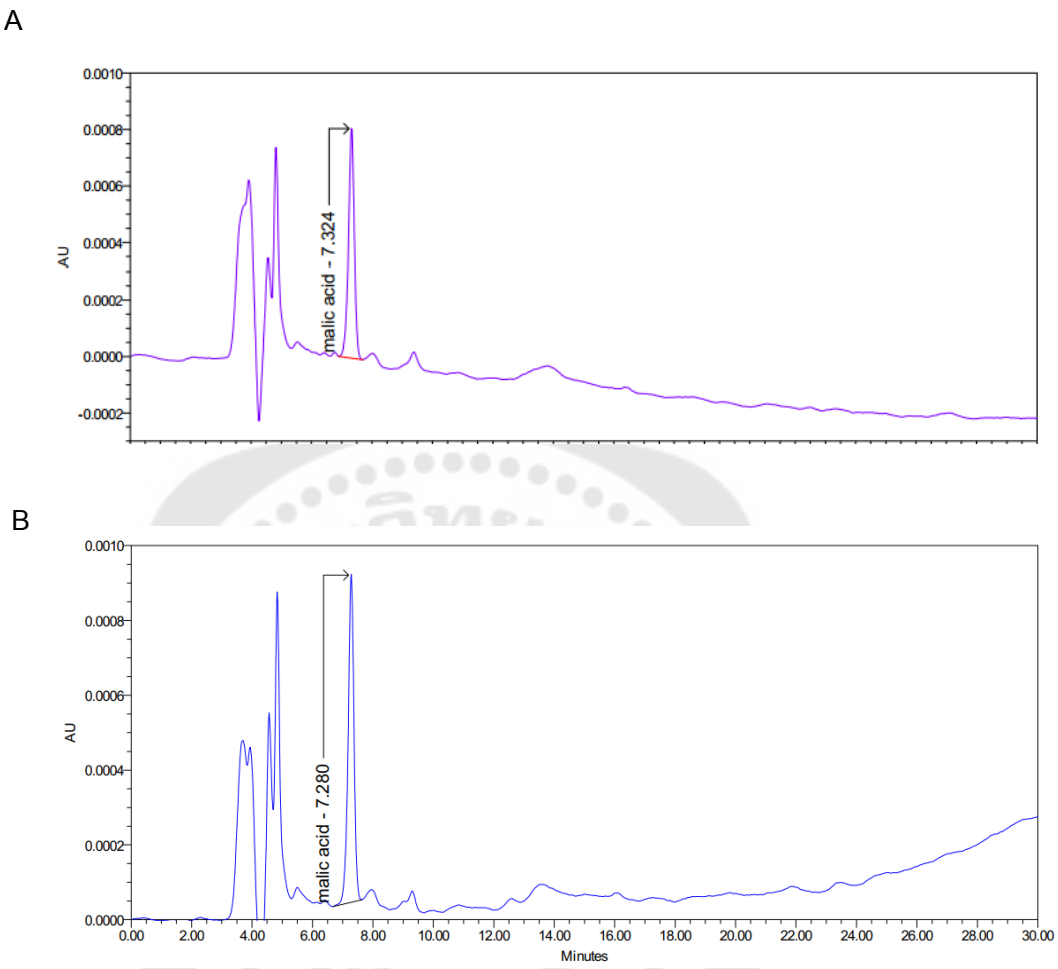

Figure 23 HPLC chromatograms illustrate the retention time of the (A) Standard malic acid, and (B) the presence of malic acid in the heated water extract of *E. latifolia* fruits.

4.3.2 GABA

The GABA content of *E. latifolia* fruit extract was quantified using HPLC analysis. The standard GABA ($Y=1.3e^{4}X + 4.12e^{3}$, R^2 =0.99994) exhibited a retention time of 15.892 min. GABA was detected in the extract with a retention time of 15.820 min (Figure 24). The GABA content of the extract, as in Table 3.

A

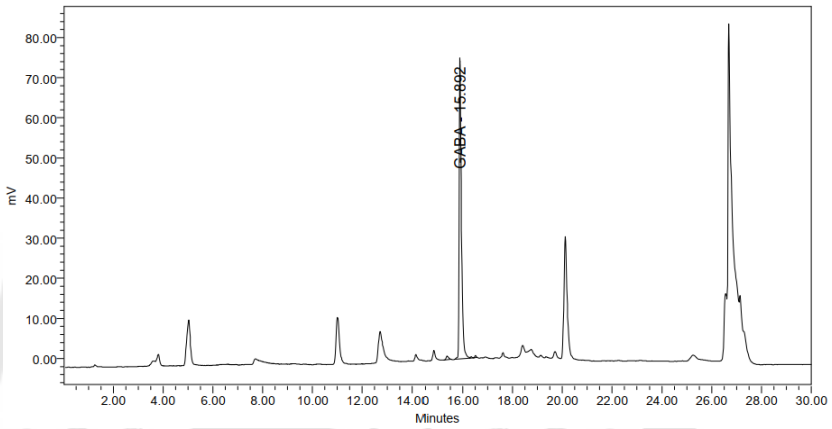

B

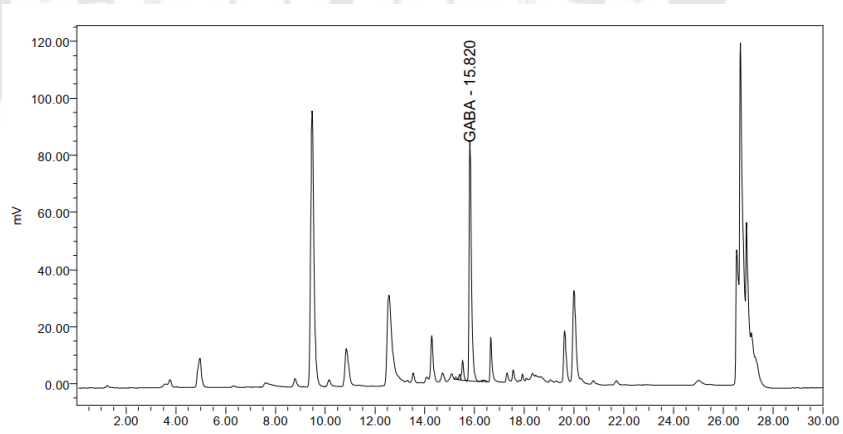

Figure 24 HPLC chromatograms depicting the retention time of the Standard (A) GABA and (B) the presence of GABA in the heated water extract of *E. latifolia* fruits.

Quantitative analysis of malic acid and GABA contents in the *E. latifolia* fruit extract revealed distinct compositional characteristics, with results shown in Table 3. The analysis indicated that malic acid was quantified at 0.55 mg/mg. In addition, GABA content analysis demonstrated substantial GABA level in the extract was found at 2.215 µg/mg. This suggests that the heating process is essential for the release or synthesis of

GABA in the extract. These findings suggest that heating not only modulates the concentration of existing compounds such as malic acid but also facilitates the formation of bioactive compounds like GABA, which are crucial for the extract's potential health benefits.

Table 3 Malic acid and GABA contents in the heated water extract of *E. latifolia* fruits.

E. latifolia	Malic acid contents (mg/mg crude extract)	GABA contents (µg/mg crude extract)
Fruit extract	0.55	2.215

4.3.3 Metabolomics-Based Profiling of *E. latifolia* Using LC-Q-TOF-MS/MS

A comprehensive phytochemical investigation of the *E. latifolia* fruit extract was conducted through LC-Q-TOF-MS/MS. This investigation uncovered the presence of 34 secondary metabolites in the extract (Table 4). Tentative metabolite assignments were made by comparing molecular ions of $[M+H]^+$ in the positive ionization mode to their respective lower m/z fragment ions with data reported in the literature and available online public databases, as shown in Table 4 and Figure 25.

The analysis revealed several classes of compounds including amino acids. **(1)** L-Asparagine was detected at a retention time (tR) of 2.59 min and had molecular ion peaks $[M+H]^+$ at m/z of 133.060, **(2)** GABA was identified at tR 2.63 min with $[M+H]^+$ at m/z of 104.071(Figure 26), **(3)** Glutamic acid was found at tR 2.66 min with $[M+H]^+$ at m/z of 148.061. **(7)** Proline was detected at tR 2.79 min with $[M+H]^+$ at m/z of 116.070, (10) L-Tyrosine was found at tR 3.08 min with $[M+H]^+$ at m/z of 182.082, **(12)** Norleucine was identified at tR 4.48 min with $[M+H]^+$ at m/z of 132.102, and (16) L-Tryptophan was detected at tR 7.20 min with $[M+H]^+$ at m/z of 205.097.

Additionally, monosaccharides and oligosaccharides were identified such as **(5)** D-(+)-Mannose was found at tR 2.73 min with $[M+H]^+$ at m/z of 361.137, and **(6)** 2-alpha-Mannobiose was detected at tR 2.78 min with $[M+H]^+$ at m/z of 360.152.

Other organic compounds identified included **(4)**1,3,5-Benzenetriol at tR 2.72 min with $[M+H]^+$ at m/z of 127.039, and **(9)** Citric Acid at tR 3.00 min with $[M+H]^+$ at m/z of 210.062. Additionally, **(14)** 3-Nonen-1-ol, (Z) was found at tR 5.14 min with $[M+H]^+$ at m/z of 143.034, and **(15)** 3-Indoleacrylic Acid was detected at tR 7.20 min with $[M+H]^+$ at m/z of 188.071. The analysis also revealed the presence of some nucleobases and nucleosides, such as **(8)** Adenine at tR 2.91 min with $[M+H]^+$ at m/z 136.062, and **(11)** Adenosine at tR 4.19 min with $[M+H]^+$ at m/z 268.105.The extract contained various lipids and fatty acids, including **(24)** 1-Oleoyl-L-alpha-lysophosphatidic acid at tR 24.45 min with $[M+H]^+$ at m/z 437.195, **(22)** Tuberostemonine at tR 23.74 minutes with $[M+H]^+$ at m/z 393.288, **(23)** 5-trans-17-Phenyltrinorprostaglandin F2**α** ethyl amide at tR 23.75 min with $[M+H]^+$ at m/z 398.243, and **(25)** 12(13)-Epoxy-9Z-octadecenoic acid at tR 24.57 min with $[M+H]^+$ at m/z 314.270.

Analysis of the phytochemicals within the *E. latifolia* fruit extract disclosed a diverse array of compounds, including amino acids (particularly GABA), sugars, oligosaccharides, and unique compounds such as tuberostemonine and oleoyl-L-**α**-lysophosphatidic acid. High concentrations of certain metabolites, including 1,3,5-Benzenetriol and citric Acid, were also observed. These findings suggest that the heat extraction process significantly alters the metabolite composition of *E. latifolia* fruit*s*, resulting in a more diverse array of bioactive compounds.

Table 4 Tentative identification of phytoconstituents in the heated water extract of *E. latifolia* fruits using LC-Q-TOF-MS/MS in positive ion mode.

No.	Analyte Peak Name/ Library Hit	Retention Time	Area	MW	Empirical Formula	Precursor Mass	Detected Mass
1	L-Asparagine	2.59	3.183e+05	115.02660	$C_4H_8N_2O_3$	133.060	133.0596
2	GABA	2.63	7.759e+04	103.06391	$C_4H_9NO_2$	104.071	104.0707
3	Glutamic acid	2.66	5.353e+04	180.06524	$C_5H_9NO_4$	361.137	361.1370
4	1,3,5-Benzenetriol	2.72	1.690e+04	130.02781	$C_6H_6O_3$	148.061	148.0612
5	D-(+)-Mannose	2.73	1.138e+05	126.03264	$C_6H_{12}O_6$	127.039	127.0394
6	2α-Mannobiose	2.78	2.515e+05	342.11849	$C_{12}H_{22}O_{11}$	360.152	360.1521
7	Proline	2.79	6.371e+04	115.06311	$C_5H_9NO_2$	116.070	116.0710
8	Adenine	2.91	3.060e+04	135.05560	$C_5H_5N_5$	136.062	136.0615
9	Citric acid	3.00	1.756e+04	192.02842	$C_6H_8O_7$	210.062	210.0619
10	L-Tyrosine	3.08	7.182e+04	181.07514	$C_9H_{11}NO_3$	182.082	182.0820
11	Adenosine	4.19	2.343e+04	267.09684	$C_{10}H_{13}N_5O_4$	268.104	268.1051
12	Norleucine	4.48	3.713e+03	131.09559	$C_6H_{13}NO_2$	132.102	132.1025
13	2-Methylquinolin-8-ol	4.99	4.672e+04	159.06948	$C_{10}H_9NO$	160.076	160.0762
14	3-Nonen-1-ol, (Z)	5.14	1.303e+04	110.00097	$C_9H_{18}O$	143.034	143.0346

15	3-Indoleacrylic acid	7.20	4.034e+04	187.06305	$C_{11}H_9NO_2$	188.070	188.0715
16	L-Tryptophan	7.20	9.917e+03	187.06369	$C_{11}H_{12}N_2O_2$	205.097	205.0974
17	16-Phenoxytetranor Prostaglandin A2	8.05	7.859e+04	370.26011	$C_{22}H_{26}O_5$	393.249	393.2488
18	Gingerglycolipid B +Na	12.64	6.065e+05	678.50646	$C_{33}H_{58}O_{14}$	701.495	701.4941
19	Cefamandole	13.92	1.507e+05	440.33811	$C_{18}H_{18}N_6O_5S_2$	463.327	463.3272
20	Mepirizole	23.53	2.053e+05	234.19962	$C_{11}H_{14}N_4O_2$	252.233	252.2328
21	Phytosphingosine	23.71	7.853e+04	317.29306	$C_{18}H_{39}NO_3$	318.300	318.3015
22	Tuberostemonine	23.74	1.704e+05	375.25445	$C_{22}H_{33}NO_4$	393.288	393.2876
23	5-trans-17-phenyl trinor Prostaglandin F2α ethyl amide	23.75	5.098e+04	375.25454	$C_{25}H_{37}NO_4$	398.243	398.2432
24	1-Oleoyl-L-α lysophosphatidic acid	24.45	9.258e+04	414.20641	$C_{21}H_{41}O_7P$	437.195	437.1956
25	12,13-Epoxy-9(Z)-octadecenoic acid	24.57	8.459e+04	296.23692	$C_{18}H_{32}O_3$	314.270	314.2702
26	Stanozolol-d3	25.70	9.489e+04	309.23230	$C_{21}H_{32}N_2O$	332.221	332.2208
27	9,12-Octadecadiynoic acid	26.61	1.356e+05	276.21055	$C_{18}H_{32}O_2$	294.244	294.2437
28	trans-4,5-Epoxy-2(E)-decenal	28.12	4.792e+04	168.11622	$C_{10}H_{16}O_2$	186.149	186.1496
29	Corosolic acid	30.33	5.477e+04	472.35774	$C_{30}H_{48}O_4$	473.364	473.3645
30	brodifacoum	34.29	1.622e+05	484.28513	$C_{31}H_{23}BrO_3$	523.248	523.2479
31	Bacosine	36.41	7.742e+04	456.36259	$C_{30}H_{48}O_3$	457.369	457.3698

32	Palmitamide	36.86	2.411e+06	255.25667	$C_{16}H_{33}NO$	256.263	256.2634
33	Stearamide	41.09	4.573e+05	283.28896	$C_{38}H_{76}N_2O_2$	284.296	284.2958
34	Oleoyl ethylamide	42.58	9.875e+05	309.30468	$C_{20}H_{39}NO$	310.311	310.3116

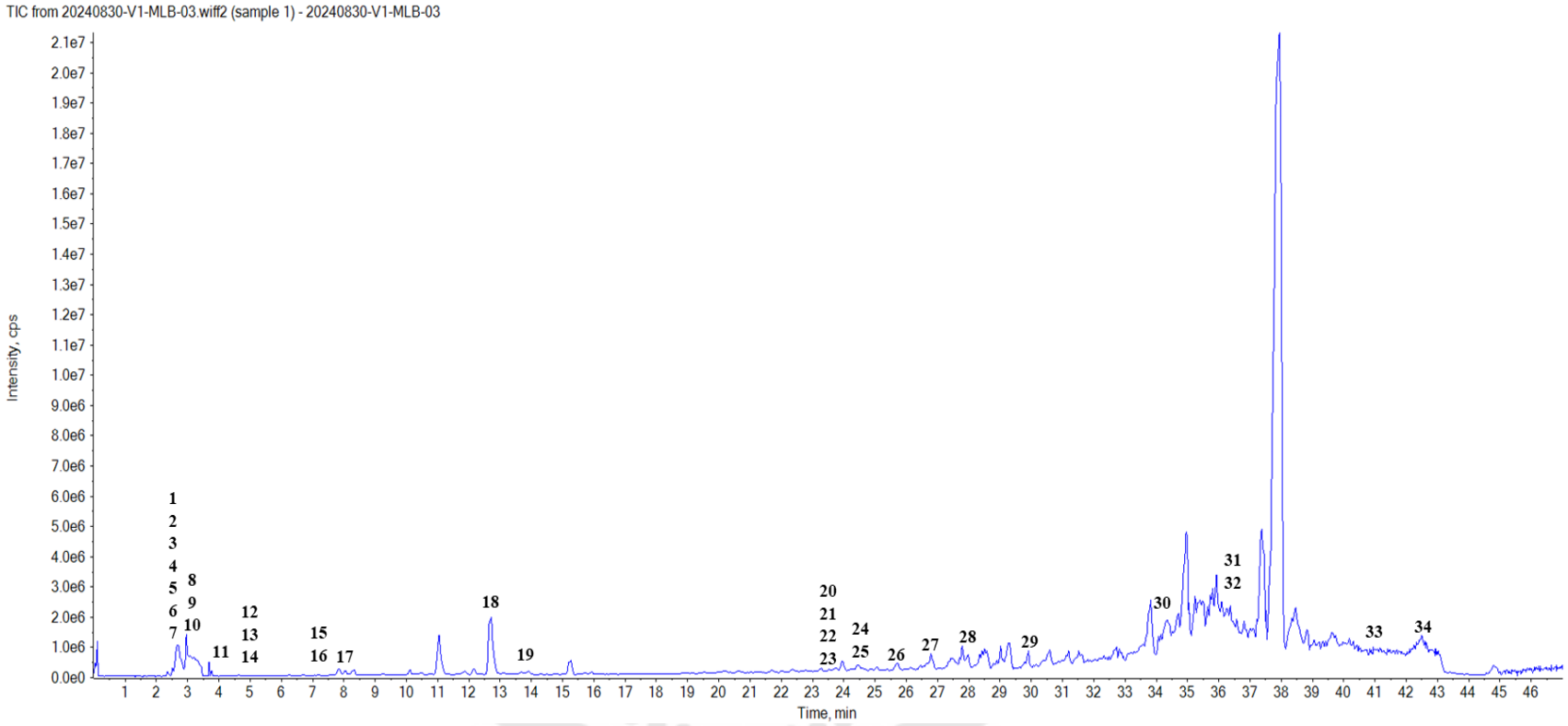

Figure 25 Chromatogram of bioactive compounds analyzed in the heated water extract of *E. latifolia* fruits using the LC-Q-TOF-MS/MS

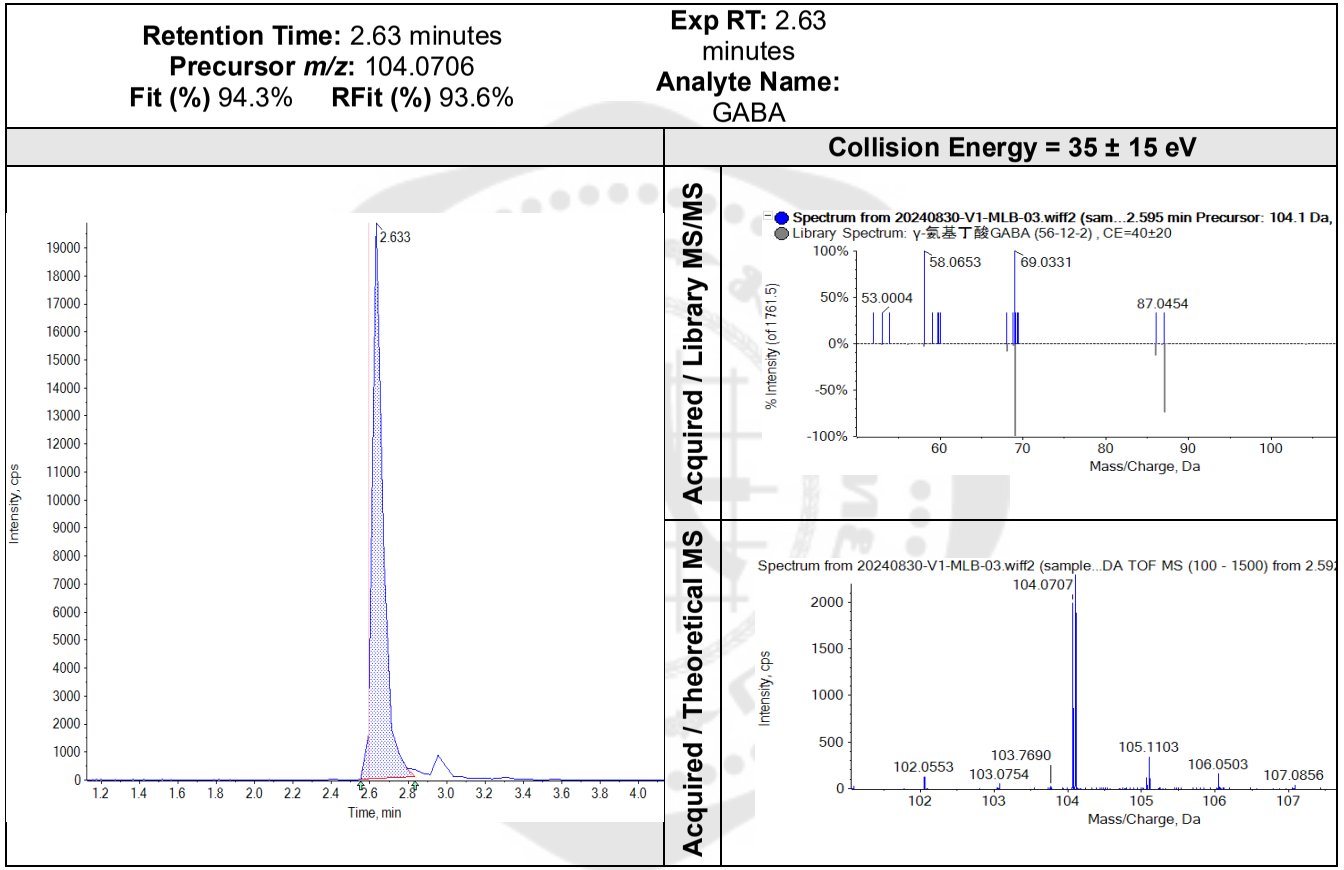

Figure 26 Chromatogram of GABA identified in the heated water extract of *E. latifolia* fruits using LC-Q-TOF-MS/MS

4.4 *In vitro* antioxidant activity

4.4.1 DPPH scavenging activity

The extract from *E. latifolia* fruit showed a concentration-dependent effect on its ability to scavenge DPPH radicals. The extract exhibited scavenging activity ranging from 28.21% to 81.54% across concentrations of 5-25 mg/mL, yielding an IC_{50} value of 14.01±0.60 mg/mL (Figure27B).

Table 5 IC_{50} values for DPPH scavenging activity in the heated water extract of *E. latifolia* fruits.

% Inhibition on DPPH free radical	Concentrations (mg/mL)					IC_{50} (mg/mL)
	5	10	15	20	25	
Fruit extract	28.21± 2.20	37.72± 1.60	50.71± 1.17	65.06± 1.64	81.54± 1.97	14.01± 0.60
STD Ascorbic acid	-	-	-	-	-	0.101±0.002

Standard Ascorbic acid was formulated at concentrations between 0.05 and 0.15 mg/mL.

A

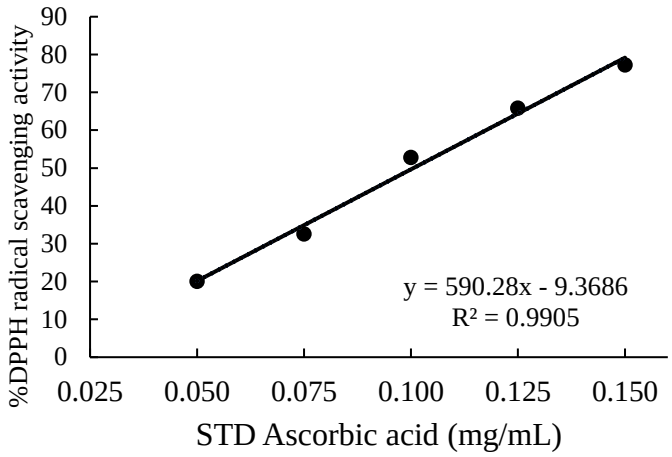

B

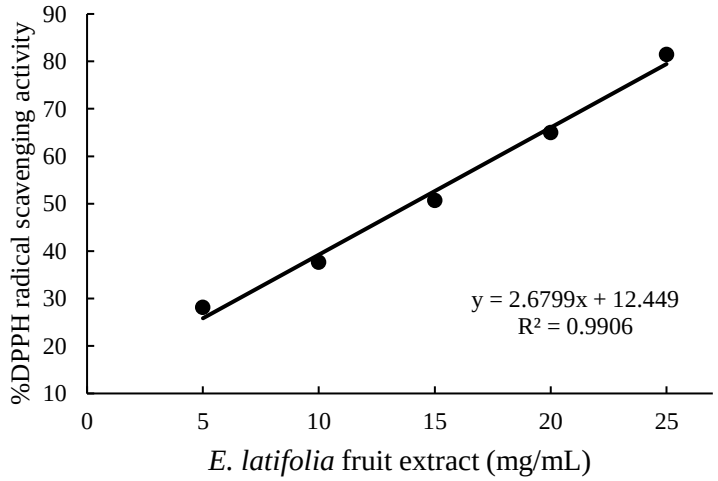

Figure 27 Percentage of DPPH scavenging activity of (A) standard ascorbic acid and (B) the heated water extract of *E. latifolia* fruits at various concentrations.

As indicated in Table 5, the *E. latifolia* fruit extract demonstrated scavenging activity across all tested concentrations. The extract attained a scavenging rate of 28.21% at a concentration of 5 mg/mL. At 25 mg/mL, it exhibited a scavenging capability of 81.54%. The IC_{50} value for the extract was determined to be 14.01 ± 0.60 mg/mL, The highest activity recorded was 81.54% at 25 mg/mL (Figure 27B). The reference standard ascorbic acid showed an IC_{50} of 0.101 ± 0.002 mg/mL (Figure 27A). These findings

confirm the antioxidant potential of the extract in facilitating efficient free radical scavenging.

4.4.2 ABTS scavenging activity

The scavenging activity against ABTS radicals exhibited by the *E. latifolia* fruit extract indicated activity patterns that depend on concentration (Table 6). The extract exhibited scavenging activities ranging from 26.50% to 68.40% at concentrations between 0.25 and 2 mg/mL (Figure 28B). Trolox, a standard antioxidant, was utilized as a reference Figure 28A.

Table 6 IC_{50} values for ABTS radical scavenging activity in the heated water extract of *E. latifolia* fruits.

% Inhibition on ABTS radical	Concentrations (mg/mL)					IC_{50} (mg/mL)
	0.25	0.50	1.00	2.00	3.00	
Fruit extract	28.21± 2.20	37.72± 1.60	50.71± 1.17	65.06± 1.64	81.54± 1.97	1.18± 0.03
STD Trolox	-	-	-	-	-	0.169±0.002

Standard Trolox was prepared at concentrations ranging from 0.1 to 0.2 mg/mL.

A

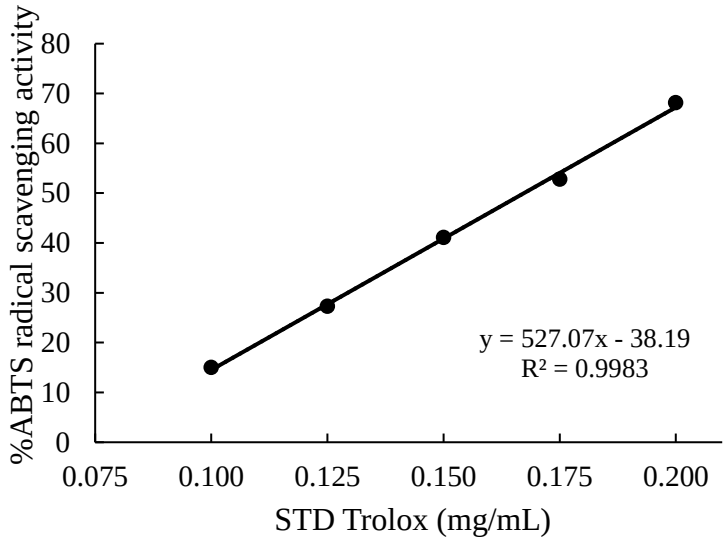

B

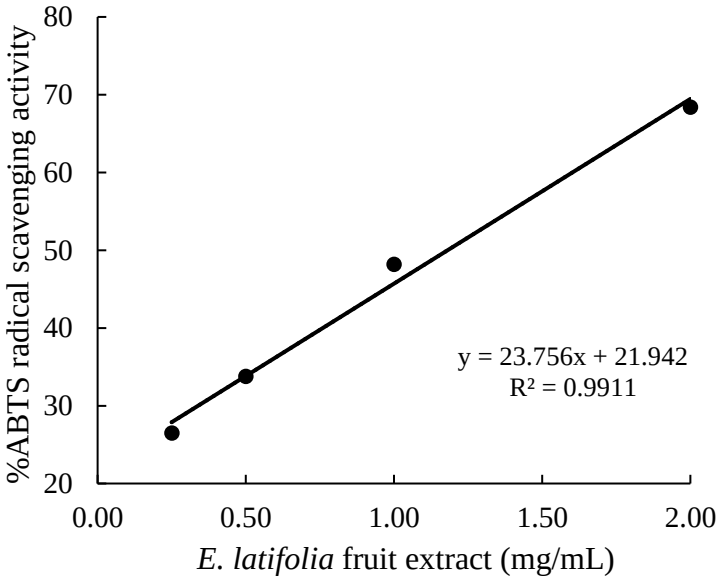

Figure 28 Percentage of ABTS scavenging activity of (A) standard Trolox and (B) the heated water extract of *E. latifolia* fruits at various concentrations.

Table 6 presents the specific percent inhibition observed at each concentration for the extract, showing an increase in scavenging activity correlated with higher concentrations. At 0.25 mg/mL, the extract achieved a scavenging activity of 28.21 ± 2.20%, progressing to the maximum scavenging capability recorded was

81.54 ± 1.97% at concentration of 3 mg/mL. The IC_{50} value for the extract, indicative of its antioxidant effectiveness, was determined to be 1.18 ± 0.03 mg/mL. This value signifies the concentration required to achieve 50% inhibition of the ABTS radical, reflecting the potent antioxidant properties of the *E. latifolia* fruit extract. In comparison, the standard antioxidant Trolox was utilized, with an IC_{50} value determined to be 0.169 ± 0.002 mg/mL (Figure 28A). These findings reinforce the antioxidant potential of the *E. latifolia* fruit extract, demonstrating substantial capacity for ABTS radical scavenging across varying concentrations.

4.4.3 Ferrous ion chelating activity

The capacity of the E. latifolia fruit extract to chelate ferrous ions was measured quantitatively, as in Table 7. The extract displayed chelating activity ranging from 3.71% to 6.53% across concentrations of 10 to 50 mg/mL. While the IC_{50} values for ferrous ion chelation could not be determined at the highest tested concentrations, the maximum chelating activity was observed at 50 mg/mL, achieving 6.53%.

Table 7 IC_{50} values of ferrous ion-chelating activity in the heated water extract of *E. latifolia* fruits.

%Fe^{2+} chelating activity	10 (mg/mL)	20 (mg/mL)	30 (mg/mL)	40 (mg/mL)	50 (mg/mL)	IC_{50} (mg/mL)
Fruit extract	3.71± 1.57	3.98± 1.41	3.89± 1.15	4.27± 1.69	6.53± 4.28	-
EDTA	-	-	-	-	-	0.18±0.01

Standard EDTA was prepared at concentrations ranging from 0.10 to 0.25 mg/mL.

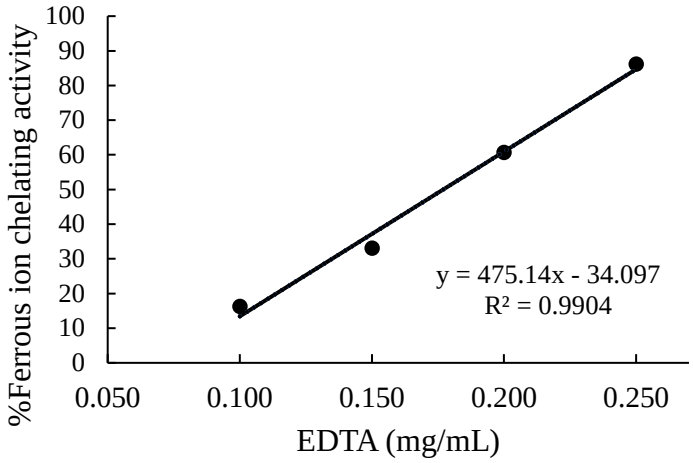

Figure 29 Percentage of ferrous ion chelating activity of the standard EDTA at different concentrations.

The standard EDTA exhibited significantly higher chelating efficiency, with an IC_{50} value of 0.18 ± 0.01 mg/mL (Figure 29). Despite, the extract demonstrated limited chelation activity across all tested concentrations. At the maximum concentration of 50 mg/mL, the extract achieved a chelation rate of only 6.53%, indicating a modest enhancement in chelating capacity because of thermal processing.

These findings suggest that while the *E. latifolia* fruit extract exhibits some capacity for ferrous ion chelation, its effectiveness is modest. The enhancement in chelating activity due to thermal processing remains insufficient to reach critically relevant levels.

4.4.4 Ferric reducing antioxidant power

The reducing capabilities of the *E. latifolia* fruit extract was evaluated using the Fe^{3+}/TPTZ methodology. The reducing potential was quantified by measuring the conversion of Fe^{3+}/TPTZ complex to TPTZ/Fe^{2+} complex, using a calibration curve of Trolox standards with concentrations ranging from 0.2 to 1.0 mg/mL. The calibration relationship was defined by the equation y=1.1752x + 0.0454 (R^2 = 0.9945), as shown in Figure 30.

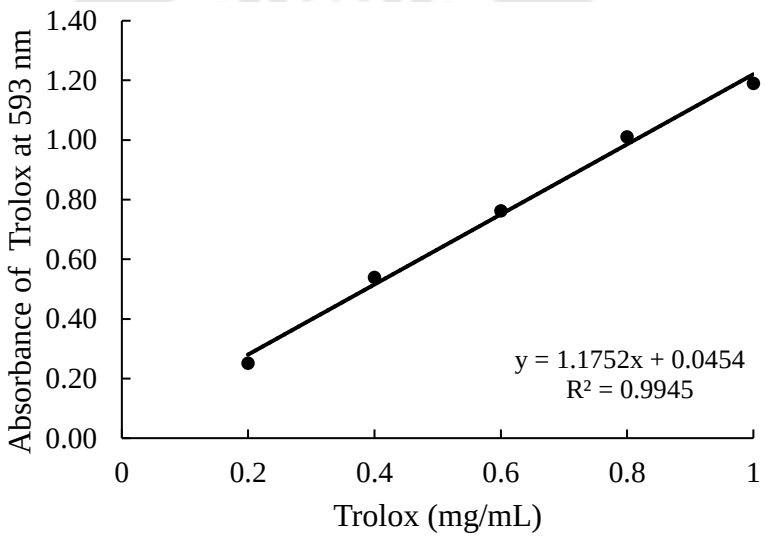

Figure 30 Calibration curves for the quantification of total ferric reducing power, using standard Trolox.

The extract exhibited a reducing power of 64.07 ± 0.01 mg TE/g extract (Table 8). This value indicates a significant capacity for electron donation in the reduction of ferric ions. The results exhibited the antioxidant properties of the *E. latifolia* fruit extract, demonstrating its potential effectiveness in reducing power assays.

Table 8 Ferric reducing power in the heated water extract of *E. latifolia* fruits.

E. latifolia	Ferric reducing power (mg TE/g extract)
Fruit extract	64.07±0.01

4.4.5 Lipid peroxidation inhibition

The lipid peroxidation inhibition capacity of the *E. latifolia* fruit extract exhibited concentration-dependent responses (Table 9). Quantitative analysis revealed that the extract demonstrated inhibition activities ranging from 33.33% to 87.07% across concentrations of 5-40 mg/mL (Figure 31).

Table 9 IC_{50} values for lipid peroxidation inhibition scavenging activity in the heated water extract of *E. latifolia* fruits.

% Lipid peroxidation inhibition	Concentrations (mg/mL)				IC_{50} (mg/mL)
	5	10	20	40	
Fruit extract	33.33±5.08	40.31±2.93	67.07±2.27	87.07±2.15	14.23±1.75
STD Trolox	-	-	-	-	0.048±0.001

Standard Trolox was prepared at concentrations ranging from 0.025 to 0.100 mg/mL.

A

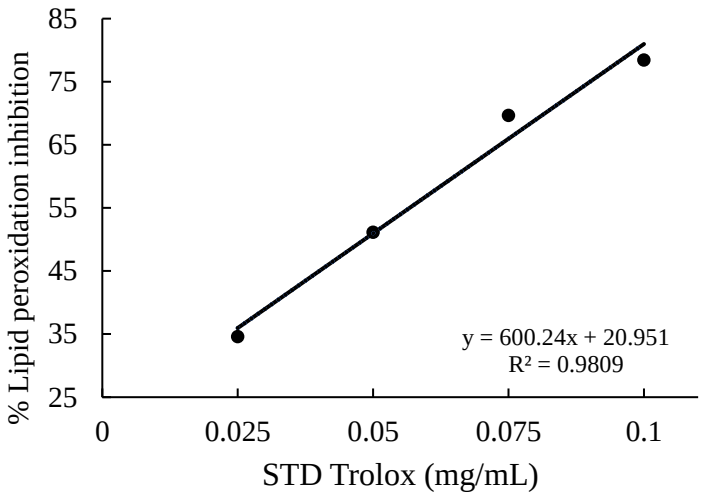

B

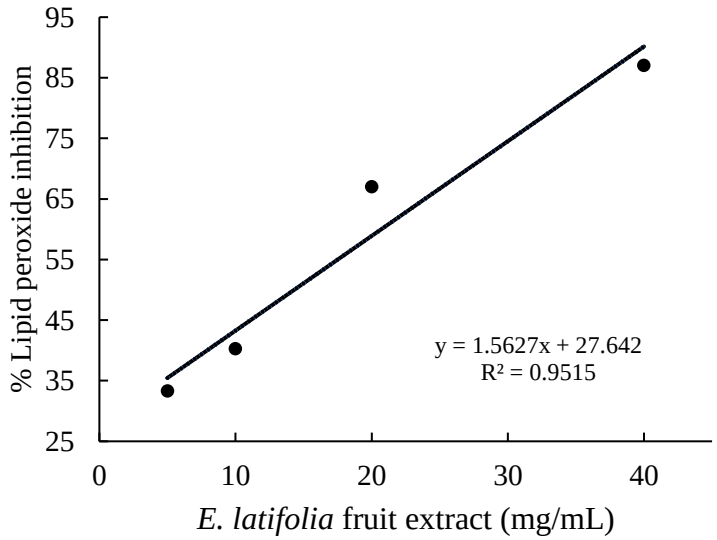

Figure 31 Percentage of lipid peroxide inhibition of (A) standard Trolox and (B) the heated water extract of *E. latifolia* fruits at various concentrations.

Analysis of IC_{50} values provided quantitative measures of extract efficacy. The extract demonstrated an IC_{50} value of 14.23 ± 1.75 mg/mL, while the reference compound Trolox exhibited an IC_{50} value of 0.048 ± 0.001 mg/mL within its tested range (0.025-0.100 mg/mL). At a concentration of 5 mg/mL, the extract achieved 33.33%

inhibition, which increased to 87.07% inhibition at 40 mg/mL. These results indicate that the extract possesses effective inhibitory potential against lipid peroxidation.

4.4.6 Superoxide radical scavenging activity

The assessment of superoxide radical scavenging activity demonstrated concentration-dependent responses from the extract, as shown in Table 10. The extract demonstrated scavenging activities ranging from 27.71% to 71.65% (5-50 mg/mL), with an IC_{50} value of 20.99 ± 1.55 mg/mL (Figure 32B). Trolox, a standard antioxidant, was utilized as reference as in Figure 32A.

Table 10 IC_{50} values for superoxide radical scavenging activity in the heated water extract of *E. latifolia* fruits.

% Inhibition on superoxide radical	Concentrations (mg/mL)				IC_{50} (mg/mL)
	5	10	20	40	
Fruit extract	27.71± 4.61	31.73± 1.73	56.95± 2.10	71.65± 1.37	20.99±1.55
STD Trolox	-	-	-	-	0.114±0.005

Standard Trolox was prepared at concentrations ranging from 0.05 to 0.125 mg/mL.

A

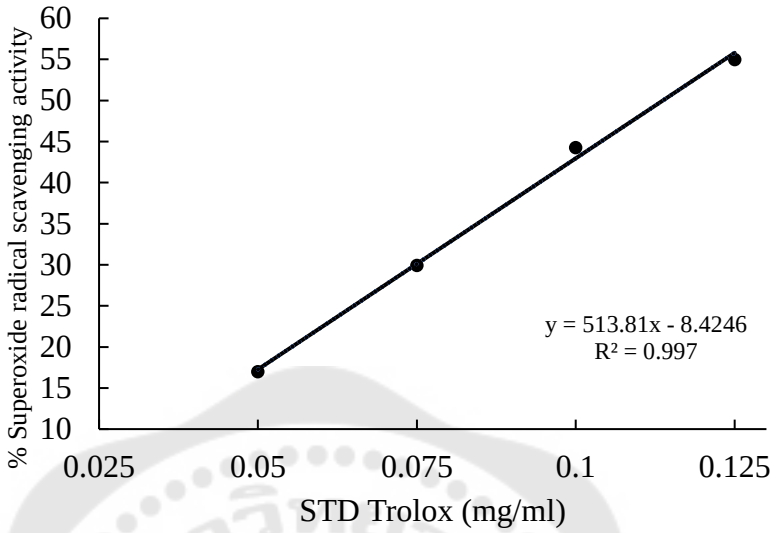

B

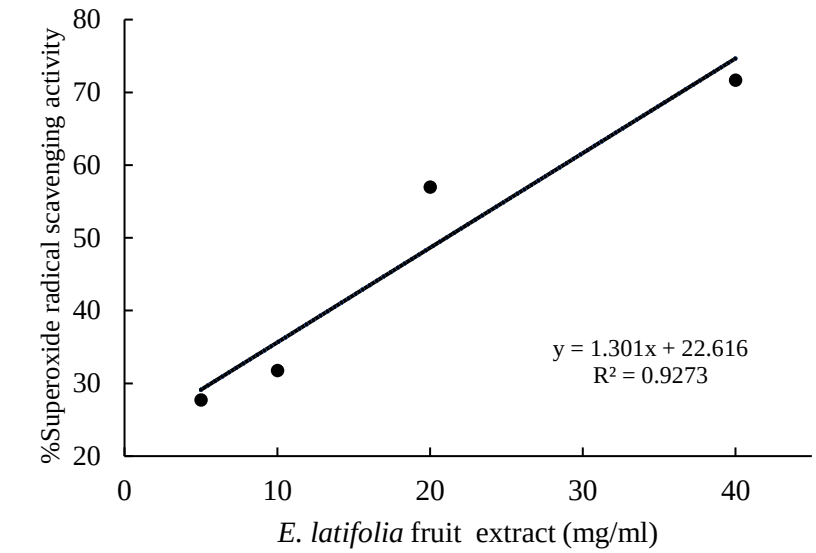

Figure 32 Percentage superoxide radical inhibition of (A) standard Trolox and (B) the heated water extract of *E. latifolia* fruits at various concentrations.

The extract exhibited concentration-dependent scavenging activity for superoxide radicals, with inhibition levels ranging from 27.71% at 5 mg/mL to 71.65% at 40 mg/mL. The IC_{50} value for the extract was determined to be 20.99 ± 1.55 mg/mL

(Figure 32B). These findings demonstrate the effective scavenging potential of the extract against superoxide radicals.

4.4.7 Hydroxyl radical scavenging activity

The capacity of the *E. latifolia* fruit extract to scavenge hydroxyl radicals was systematically evaluated across multiple concentrations (Table 11). The extract exhibited significant concentration-dependent scavenging activity, with inhibition ranging from 27.71% to 71.65% (20-80 mg/mL) and an IC_{50} value of 53.69 ± 2.54 mg/mL (Figure 33B). Ascorbic acid, a standard, was utilized as a reference Figure 33A.

Table 11 IC_{50} values for hydroxyl radical scavenging activity in the heated water extract of *E. latifolia* fruits.

% Inhibition on hydroxyl radical	Concentrations (mg/mL)				IC_{50}
	20	40	60	80	
Fruit extract	27.71±4.61	31.73±1.73	59.95±2.10	71.65±1.37	53.69±2.54 mg/mL
STD Ascorbic acid	-	-	-	-	364.78±4.84 ng/mL

Standard Ascorbic acid was prepared at concentrations ranging from 50 to 500 ng/mL.

A

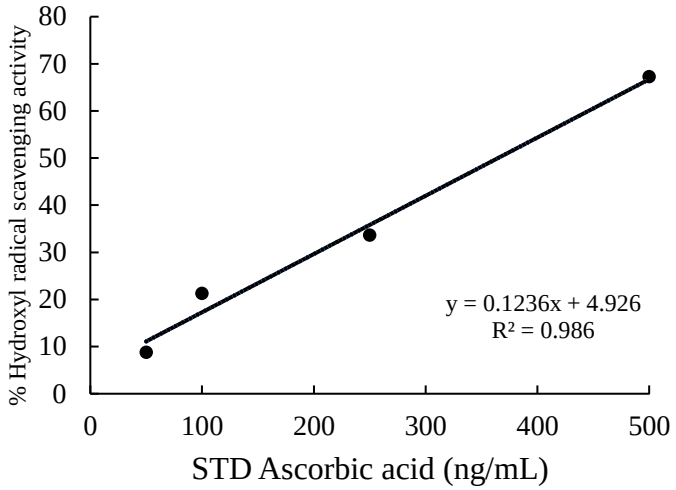

B

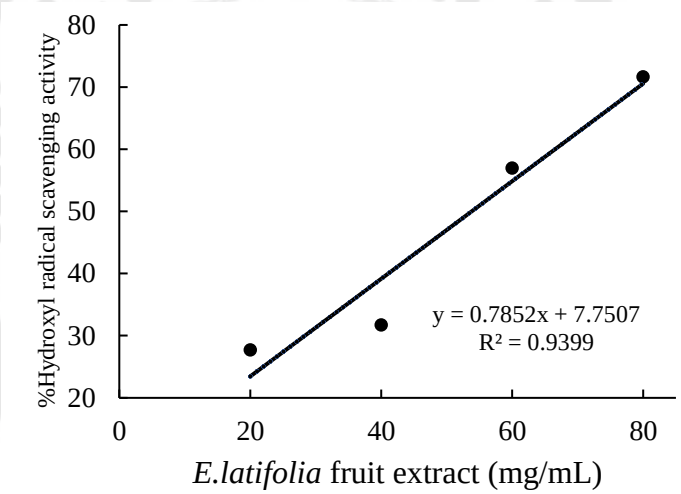

Figure 33 Percentage hydroxyl radical inhibition of (A) standard Ascorbic acid and (B) the heated water extract of *E. latifolia* fruits at various concentrations.

At 20 mg/mL, the extract demonstrated 27.71% hydroxyl radical inhibition. At 40 mg/mL, the inhibition increased to 31.73%. As the concentration increased, the extract continued to show enhanced performance, achieving 59.95% inhibition at 60 mg/mL. At the highest concentration tested (80 mg/mL), the extract reached 71.65%

inhibition. The IC_{50} value of the extract indicates its capacity to neutralize hydroxyl radicals, requiring a

concentration of 53.69 ± 2.54 mg/mL to achieve 50% inhibition. These results emphasize the effective hydroxyl radical scavenging potential of the *E. latifolia* fruit extract.

4.4.8. Nitric oxide radical scavenging activity

The evaluation of nitric oxide radical scavenging capability demonstrated that the extract displayed concentration-dependent scavenging activities, which ranged from 31.02% to 58.06% (20-50 mg/mL). The IC_{50} value for the extract was determined to be 41.51 ± 1.55 mg/mL (Figure 34B). The gallic acid positive control demonstrated an IC_{50} value of 63.24 ± 2.99 µg/mL (Figure 34A).

Table 12 IC_{50} values for NO radical scavenging activity in the heated water extract of *E. latifolia f*ruits

% Inhibition on NO free radical	Concentrations (mg/mL)				IC_{50}
	20	30	40	50	
Fruit extract	31.02±3.06	39.31±3.02	48.02±1.77	58.06±2.14	41.51±1.55 mg/ml
STD Gallic acid	-	-	-	-	66.65±3.53 µg/ml

Standard Gallic acid was prepared at concentrations ranging from 40 to 100 µg/mL.

A

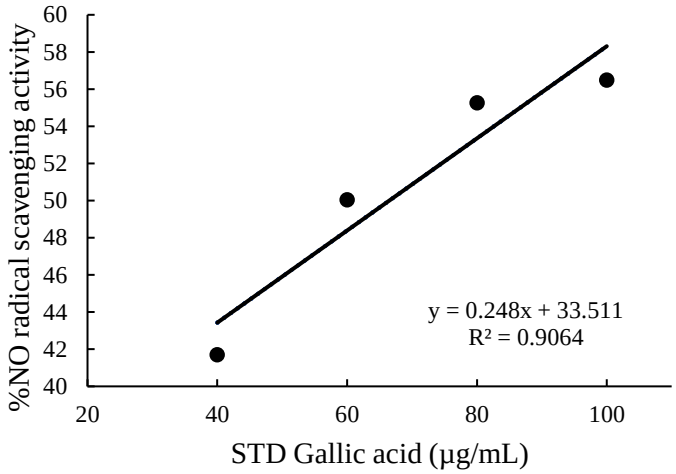

B

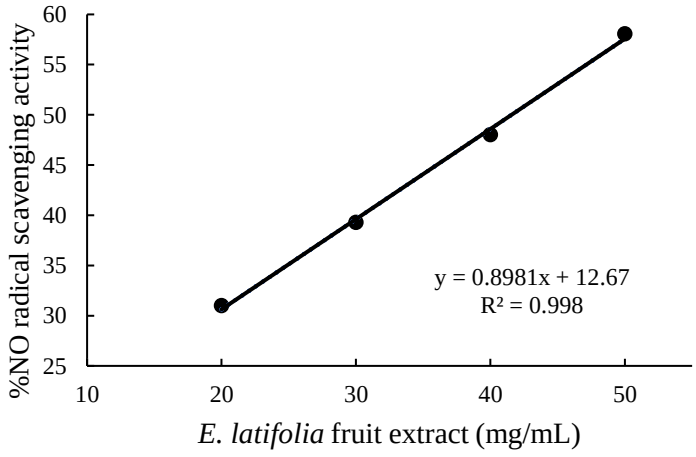

Figure 34 Percentage of NO radical scavenging activity of (A) standard Gallic acid and (B) the heated water extract of *E. latifolia* fruits at various concentrations.

At the lowest concentration (20 mg/mL), the extract achieved scavenging efficiency of 31.02%. At the maximum concentration (50 mg/mL), the extract achieved a scavenging activity of 58.06%. The IC_{50} value for the extract was determined to be 41.51± 1.55 mg/mL, indicating its effective capacity to nitric oxide scavenging capacity of the *E. latifolia* fruit extract

4.4.9 Hydrogen peroxide scavenging activity

The capacity of the *E. latifolia* fruit extract to scavenge hydrogen peroxide (H_2O_2) was evaluated quantitatively (Table 13). The extract also exhibited concentration-dependent activity ranging from 12.59% to 68.50% at concentrations of 1.25 to 10 mg/mL, with an IC_{50} value of 6.88 ± 0.26 mg/mL (Figure 35B). Ascorbic acid, used as a standard, exhibited superior scavenging potential with an IC_{50} value of 88.52 ± 1.88 ng/mL (Figure 35A).

Table 13 IC_{50} values for H_2O_2 scavenging activity in the heated water extract of *E. latifolia* fruits

% Inhibition on H_2O_2	Concentrations (mg/mL)				IC_{50}
	1.25	2.5	5	10	
Fruit extract	12.59±1.31	28.62±2.94	37.52±0.61	68.50±1.84	6.88±0.26 mg/ml
STD Ascorbic acid	-	-	-	-	88.52±1.88 ng/ml

Standard Ascorbic acid was prepared at concentrations ranging from 5 to 100 ng/mL.

A

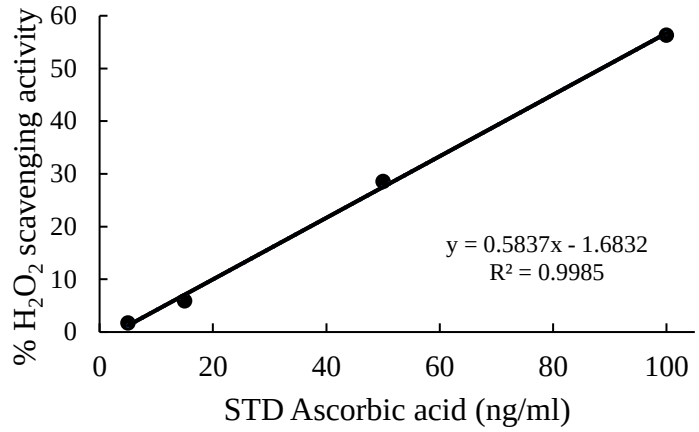

B

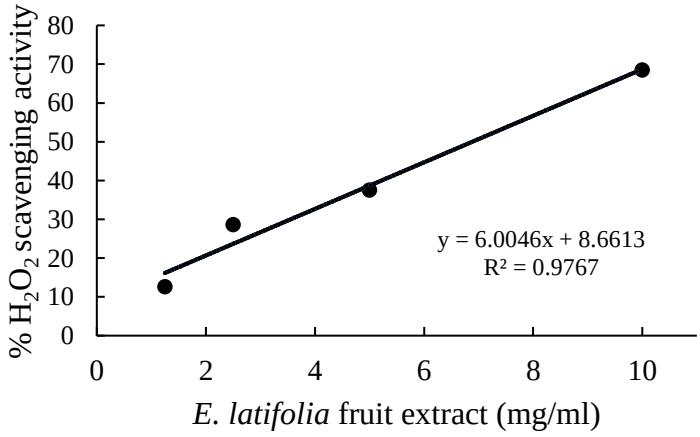

Figure 35 Percentage of H_2O_2 scavenging activity of (A) standard ascorbic acid and (B) the heated water extract of *E. latifolia* fruits at various concentrations.

At the lowest concentration (1.25 mg/mL), the extract achieved scavenging efficiency of 12.59%. At the highest concentration tested (10 mg/mL), the extract demonstrated a scavenging activity of 68.50%. The IC_{50} value for the extract was determined to be 6.88 ± 0.26 mg/mL, indicating its effective capacity to neutralize hydrogen peroxide. These findings demonstrate the substantial hydrogen peroxide scavenging potential of the *E. latifolia* fruit extract.

Table 14 Total phenolic, flavonoid, and antioxidant activities IC_{50} values of the heated water extract of *E. latifolia* fruits.

Assessment	*E. latifolia* fruit extract (mg/mL)	Standard			
		Gallic acid (µg/mL)	EDTA (mg/mL)	Trolox (mg/mL)	Ascorbic acid (ng/mL)
Total phenolic content	24.38±0.40[a]	-	-	-	-
Total flavonoid content	0.13±0.06[b]	-	-	-	-
DPPH radical scavenging activity	14.01± 0.60	-	-	-	0.101±0.002 (mg/mL)
ABTS radical scavenging activity	1.18± 0.03	-	-	0.169±0.002	-
Ferrous ion chelation activity	-	-	0.18±0.01		-
Ferric reducing antioxidant power	64.07±0.01[c]	-	-		-
Lipid peroxidation inhibition	14.23±1.75	-	-	0.048±0.001	-
Superoxide radical scavenging activity	20.99±1.55	-	-	0.114±0.005	-
Hydroxyl radical scavenging activity	53.69±2.54	-	-	-	364.78±4.84
Nitric oxide radical scavenging activity	41.51±1.55	66.65±3.53	-	-	-
Hydrogen peroxide scavenging activity	6.88±0.26		-	-	88.52±1.88

Results expressed as mean ± SD, [a] mg GAE/g extract [b] mg QE/g extract [c] mg TE/g extract.

4.5. *In vitro* cell-based study of *E. latifolia* fruit extract

4.5.1 Effect of *E. latifolia* fruit extract on cell viability of human submandibular gland (HSG) cells

Assessing the toxicity of *E. latifolia* fruit extract in HSG (HTB-41) cells is a crucial step to confirm that only non-toxic concentrations are employed in subsequent experiments. Due to their relevance in pharmacological studies, HSG cells originating from the human submandibular gland were selected as an appropriate model for toxicity assessment.

To determine the non-cytotoxic concentrations, HSG cells were treated with the extract at varying concentrations ranging from 0 to 100 µg /mL. Cell viability was measured after 24 hours using a resazurin cell viability assay. The results indicated that the extract did not significantly alter cell viability across the tested concentration range compared to the untreated control ($p>0.05$) (Figure 36). This finding confirms that the extract does not cause cytotoxicity or induces proliferation in HSG cells. It ensures that any observed effects in further experiments can be directly attributed to the extract's specific properties rather than to cellular stress or growth stimulation.

Based on these findings, concentrations of 25, 50, and 100 µg/mL were chosen for subsequent experiments to evaluate the pharmacological activity of the extracts, as these concentrations showed no toxicity to HSG cells.

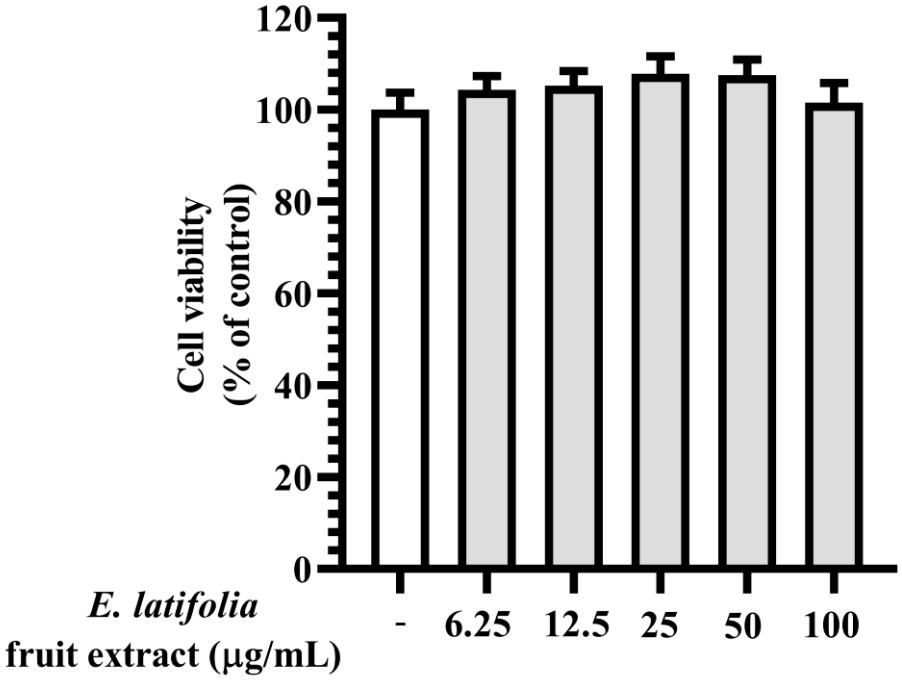

Figure 36 Cell viability of the heated water extract of *E. latifolia* fruits at various concentrations. Data are expressed as mean ± SEM (n = 4).

4.5.2 Effect of tert-butyl hydroperoxide (t-BHP) on cell viability of human submandibular gland cells

Cytotoxicity testing of t-BHP in HSG cells is a crucial step in determining safe concentrations that induce oxidative stress without markedly affecting cell viability. This ensures that the effects observed in subsequent experiments are specifically attributed to the targeted biochemical pathways rather than to excessive toxicity.

To evaluate the cytotoxicity of t-BHP, cell viability assays were performed on HSG cells using various concentrations and exposure times. The experimental design involved treating HSG cells with a range of t-BHP concentrations, from 0.07 to 5 mM for 4, 6, and 24 hours. Cell viability was then measured using the resazurin cell viability assay, and the results were expressed as a percentage of the untreated control. The viability of HSG cells under these conditions was illustrated in Figure 37.

After 4 h of incubation, the effect on HSG cell viability was mild (not especially pronounced). Viability decreased slightly from 94.59±0.28% at 0.07 mM to 75.83±0.29% at 5 mM, compared to 100% viability in the untreated control. In contrast, 24-h exposure to t-BHP resulted in a dramatic decrease in cell viability, with 97.42±1.51% cell death at 0.07 mM and 7.05 ±0.04% cell death at 5mM. For the 6-hour exposure, cell viability gradually decreased from 90.80± 0.37% at 0.07mM to 42.40 ±0.14% at 5mM.

Based on these results, a 6-h incubation period and a t-BHP concentration of 0.4 mM (400 μM) were determined to be the optimal conditions for subsequent experiments in this study. At this concentration, cell viability was approximately 55.64±0.22%, providing an appropriate balance between inducing cellular stress and maintaining sufficient cell survival for further analysis.

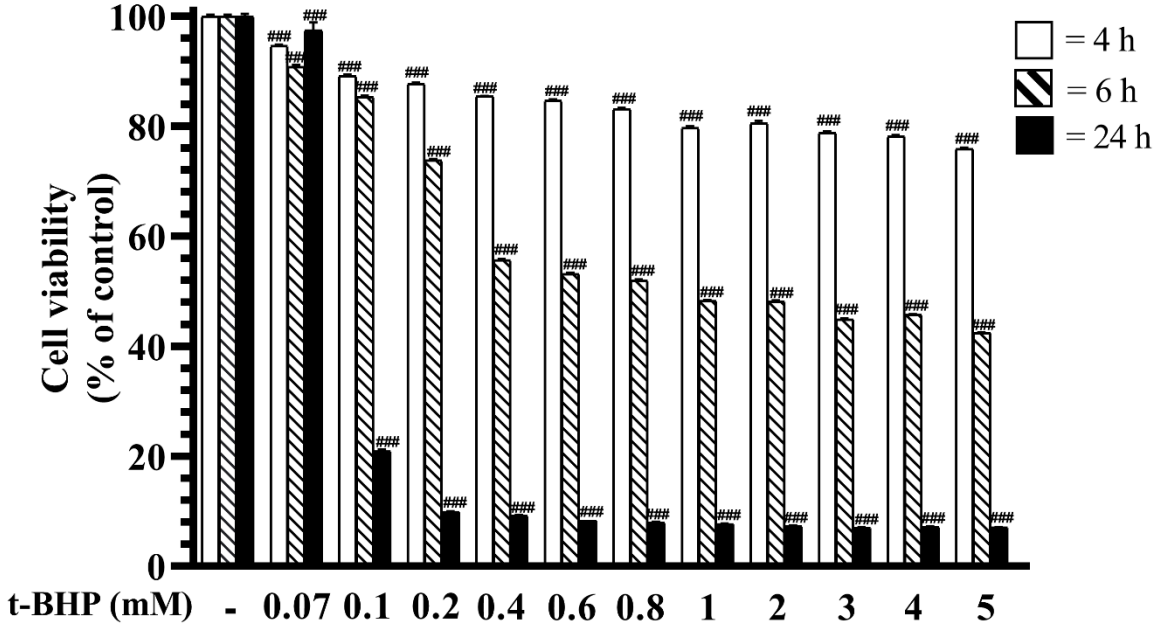

Figure 37 Cytotoxic effect of t-BHP on relative HSG cell viability induced by various concentrations (0 to 5 mM) and exposure times (4, 6 and 24 h).

Data are presented as mean ± SEM ($n \geq 4$).

$^{###}p<0.001$ compared with untreated control group.

4.5.3 Effect of *E. latifolia* fruit extract on t-BHP-induced toxicity in HSG cells

The t-BHP-induced oxidative damage in HSG cells was used as a model to determine the protective effect of the *E. latifolia* fruit extract. Exposure to 400μM t-BHP was for 6 h significantly decreased percent cell viability ($p < 0.001$) compared to the untreated control group (Figure 38).

Co-treatment of HSG cells with the extract and t-BHP showed significant improvements in cell viability. At concentration of 25, 50, and 100 μg/mL, cell viability was 79.21 ±1.22, 88.98 ±0.82, and 96.60± 0.74, respectively (all $p<0.001$), compared to the t-BHP alone group (Figure 38).

These results indicate that the extract significantly enhances cell viability at all tested concentrations, demonstrating protective effects against t-BHP-induced oxidative damage in HSG cells. This supports their use in further experiments to maximize antioxidant benefits.

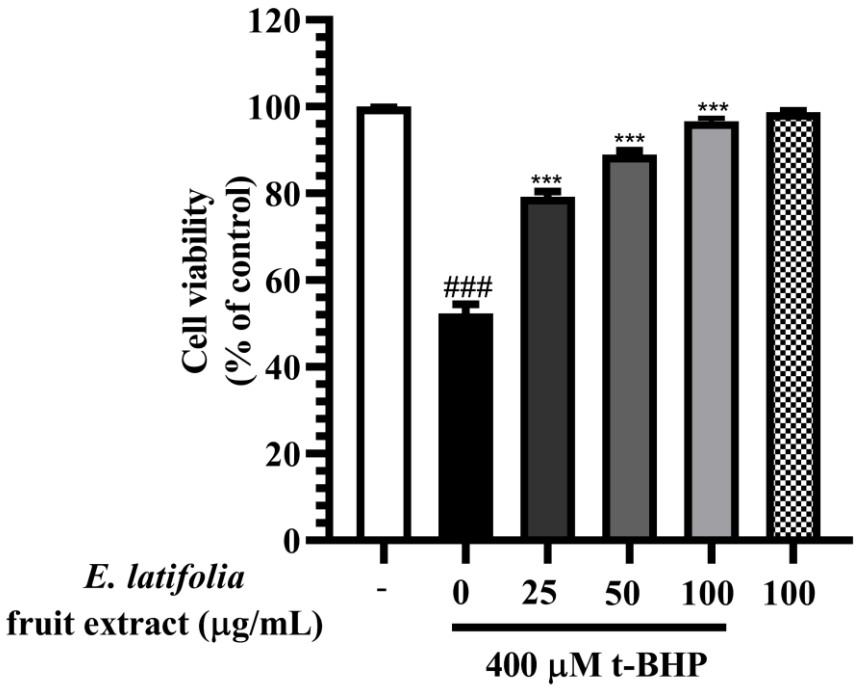

Figure 38 Protective effect of the heated water extract of *E. latifolia* fruits on t-BHP-induced HSG cell viability.

Values were represented as mean ± SEM ($n \geq 4$); $^{###}p<0.001$ as compared with untreated control group; $^{***}p<0.001$ as compared with only t-BHP treated group.

4.5.4 Effect of the *E. latifolia* fruit extract on t-BHP-induced HSG cells apoptosis

4.5.4.1 Morphological assessment of apoptosis using phase contrast and Hoechst 33342 staining

Phase contrast microscopy was used to observe live, unstained cells, providing insight into their natural state without the need for dyes or labels that could potentially alter cellular behavior. Moreover, Hoechst 33342 staining was utilized to visualize nuclear chromatin under a confocal microscope. This technique allowed for the identification of apoptotic characteristics, such as fragmentation and chromatin condensation, offering a more detailed view of nuclear structure and organization.

In Figure 39A and 39B, the cells exposed to 400 µM t-BHP demonstrated markedly condensed and fragmented nuclear chromatin, indicative of apoptosis. In contrast, cells treated with the highest concentration of *E. latifolia* fruit extract (100 µg/mL) showed some degree of chromatin condensation and fragmentation, but to a lesser extent than t-BHP-treated cells. Regarding cell morphology, untreated control cells displayed typical characteristics: flat, polygonal shapes with round, central nuclei and low fluorescence intensity when stained with Hoechst dyes. These cells were closely connected with clear outlines. Exposure to 400 µM t-BHP caused significant cell morphological changes, including increased roundness, reduced size, looser intercellular connections, and significantly and heightened fluorescence intensity of Hoechst dyes. In contrast, co-treatment with the extract (100 µg/mL) resulted in cell morphology more like untreated cells, with lower intensity of Hoechst dyes, compared to t-BHP-treated cells. Moreover, the extract effectively alleviated t-BHP-induced oxidative stress, exhibiting antioxidant effects. Cells treated with the extract were larger and more polygonal with rounded nuclei, in contrast to the smaller, altered shape of t-BHP-treated cells.

A

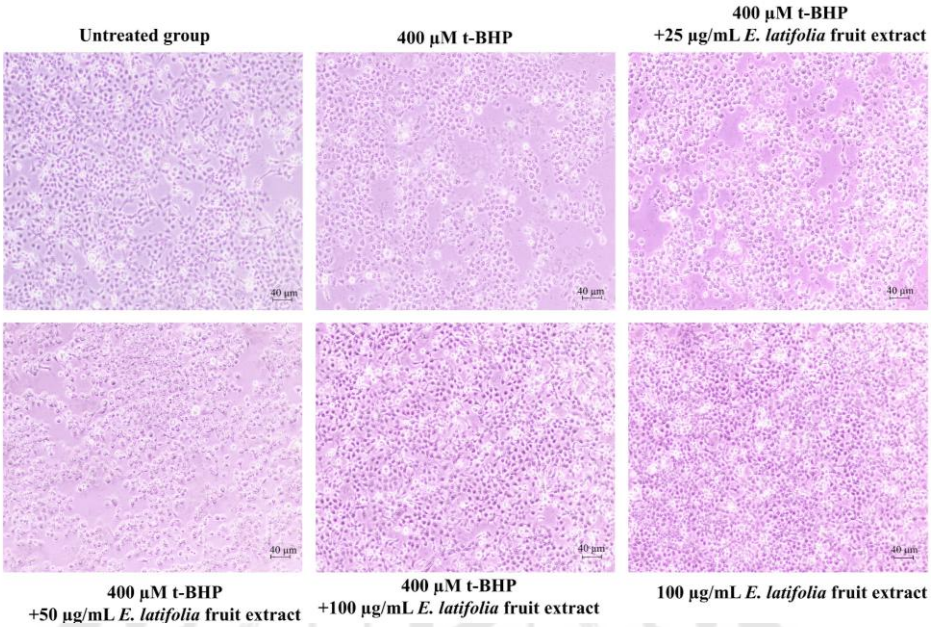
Untreated group
400 µM t-BHP
400 µM t-BHP
+25 µg/mL E. latifolia fruit extract
40 µm
400 µM t-BHP
+50 µg/mL E. latifolia fruit extract
400 µM t-BHP
+100 µg/mL E. latifolia fruit extract
100 µg/mL E. latifolia fruit extract

B

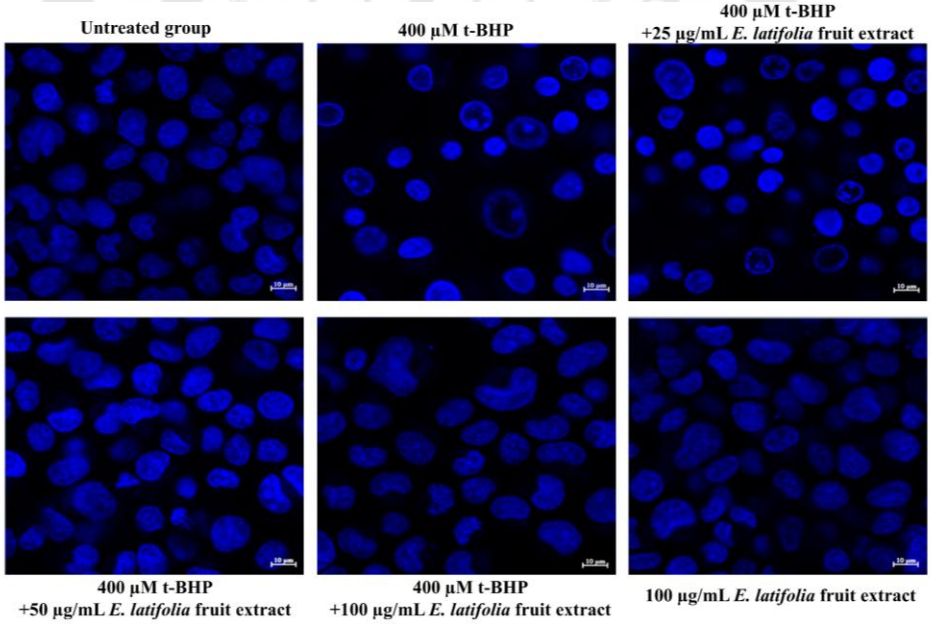
Untreated group
400 µM t-BHP
400 µM t-BHP
+25 µg/mL E. latifolia fruit extract
10 µm
400 µM t-BHP
+50 µg/mL E. latifolia fruit extract
400 µM t-BHP
+100 µg/mL E. latifolia fruit extract
100 µg/mL E. latifolia fruit extract

Figure 39 (A) Morphological features and (B) nuclear alterations stained with Hoechst 33342 during apoptosis in HSG cells, visualized using phase contrast (scale bar: 20 μm) and confocal laser scanning microscope (scale bar: 10 μm; Zeiss, Germany).

4.5.4.2 Analysis of cell death using Acridine Orange (AO)/Ethidium Bromide (EB) Staining

Apoptotic morphological changes were identified through acridine orange-ethidium bromide (AO/EB) fluorescent staining of t-BHP-induced HSG cell and compared with the extract treatment. The AO/EB staining method reveals cellular states through color: green nuclei indicate viable cells, green nuclei signify viable cells, greenish-yellow nuclei indicate early apoptosis, condensed orange-red nuclei denote late apoptosis, and bright red is indicative of dead cells.

Figure 40 indicated that the untreated cells and the group treated with 100 μg/mL *E. latifolia* fruit extract alone appeared with normal nuclei, almost entirely presenting bright green. In contrast, cells treated with 400μM t-BHP showed significantly increased intensity of orange and red fluorescence, indicating hallmark signs of apoptosis, including condensed chromatin, fragmented nuclei, formation of apoptotic bodies, and membrane blebbing. These distinctive features were clearly observable in the AO/EB-stained cells, providing significant evidence of the apoptotic process.

Combination treatment of 400μM t-BHP and *E. latifolia* fruit extract significant decreased red fluorescence while increasing green fluorescence in dose-dependent manner. This effect was most pronounced at the highest concentration (100 μg/mL), where cell morphology was similar to the extract-alone group when compared with the t-BHP-induced group.

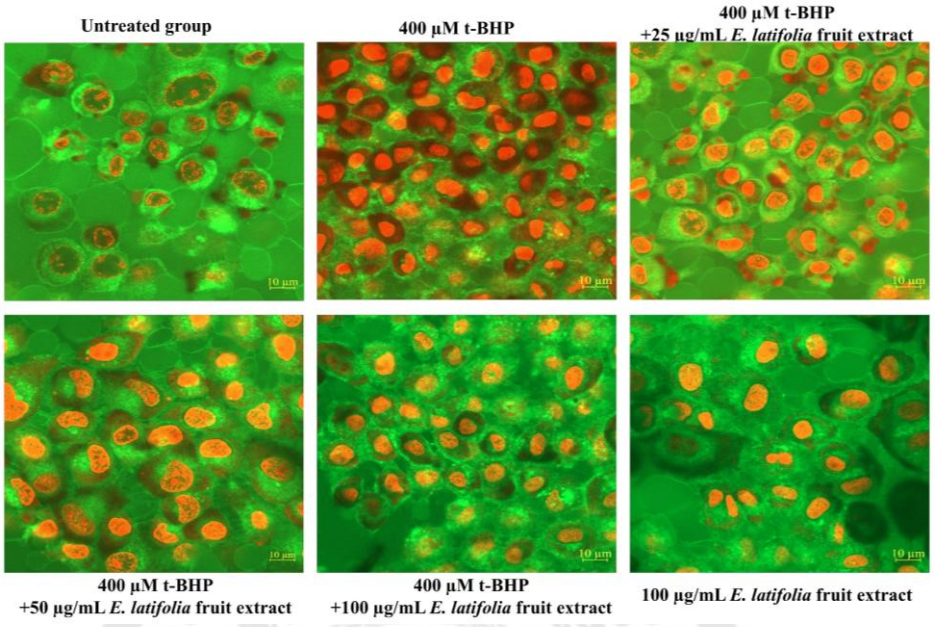

Figure 40 Apoptotic morphology detection by acridine orange-ethidium bromide (AO/EB) fluorescent staining of HSG cells visualized using confocal laser scanning microscope (scale bar: 10 µm; Zeiss, Germany).

4.5.5 Effect of *E. latifolia* fruit extract on t-BHP-induced intracellular ROS

The preventive effect of the extract on intracellular ROS induced by t-BHP was evaluated by measuring fluorescent intensity of DCF. As illustrated in Figure 41, t-BHP, a known inducer of oxidative stress, significantly increased intracellular ROS levels, resulting in the highest intensity of green fluorescence observed (Figure 41A). Quantitatively, the ROS-related fluorescence intensity increased to 3.66 ± 0.14-fold compared to the control group (p<0.001) (Figure 41B).

In contrast, the combination of t-BHP with *E. latifolia* at 100 µg/mL dramatically reduced the green fluorescence intensity, indicating a substantial decrease in ROS production down to 1.22 ± 0.06-fold of the control. Similarly, lower concentration of the extract at 25 and 50 µg/mL were able to gradually lower the fluorescence and significantly decreased the ROS levels to 2.62 ± 0.10 and 1.85± 0.22-folds of the control, respectively (p<0.001), compared to t-BHP group. These findings demonstrate that the extract's ability to reduce intracellular ROS in a statical significance. Moreover, treatment with the extract alone did not increase intracellular ROS generation, producing an effect similar to the untreated control group (p=0.872).

A

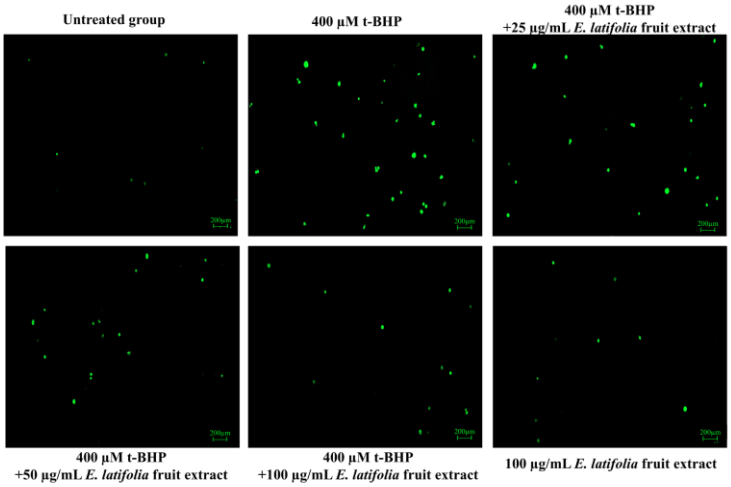

B

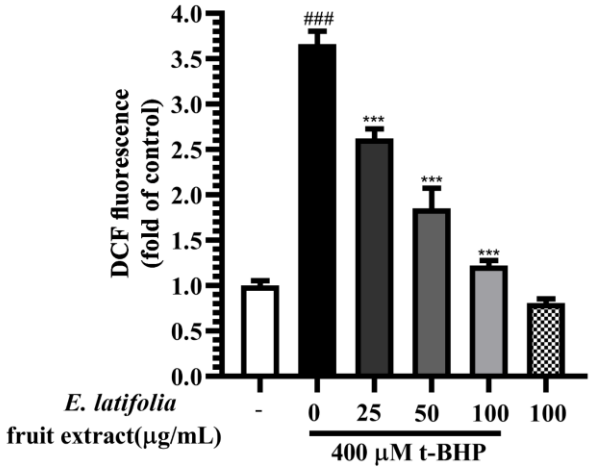

Figure 41 Antioxidant effect of the heated water extract of *E. latifolia* fruits on intracellular ROS of t-BHP-induced cells oxidative stress. (A) Fluorescence images and (B) the percentage of DCF fluorescence intensity.

Values were represented as mean ± SEM (n = 4); $^{###}p<0.001$ as compared with untreated control group; $^{***}p<0.001$ as compared with only t-BHP treated group.

4.5.6 Effect of *E. latifolia* fruit extract on mRNA expression of salivary genes in t-BHP-induced HSG cells using real-time RT-PCR analysis

4.5.6.1 Effect *of E. latifolia* fruit extract on Bax and Bcl-2 mRNA expression

The effect of the extract on cellular apoptosis was investigated by measuring the Bax/Bcl-2 mRNA expression ratio in t-BHP-induced HSG cells. As illustrated in Figure 42, treatment with 400 µM t-BHP significantly increased the Bax/Bcl-2 mRNA ratio to 6.33 ± 0.67 compared to untreated control group *(p*<0.001). Conversely, combining 400 µM t-BHP with various concentrations of the extract (25, 50, and 100 µg/mL) resulted in a gradual reduction of the Bax/Bcl-2 mRNA ratio, with relative expression levels of 4.29 ± 0.30, 1.94 ± 0.17, and 1.18 ± 0.05-folds of the control, respectively. This indicated a significant decrease in Bax/Bcl-2 mRNA expression compared to t-BHP-induced cells alone, with reductions being statistically significant at *p*<0.01, *p*<0.001, and *p*<0.001, respectively.

Treatment with *E. latifolia* extract alone did not significantly alter the Bax/Bcl-2 ratio compared to untreated cell (*p*>0.999). These findings suggest that *E. latifolia* fruit extract effectively reduces the Bax/Bcl-2 ratio at the mRNA expression level, thereby shifting the balance between pro- and anti-apoptotic factors towards cell survival.

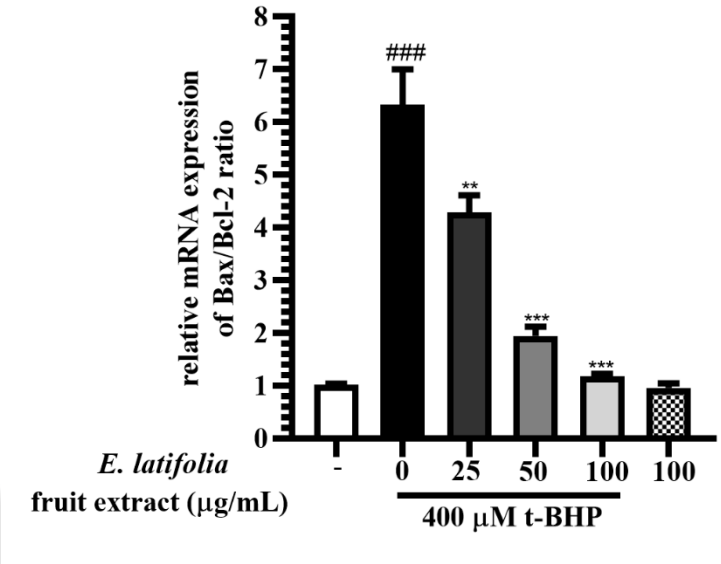

Figure 42 The relative mRNA expression levels of Bax/Bcl-2 ratio in t-BHP induced HSG cells and the co-treatment with the heated water extract *E. latifolia* fruits. GAPDH was used as the internal control.

Values were represented as mean ± SEM (n = 4); $^{###}p<0.001$ as compared with untreated control group; $^{**}p<0.01$ and $^{***}p<0.001$ as compared with only t-BHP treated group.

4.5.6.2 Effect of *E. latifolia* fruit extract on AQP5 mRNA expression

The modulation of AQP5 mRNA expression in t-BHP-induced HSG cells by *E. latifolia* fruit extract was explored, as illustrated in Figure 43. This study found that combining 400 µM t-BHP with 25 µg /mL of the extract slightly increased AQP5 gene expression, but the change was not significant compared to t-BHP alone (p=0.448), with relative expression at 0.80 ± 0.05-fold of the control.

However, higher concentrations of the extract (50 and 100 µg /mL) led to a significant increase in AQP5 gene expression, with relative levels at 0.97 ±0.05 and 1.25 ± 0.11-fold of the control, respectively, compared to cells treated with t-BHP alone (p<0.05 and p<0.001, respectively).

The extract alone group at 100 µg /mL significantly enhanced AQP5 mRNA expression to 1.75± 0.09-fold of the control, compared to both untreated and t-BHP alone (p<0.001). In contrast, the t-BHP alone group showed a marked decrease in AQP5 expression compared to untreated control, with relative expression of 0.59 ±0.10 (p<0.01). The results suggest a trend of *E. latifolia* fruit extract to upregulate AQP5 expression in t-BHP-induced HSG cells.

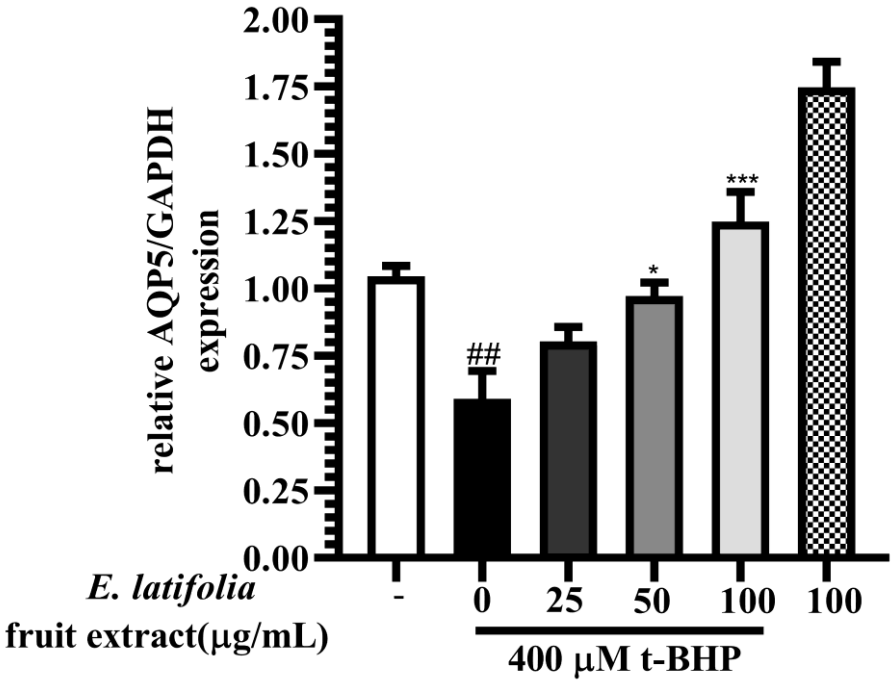

Figure 43 The relative mRNA expression levels of AQP5 in t-BHP induced HSG cells and the co-treatment with the heated water extract of *E. latifolia* fruits. GAPDH was used as the internal control.

Values were represented as mean ± SEM (n = 4); $^{\#\#}p<0.01$ compared to untreated control group; $^{*}p<0.05$ and $^{***}p<0.001$ as compared with only t-BHP treated group.

4.5.6.3 Effect of *E. latifolia* fruit extract on AMY1 mRNA expression

The effect of *E. latifolia* fruit extract on AMY1 mRNA expression in t-BHP-induced HSG cells was investigated. Results revealed that HSG cells treated with 400 µM t-BHP exhibited a significant decrease in AMY1 expression compared to the untreated control group, with a relative expression of 0.29 ± 0.06 (p<0.001) (Figure 44).

In contrast, combining 400 µM t-BHP with three concentrations of the extract (25, 50, and 100 µg/mL) led to a significant increase in AMY1 expression levels compared to t-BHP-induced cells alone, with a relative expression levels were 0.49 ± 0.03, 0.58 ± 0.05 and 0.90 ± 0.03-fold of the control, respectively, with statistical significance of p<0.05, p<0.01, and p<0.001, respectively. While treatment with the extract alone at 100 µg/mL showed no significant difference in AMY1 gene expression compared to untreated cells (p=0.897).

These observations indicate that *E. latifolia* fruit extract may upregulate AMY1 expression in t-BHP-induced HSG cells in a dose-dependent manner. In particular, the 100 µg/mL concentration of the extract markedly enhanced AMY1 expression levels, suggesting a potential preventive effect against t-BHP-induced dysfunction in HSG cells. Moreover, the gene expression analysis demonstrated that all tested concentrations significantly elevated AMY1 levels in t-BHP-treated HSG cells, implying that the extract could support salivary function following oxidative stress exposure.

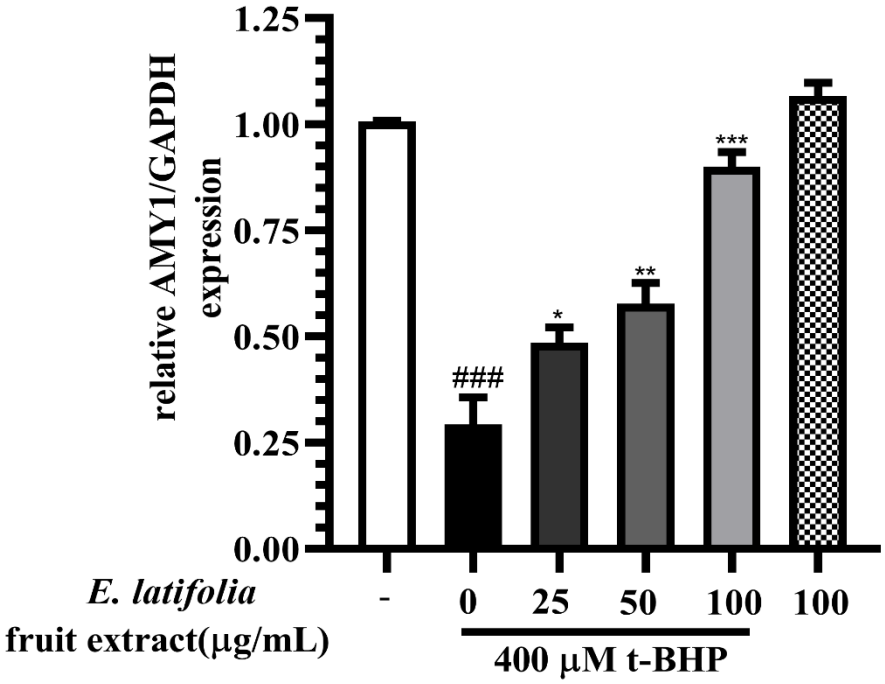

Figure 44 The relative mRNA expression levels of AMY1 in t-BHP induced HSG cells and the co-treatment with the heated water extract of *E. latifolia* fruits. GAPDH was used as the internal control.

Values were represented as mean ± SEM (n = 4); $^{###}p<0.001$ as compared with untreated control group; $^{*}p<0.05$, $^{**}p<0.01$ and $^{***}p<0.001$ as compared with only t-BHP treated group.

4.5.7 Effect of *E. latifolia* fruit extract on protein expression in t-BHP-induced HSG cells using western blot analysis

4.5.7.1 Effect of *E. latifolia* fruit extract on Bax and Bcl-2 protein expression

To investigate the effect of the extract on t-BHP-induced HSG cells involving the apoptotic signaling pathway of the Bcl-2 family, the Bax/Bcl-2 protein expression ratio was measured using GAPDH as an internal reference, as shown in Figure 45. Treatment with 400 µM t-BHP significantly increased the Bax/Bcl-2 ratio to 2.98 ± 0.21 compared to the untreated control group *(p*<0.001). In contrast, combining 400 µM t-BHP with extracts at 25, 50, and 100 µg/mL resulted in a gradual decrease in the Bax/Bcl-2 ratio compared to t-BHP alone, with levels at 2.30 ± 0.14, 1.40 ± 0.19, and 1.04 ± 0.12-folds of the control, respectively. This demonstrated a trend of decreasing the Bax/Bcl-2 protein expression ratio, with a statistical significance at *p*<0.01, *p*<0.001, and *p*<0.001, respectively.

Treatment with the extract alone did not significantly change the Bax/Bcl-2 ratio compared to untreated group. These findings suggest that *E. latifolia* fruit extract effectively lowered the Bax/Bcl-2 ratio at the protein expression level, potentially diminishing apoptotic signaling pathway and enhanced cell survival.

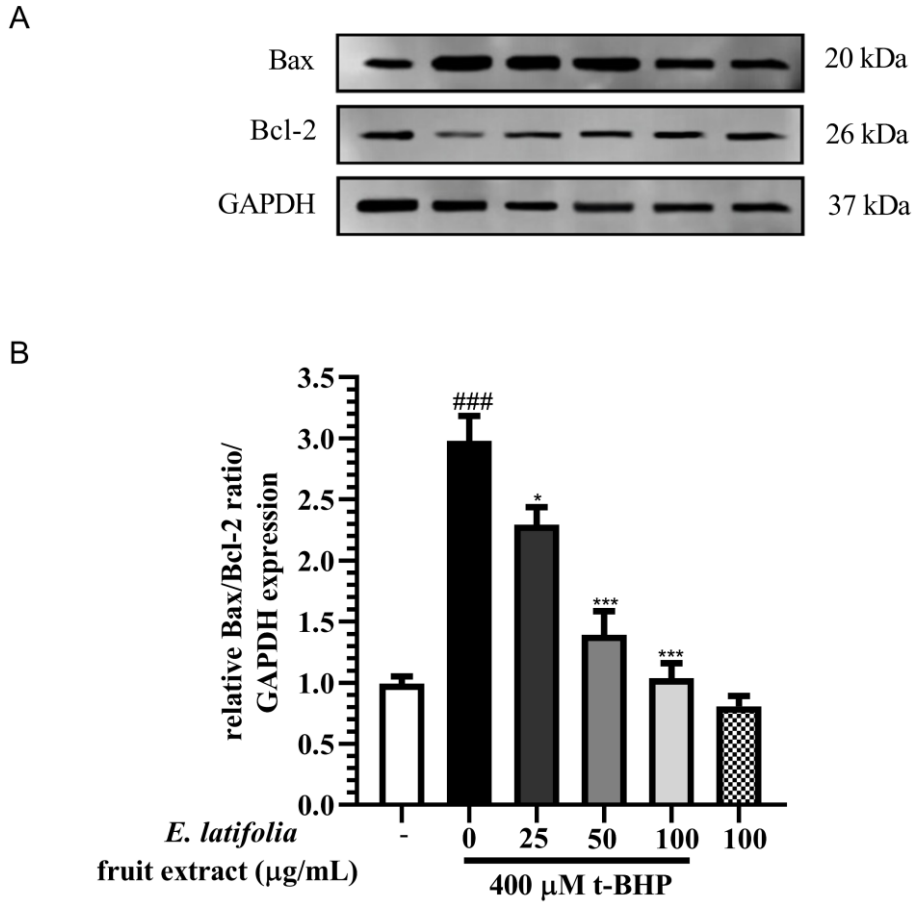

Figure 45 Relative expression of Bax/Bcl-2 ratio in t-BHP induced HSG cells and the co-treatment with the heated water extract of *E. latifolia* fruits. (A) Representative protein bands of Bax, Bcl-2, and GAPDH. (B) Bax/Bcl-2 ratio normalized to GAPDH protein levels

Values were represented as mean ± SEM (n = 4); $^{###}p<0.001$ as compared with untreated control group; $^{*}p<0.05$ and $^{***}p<0.001$ as compared with only t-BHP treated group.

4.5.7.2 Effect of *E. latifolia* fruit extract on phosphorylation of P38 protein expression

The protective effect of *E. latifolia* fruit extract was investigated. In particular, this study examined the phosphorylation levels of P38 (P-P38) under stress conditions induced by t-BHP in HSG cells, as illustrated in **Figure 46**. GAPDH protein was used as an internal reference for this analysis.

P-P38 protein expression significantly increased after treatment with 400 µM t-BHP alone compared to the untreated control group, with a relative expression of 1.66 ± 0.11-fold (p<0.001). The combination of 400 µM t-BHP with 25 µg/mL of the *E. latifolia* fruit extract slightly reduced P-P38 protein expression, but not significantly, with the relative P-P38 expression at 1.51 ± 0.07-fold of the control, compared to t-BHP alone (p=0.548).

However, combining 400 µM t-BHP with the extract at 50 and 100 µg/mL led to a significant decrease in P-P38 protein expression, with relative expression levels of 1.94 ± 0.17 and 1.18 ± 0.05-folds of the control, respectively, compared to t-BHP-induced cells alone. These reductions were statistically significant at p<0.01. *E. latifolia* fruit extract alone at a concentration of 100 µg/mL showed no significant difference in protein expression compared to untreated cells (p=0.826). These results suggest that treatment with the extract demonstrated a trend towards reducing P-P38 protein expression and could effectively decrease its levels even under oxidative stress conditions.

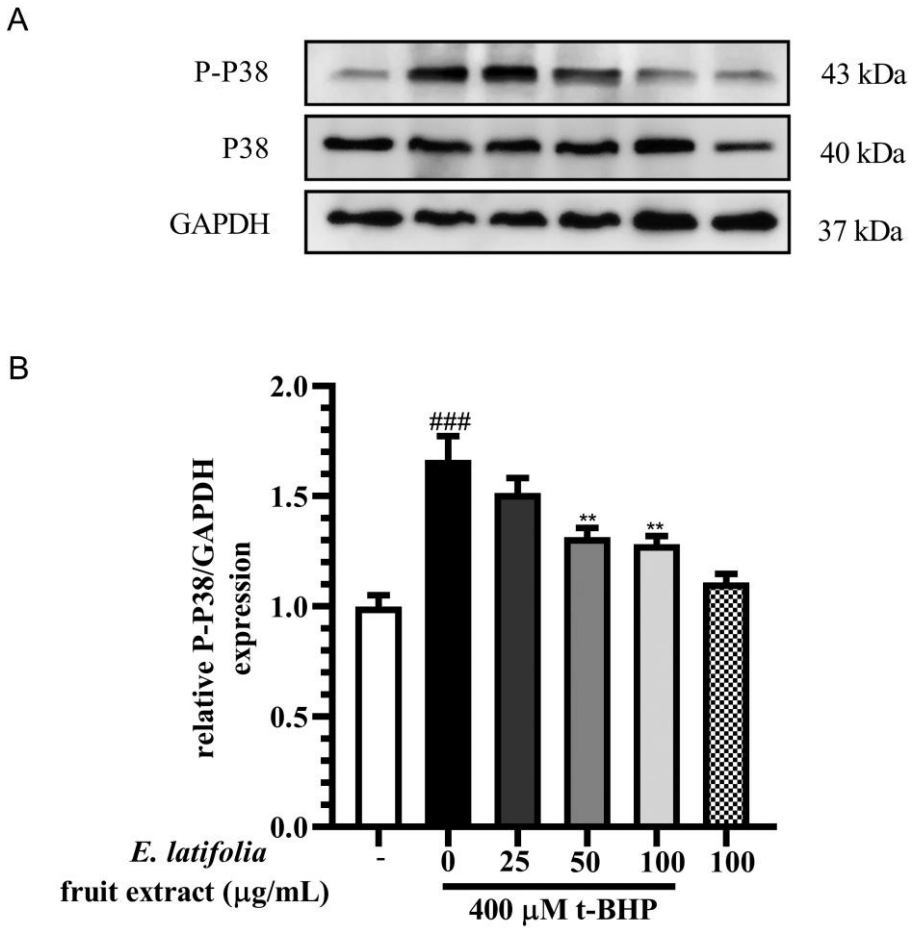

Figure 46 Phosphorylation of P38 expression in t-BHP induced HSG cells and the co-treatment with the heated water extract of *E. latifolia* fruits. (A) Representative protein bands of P-P38, total P38, and GAPDH. (B) Calculation of the P-P38/GAPDH protein ratio.

Values were represented as mean ± SEM (n = 4); $^{###}p<0.001$ as compared with untreated control group; $^{**}p<0.01$ as compared with only t-BHP treated group.

4.5.7.3 Effect of *E. latifolia* fruit extract on caspase-3 protein expression

To investigate the effect of *E. latifolia* fruit extract on t-BHP-induced HSG cells in relation to the apoptotic pathway involving caspase-3 protein changes, this study assessed cleaved caspase-3 protein expression using GAPDH as an internal reference, as shown in Figure 47.

This study found that treatment with t-BHP alone showed a marked increase cleaved caspase-3 protein expression compared to untreated control, with a relative expression of 1.79 ±0.10 fold (p<0.001). The combination of 400 µM t-BHP with 25 µg /mL of the extract showed no difference compared to t-BHP alone (p>0.999), and did not decrease the cleaved caspase-3 protein expression, with relative protein expression at 1.77± 0.18-fold of the control.

However, higher concentrations of the extract (50 and 100 µg /mL) led to a significant decrease in cleaved caspase-3 protein expression, with relative expression at 1.49 ±0.07 and 1.28 ± 0.05-folds of the control, respectively, compared to t-BHP-induced cells alone (p<0.05 and p<0.001, respectively).

The extract alone at 100 µg /mL significantly reduced the protein expression of cleaved caspase-3 compared to t-BHP alone and showed no significant difference to untreated group (p=0.967). The results suggest that the *E. latifolia* fruit extract could downregulate cleaved caspase-3 protein expression under oxidative stress conditions in HSG cells.

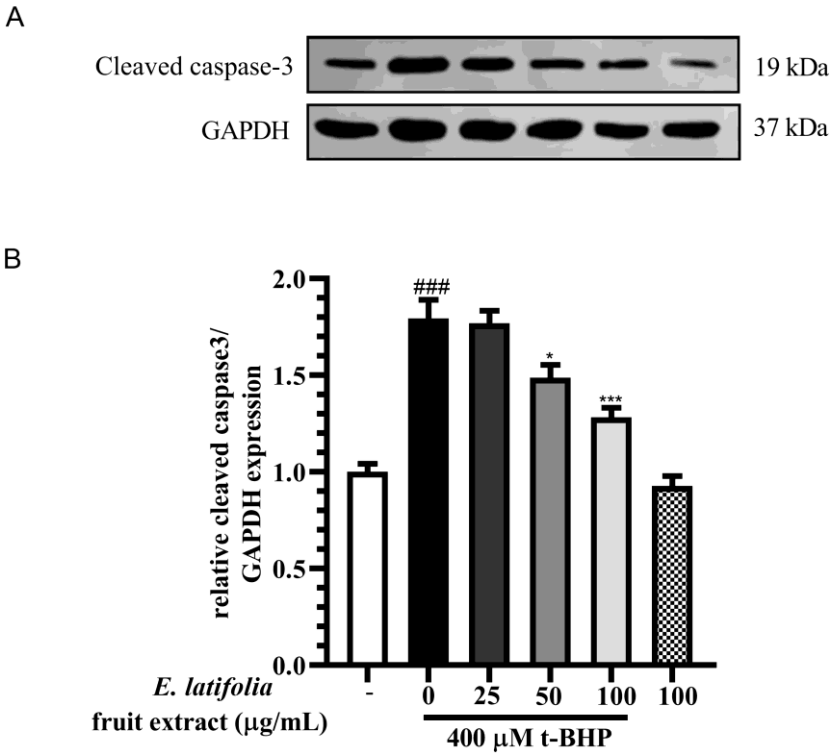

Figure 47 Cleaved caspase-3 protein expression in t-BHP induced HSG cells and the co-treatment with the heated water extract of *E. latifolia* fruits. (A) Representative protein bands of cleaved caspase-3 and GAPDH determined by western blot. (B) Protein ratio calculation of caspase-3 and GAPDH.

Values were represented as mean ± SEM (n = 4); $^{###}p<0.001$ as compared with untreated control group; $^{*}p<0.05$ and $^{***}p<0.001$ as compared with only t-BHP treated group.

4.5.7.4 Effect of *E. latifolia* fruit extract on AQP5 protein expression

The effect of *E. latifolia* fruit extract on water channel protein aquaporin-5 (AQP5) was investigated by measuring the AQP5 protein expression under stress conditions induced by t-BHP in HSG cells, using GAPDH as an internal reference, as shown in Figure 48.

Treatment with 400 µM t-BHP significantly decreased the AQP5 protein expression level to 0.60 ± 0.04 compared to the untreated control group *(p*<0.001). Conversely, combining 400 µM t-BHP with the extract (25, 50, and 100 µg/mL) resulted in a gradual elevation of the expression levels compared to t-BHP-induced cells alone, with relative expression levels of 0.88 ± 0.04, 0.93 ± 0.04, and 0.97 ± 0.05-folds of the control, respectively. This indicated a marked increase in AQP5 protein expression, with statistical significance at *p*<0.01, *p*<0.001, and *p*<0.001, respectively.

Treatment with the extract alone did not significantly change the AQP5 protein expression compared to the untreated group. These findings suggest that the extract treatment effectively increased the AQP5 water channel at the protein expression, thereby potentially rescuing AQP5 protein levels under t-BHP induced cellular oxidative damage.

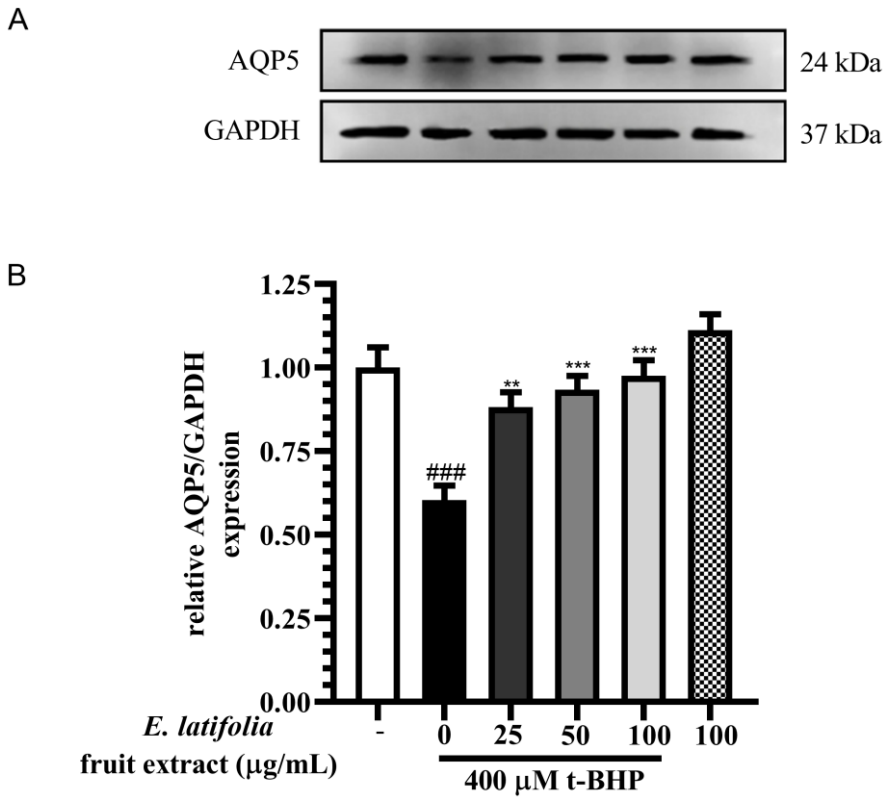

Figure 48 Aquaporin-5 protein expression in t-BHP induced HSG cells and the co-treatment with the heated water extract of *E. latifolia* fruits. (A) Representative protein bands of AQP5 and GAPDH determined by western blot. (B) Protein ratio of AQP5 and GAPDH.

Values were represented as mean ± SEM (n = 4); $^{###}p<0.001$ as compared with untreated control group; $^{**}p<0.01$ and $^{***}p<0.001$ as compared with only t-BHP treated group.

4.5.8 Effect of *E. latifolia* fruit extract on amylase activity in t-BHP-induced HSG cells

The quantification of nitrophenol was performed using calibration curves specific to each time point. For the initial 5-min measurement ($T_{initial}$), the calibration curve equation y=0.0316x+0.0469 was employed, as illustrated in Figure 49. Subsequent time points (T_{final}) varied depending on the sample and utilized distinct equations for calculation, as detailed in Table 15. The complete set of nitrophenol calibration curves for each time point can be found in Figure 55, providing a comprehensive reference for the analytical methodology utilized in this study.

Table 15 Nitrophenol standard curve parameters at each time point.

Time	Equation from STD nitrophenol	R^2
$T_{initial}$ at 5 min	y=0.0316x+0.0469	0.9987
T_{final} at 10 min	y=0.0318x+0.0486	0.9991
T_{final} at 15 min	y=0.0320x+0.0485	0.9991
T_{final} at 20 min	y=0.0322x+0.0489	0.9989
T_{final} at 25 min	y=0.0324x+0.0485	0.9990
T_{final} at 30 min	y=0.0326x+0.0488	0.9989
T_{final} at 35 min	y=0.0327x+0.0468	0.9990
T_{final} at 40 min	y=0.0327x+0.0485	0.9992

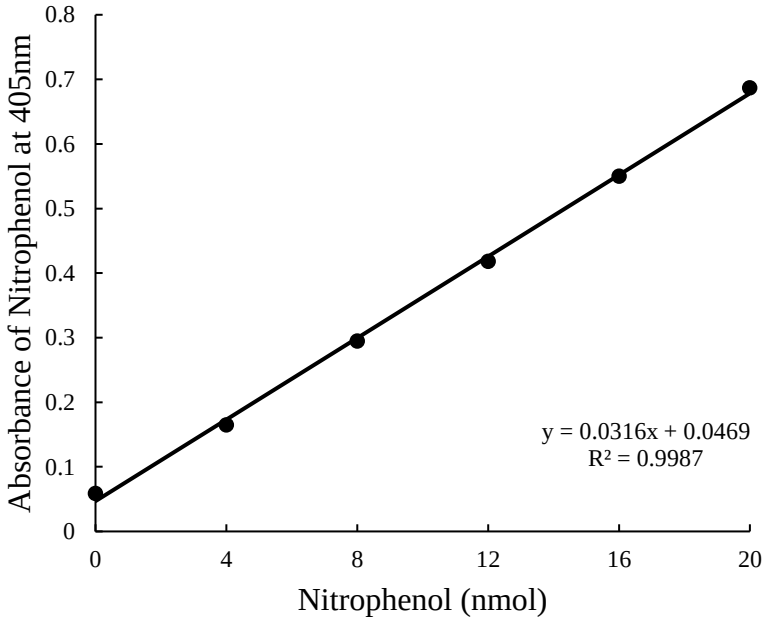

Figure 49 Standard curve of nitrophenol for amylase activity quantification at $T_{initial}$=5 min

Amylase activity in HSG cells under t-BHP-induced stress conditions was evaluated following treatment with *E. latifolia* fruit extract (Figure 50). Quantification was performed using a nitrophenol calibration curve ranging from 4 to 20 nmol (Figure 49). Exposure to 400 μM t-BHP alone significantly reduced amylase activity to 0.85 ± 0.36 nmol/min/mL compared to the untreated control (p<0.001). Co-treatment with 25 μg/mL *E. latifolia* fruit extract slightly increased amylase activity to 1.73 ± 0.39 nmol/min/mL, though this change was not statistically significant (p=0.561). However, higher concentrations of *E. latifolia* fruit extract (50 and 100 μg/mL) in combination with 400 μM t-BHP resulted in significant increases in amylase activity to 4.77 ± 0.46 and 3.87 ± 0.43 nmol/min/mL, respectively (p<0.001 for both). Interestingly, co-treatment with 50 μg/mL of the extract exhibited the most pronounced effect in enhancing amylase activity in t-BHP-induced HSG cells. In addition, the extract treatment alone did not significantly alter amylase activity compared to untreated cells (p>0.999). These findings suggest that the

extract exhibited a protective effect on amylase activity under oxidative stress conditions, potentially mitigating t-BHP-induced cellular damage.

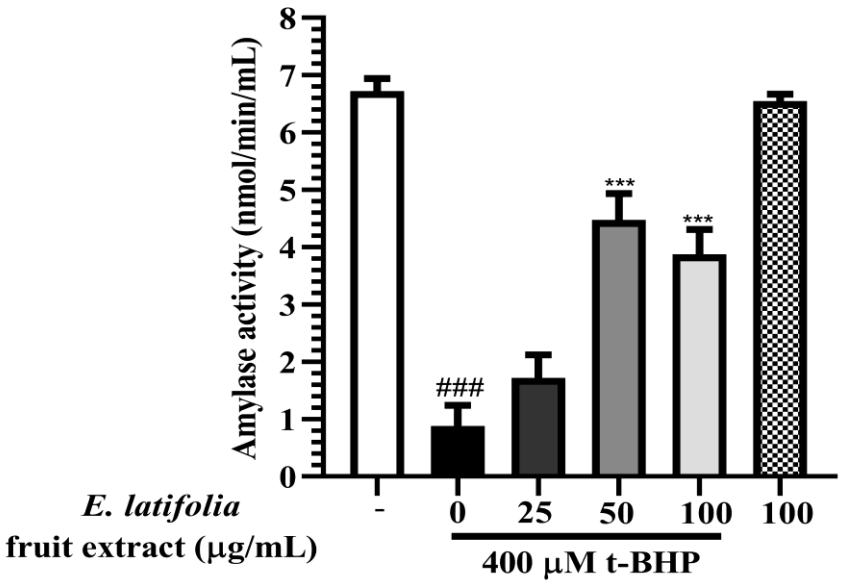

Figure 50 Amylase activity in t-BHP induced HSG cells and the co-treatment with the heated water extract of *E. latifolia* fruits.

Values were represented as mean ± SEM ($n \geq 4$); $^{###}p<0.001$ as compared with untreated control group and $^{***}p<0.001$ as compared with only t-BHP treated group.

CHAPTER 5
DISCUSSION AND CONCLUSION

An imbalance between reactive oxygen species (ROS) and antioxidant levels leads to the phenomenon known as oxidative stress, significantly contributing to various diseases, including oral health disorders[150]. This imbalance leads to cellular damage through the oxidation of lipids, proteins, and DNA, resulting in pathological conditions such as oral health issues and cancer progression[151]. Elaeagnus latifolia Linn. (E. latifolia), known as Malod in Thailand, is renowned for its potent antioxidant properties, attributed to its rich valuable bioactive compounds that provide protection against oxidative stress[152].

The levels of antioxidant and bioactive compounds in E. latifolia fruits vary across ripening stages, influencing their potential health benefits. Research on various fruits, including peaches, apples, and grapes, has demonstrated that unripe fruits often contain higher levels of polyphenols and exhibit antioxidant activity compared to ripe fruits [153-155]. Similarly, studies on Carissa carandas have indicated that unripe fruits display stronger radical-scavenging activity, demonstrating the importance of the ripening stage in determining antioxidant effectiveness (27). In line with these findings, Niwaspragrit et al. observed elevated levels of polyphenols and flavonoids in unripe E. latifolia fruits, correlating with enhanced antioxidant properties(112). These observations guided the focus on unripe E. latifolia fruit to maximize the therapeutic potential of its bioactive compounds.

Methanol and ethanol extractions are widely used to isolate diverse bioactive compounds from E. latifolia fruits, including both polar and non-polar phytochemicals[119, 156]. While methanol extracts generally yield higher concentrations of these compounds, water extracts can exhibit comparable or superior antioxidant activity, as evidenced in Oldenlandia corymbosa[157]. This suggests that water may extract certain synergistic phytoconstituents that enhance antioxidant activity, despite lower polyphenol levels.

However, research on water extracts of E. latifolia is still limited. Therefore, this study utilizes water-based extraction, aligning with green chemistry principles by replacing hazardous organic solvents with an environmentally sustainable, cost-effective alternative that effectively recovers valuable bioactive components[158]. This study focused on optimizing E. latifolia' s bioactive yield using heated water extraction methods. Heating facilitates the production of stable bioactive compounds, contributing to the antioxidant profile of E. latifolia. This thermal disruption of plant cell walls, releasing phenolic compounds from the plant matrix and making them more accessible to the solvent[159, 160], as observed in studies involving heating tomato and black mulberry extracts[161, 162]. Heated water extraction effectively alters the total flavonoid content of E. latifolia fruits by converting flavonoid glycosides into more readily extractable aglycone forms. This process corresponds with findings from studies on tomato and E. rhamnoides (sea buckthorn) fruits, where thermal disruption of cell walls facilitated flavonoid release[163, 164]. Advanced extraction methods, such as ultrasound-assisted extraction and ohmic heating, can further optimize flavonoid yield[165]. However, careful temperature control is essential to avoid thermal degradation of these sensitive compounds[166].

To comprehensively evaluate the antioxidant potential of E. latifolia extracts, a dual-assay approach was employed using DPPH and ABTS methods. The DPPH assay detects hydrogen-donating antioxidants in non-polar environments, the ABTS assay measures a broader spectrum of antioxidants in both water and organic solvents[167]. Research has established the antioxidant potential of 70% methanol extract of E. latifolia fruits, demonstrating moderate antioxidant activity(14) and the flower extract demonstrated significant DPPH scavenging activity(116). Furthermore, the ethanolic extract of E. latifolia fruits exhibited considerable antioxidant potential in the ABTS assay(119). Consistent with these findings, our findings indicate that thermal processing is effective for the antioxidant activity of the water extracts, as evidenced by IC50 values and scavenging efficiency in both DPPH and ABTS assays.

The antioxidant profile of E. latifolia fruit extract was further characterized through ferric reducing antioxidant power (FRAP) and ferrous ion chelating activity (FIC) assays. The FRAP assay quantifies electron-donating capacity through the reduction of ferric to ferrous ions[168], the chelating assay measures the ability to bind Fe2+ ions, preventing

Fenton reaction-mediated oxidative damage[169]. Comparative studies across Elaeagnus species have shown varying antioxidant mechanisms. The acetone extract of E. indica leaves demonstrated substantial FRAP activity due to high phenolic content[156], while methanolic extracts of E. kologa fruits exhibited significant chelating effects [170]. In contrast, previous research on the 70% methanolic extract of E. latifolia fruits showed significant ferrous ion chelating activity but limited reducing power (14).

Our analysis of E. latifolia fruits revealed that heated water extract exhibited both reducing power and chelating activity, although the chelating effect was modest compared to EDTA controls. This suggests that the extract may have limited effectiveness as an iron chelator, whereas the observed reducing power indicates its potential as a reducing agent. Further investigation into the isolation of specific bioactive compounds is warranted to optimize both properties.

The antioxidant capacity of E. latifolia fruits extends to their interaction with specific reactive species. Research within the Elaeagnus genus has demonstrated a variety of radical-specific activities, with the heated water extract E. umbellata fruit, the acetone extract of E. indica leaves and the water extract of E. pyriformis fruit exhibiting remarkable superoxide scavenging abilities[156, 171, 172].

Previous studies on methanolic extract of E. latifolia fruits specifically emphasized its effectiveness in neutralizing superoxide radicals(14). Regarding hydroxyl radical scavenging, the Elaeagnus genus has demonstrated diverse capabilities. The E. umbellata fruits extract and E. indica leaves extract showed potent scavenging effects[156, 171], while the E. latifolia fruits extract exhibited specific hydroxyl radical scavenging

capacity and DNA protective properties(14). The nitric oxide scavenging profile also varies across Elaeagnus species, with the ethanolic extract of E. latifolia fruits demonstrating the ability to significantly reduce nitric oxide levels in acetaminophen-induced liver damage through NF-KB target gene modulation[173]. Our experiments revealed significant radical scavenging capabilities, with the E. latifolia fruit extract enhancing effectiveness against superoxide, hydroxyl, and nitric oxide radicals, as indicated by the IC50 values. These findings suggest that thermal processing may optimize the bioavailability or efficacy of active compounds, emphasizing its potential as a valuable method for utilizing E. latifolia in antioxidant-based health products.

Hydrogen peroxide (H2O2) scavenging activity varies within the Elaeagnus genus. The water extract of Hippophae salicifolia fruits showed superior activity among actinorhizal fruits, while the water extract of E. pyriformis fruits demonstrated the lowest direct H2O2 scavenging capacity among all tested fruits[174]. Meanwhile, the methanolic extract of E. latifolia leaves achieved an IC50 of 444.59 µg/mL for H2O2 scavenging capacity(116). Our results indicated effective H2O2 neutralization, likely due to heat-induced changes that optimize the availability of active compounds.

Lipid peroxide scavenging represents a distinct protective mechanism against cellular oxidative damage, and research across Elaeagnus species reveal varying degrees of lipid peroxidation inhibition. The methanolic extract of E. angustifolia fruits and the heated water extract of E. umbellata fruits effectively reduced malondialdehyde formation[175-177], while previous studies indicated moderate efficacy for E. latifolia fruits extract(14). Our findings revealed that thermal processing of E. latifolia fruit exhibited lipid peroxidation inhibition capacity, suggesting that heated water extraction may activate or release additional membrane-protective compounds. This enhancement broadens the potential applications of E. latifolia fruit extract in antioxidant applications.

The presence of malic acid in the heated water extract of E. latifolia fruits carries significant potential benefits for oral health. Studies have demonstrated malic acid's dual

effects on salivary function and antioxidant capacity within the oral cavity. In stressed rat models, malic acid has been shown to normalize oxidative stress markers and neurotransmitter levels[178, 179]. This clinical significance was particularly evident in the treatment of dry mouth, where a 1% malic acid spray effectively increases salivary flow[180]. The enhanced salivation provided natural protection against dental caries and infections while bolstering the oral cavity's antioxidant defense system against conditions such as gingival inflammation[181].

The E. latifolia fruit extract was found to contain GABA, a neurotransmitter recognized for its ability to reduce neuronal excitability. Importantly, GABA also exhibits potent antioxidant properties outside the nervous system. Key protective mechanisms include stimulating important antioxidant enzymes such as superoxide dismutase and catalase, coupled with the upregulation of the Nrf2 pathway, which strengthens cellular defenses by increasing the expression of detoxifying enzymes[182-184]. These antioxidant effects have been demonstrated in various biological systems, from muscle cells to plant tissues, where GABA consistently reduces oxidative damage and improves cell viability under stress conditions[182, 183].

Our HPLC analysis confirmed the presence of both malic acid and GABA in the heated water extract of E. latifolia fruits, aligning with the findings by Niwaspragrit and Meeploy, respectively(108, 112). The presence of malic acid and GABA in the extracts suggests the potential for synergistic antioxidant effects. The comprehensive antioxidant profile, encompassing phenolic compounds and flavonoids, has the potential to deliver enhanced defense against oxidative stress-related issues within the oral cavity. These phenolic compounds and flavonoids may contribute synergistic benefits that exceed those of individual compounds alone. The combination of these antioxidant compounds could contribute to maintaining oral tissue integrity, reducing the risk of inflammatory conditions, and supporting overall oral health through multiple mechanisms[185].

The metabolic profiling of the heated water extract of E. latifolia fruits was performed utilized LC-Q-TOF-MS/MS, revealing a diverse array of bioactive compounds with potential health benefits. The identification of GABA (tR=2.63 min, [M+H]+ m/z 104.071), confirmed by HPLC, was significant given its established antioxidant and neuroprotective properties[182, 184]. Its presence, along with 1,3,5-benzenetriol (phloroglucinol) (tR=2.72 min, m/z 127.039), a potent ROS scavenger with demonstrated antioxidant, antibacterial, and antidiabetic properties[186]. Similar findings in the methanolic extract of E. umbellata berries, identified phloroglucinol. The identification of several amino acids (L-asparagine, glutamic acid, and proline) further supports this, given their roles in protein synthesis, tissue repair, and protection against oxidative damage[187-189].

The presence of citric acid (tR = 3.00 min; [M+H]+ m/z 210.062), a key component of the Krebs cycle that may support cellular energy production and exhibit antioxidant effects, potentially benefiting salivary gland cells[190, 191], particularly beneficial for meeting the metabolic requirements of salivary gland cells, especially during oxidative stress. Previous investigations of related Elaeagnus species have identified multiple organic acids, including citric acid and malic acid, as important contributors to the overall antioxidant capacity[119, 192]. The identification of mannobiose and D-(+)-Mannose suggests a role for these oligosaccharides in metabolic function and maintaining a balanced oral microbiome[193, 194], consistent with findings in the water extract of E. angustifolia pulps[195]. Our analyasis found L-Tyrosine (tR = 3.08 min; m/z 182.082), suggests a potential role in supporting neurotransmitter synthesis in response to stress. This findings aligns with the study by Abizov et al., reported the presence of amino acid, including tyrosine, in the water extract of E. angustifolia fruits[191]. while adenosine (tR = 4.19 min; m/z 268.105) may be important for energy metabolism and cellular signaling under oxidative stress conditions[196]. The presence of adenosine has not been extensively documented previously within the Elaeagnus genus making this

finding particularly noteworthy. Furthermore, the extract includes corosolic acid (tR=30.33 min; [M+H]+ m/z =473.364) and palmitamide (tR=36.86 min; [M+H]+ m/z =256.263), both known for their antioxidant and anti-inflammatory properties[197, 198] further strengthens the extract's protective potential. The next logical step is to investigate the protective effects of this extract in cell-based models, exploring their mechanisms in combating oxidative damage within salivary gland cells.

The human submandibular gland (HSG) cells are an important model for studying oxidative damage and antioxidant strategies due to their vital role in saliva production and oral health[199]. Dysfunction in these glands, linked to conditions like hyposalivation, diabetes, radiation-induced damage, and dry mouth, is closely associated with oxidative stress, making HSG cells ideal for investigating oxidative damage mechanisms and the interplay between ROS production and antioxidant defenses[200].

Tert-butyl hydroperoxide (t-BHP) is identified as a powerful inducer of oxidative stress, distinct from hydrogen peroxide (H2O2). T-BHP activates NADPH oxidase for superoxide radical generation and disrupts mitochondrial electron transport, enhancing ROS production[201, 202]. It induces stronger cellular responses, including apoptosis and ferroptosis, which are not typically observed with H2O2[202, 203]. T-BHP may convert to H2O2 through specific proton transfer mechanisms[204] and it significantly affects cellular protective mechanisms by modulating glutathione synthesis and nuclear factor pathways[205, 206]. On the other hand, H2O2 is valuable for studying signaling and mitochondrial function, t-BHP's unique properties make it particularly useful for investigating severe oxidative stress responses[207-209]. These specific pathways are crucial for developing therapeutic interventions for oxidative stress-related conditions, including submandibular gland dysfunction.

At low concentration of t-BHP (50 μM), it induces caspase-dependent apoptosis in endothelial cells[210]. With increasing concentrations (100-200 μM), a significant

reduction in cell viability is observed in HepG2 cells, correlating with oxidative stress and decreased glutathione levels[211]. Around 200 μM, t-BHP triggers both oxidative stress and apoptosis with DNA fragmentation[212]. At higher concentrations of t-BHP (≥500 μM), the response shifts from apoptosis to necroptosis[210]. Our findings indicate that 400 μM t-BHP is optimal for studying oxidative damage and apoptosis in HSG cells, aligning with IC50 values from cytotoxicity assays.

Cytotoxicity assessment of the E. latifolia fruit extract revealed that concentrations ranging from 6.25 to 100 μg/mL are nontoxic to HSG cells. The extract at 25, 50, and 100 μg/mL effectively protected cells from oxidative damage and death induced by 400 μM t-BHP, likely due to its potent free radical scavenging properties demonstrated in in vitro assays. Previous studies indicated that the water extract of E. angustifolia fruits reduced tissue damage in mice exposed to graphene oxide nanoparticles[213], and E. latifolia fruit extract significantly diminished liver damage and oxidative stress in models of acetaminophen-induced hepatotoxicity[173].

Oxidative stress occurs when excessive ROS production disrupts intracellular redox balance, resulting in oxidative damage and inflammation[214]. In this study, we measured intracellular ROS using the H2DCFH-DA assay, which indicates ROS levels through fluorescence. The findings revealed that t-BHP exposure significantly increased DCF fluorescence, indicating elevated ROS levels. In contrast, co-treatment with the E. latifolia fruit extract reduced fluorescence, suggesting effective ROS scavenging and restoration of redox balance. This antioxidant action helps maintain the structural and functional integrity of salivary gland tissues, enhancing saliva production and quality while reducing tissue degradation and inflammatory responses. These results align with findings by Ianuzzi et al., who noted that bioactive compounds from the methanolic extract of E. umbellata fruits effectively reduce ROS in human gingival fibroblasts[215], and cis-3-O-p-hydroxycinnamoyl ursolic acid extracted from E. oldhamii leaves demonstrates antioxidant properties while promoting apoptosis in cancer cells[216].

Apoptosis is characterized by distinct morphological hallmarks that can be visualized using Hoechst and acridine orange-ethidium bromide (AO/EB) staining method. These apoptotic features include chromatin condensation, nuclear fragmentation, and alterations in cell shape and size, often leading to increased fluorescence intensity[217]. In this study, exposure of HSG cells to t-BHP induced characteristic morphological changes, evidenced by heightened fluorescence intensity associated with apoptotic cell death. In contrast, co-treatment with between t-BHP and E. latifolia fruit extract demonstrated protective effects against t-BHP-induced morphological alterations, reducing Hoechst staining intensity and preserving normal cell morphology.

Similar analyses with AO/EB staining showed that t-BHP exposure typically resulted in orange to red fluorescence patterns indicative of late-stage apoptosis, while co-treatment with the extract reversed these changes, increasing green fluorescence related to viable cells. These viable cells retain their integrity and exhibit bright green nuclei due to acridine orange uptake, indicating that they are not undergoing apoptosis or necrosis. This suggests a reduction in both apoptotic and necrotic cell populations, indicating that the extract may exert anti-apoptotic effects.

Previous investigations revealed the effect of the ethanolic extract of E. latifolia fruits on key apoptotic regulators. The extract has been shown to significantly downregulate Bax expression while upregulating Bcl-2 in acetaminophen-treated mice liver tissues, resulting in a decreased Bax/Bcl-2 ratio indicative of reduced apoptotic activity and enhanced cell survival[173]. In our study, t-BHP-induced HSG cell death was accompanied by an elevated Bax/Bcl-2 ratio at both mRNA and protein levels, signaling the presence of apoptosis. These findings align with the previous research demonstrating that t-BHP treatment significantly increased the Bax/Bcl-2 ratio in various cell types[218-220]. However, co-treatment with E. latifolia fruit extract reversed this effect by downregulating Bax and upregulating Bcl-2, decreasing the Bax/Bcl-2 ratio. This

modulation suggests an anti-apoptotic effect of the extract. The Bax/Bcl-2 ratio governs cell fate in apoptosis; Bax promotes apoptosis by increasing mitochondrial membrane permeability, while Bcl-2 stabilizes the membrane, thus regulating mitochondrial integrity and intracellular calcium levels[221, 222]. Moreover, p38 MAPK activation occurs prior to Bax translocation, and inhibiting p38 MAPK's effect on Bcl-2 significantly increases Bax translocation, cytochrome c release, and apoptosis. Consequently, p38 MAPK is thought to play a crucial role in regulating the balance between Bax and Bcl-2, thereby influencing the apoptotic process[223].

Our study demonstrated that t-BHP-induced HSG cell death was accompanied by significant increases in cleaved caspase-3 and p38 phosphorylation levels. Consistent with prior studies, these results demonstrate an increase in p38 phosphorylation after exposure to t-BHP[210]. The p38 MAPK pathway is a key mediator of cell death in response to oxidative stress and inflammation, regulating diverse biological functions, including apoptosis and autophagy[224]. Dysregulation of p38 MAPK pathway is linked to conditions such as dry mouth, as its activation can contribute to inflammation and tissue damage[224, 225] . Additionally, p38 MAPK directly regulates the activity of caspases. For instance, active p38 MAPK can phosphorylate cleaved caspase-3 on serine-150, a critical step in the apoptotic cascade[226, 227].

Our results correlated with prior research showing increased p38 phosphorylation in salivary gland cells, leading to caspase-3 activation[228]. Cleaved caspase-3 plays a crucial role in the apoptotic process through its involvement in the execution phase of apoptosis and non-apoptotic functions. In the apoptotic pathway, cleaved caspase-3 acts as an executioner caspase, which facilitates the cleavage of various cellular substrates, leading to the morphological and biochemical changes associated with the process of apoptosis[229]. Recent studies also suggest non-apoptotic roles for cleaved caspase-3, such as promoting oncogenic transformation and regulating angiogenesis[230].

Furthermore, we demonstrated that co-treatment with the E. latifolia fruit extract significantly downregulated p38 phosphorylation and cleaved caspase-3 levels in t-BHP-induced HSG cells. These findings align with previous studies showed that the ethanolic extract of E. glabra leaves reduced p38 phosphorylation by significantly lowering P-P38 levels in LPS-activated BV-2 microglial cells[231] and the heated water extract of E. umbellata flowers modulate apoptosis by downregulating caspase-3 and other apoptotic markers in response to cadmium-induced cytotoxicity in HepG2 cells[232]. These findings suggest that E. latifolia fruits could inhibit intracellular ROS generation through its antioxidant and anti-apoptotic activities.

Aquaporin-5, encoded by the AQP5 gene, a water-selective channel located in the apical membrane of salivary glands, enables rapid water transport essential for gland function[233]. Disruption in AQP5 expression can lead to physiological issues, including conditions like Sjögren's syndrome and xerostomia (dry mouth)[234]. Our study found that t-BHP treatment decreased AQP5 mRNA and protein levels in HSG cells, indicating that oxidative stress impairs normal fluid transport functions. This reduction may be influenced by transcription factors such as NF-kB, which regulates AQP5 during inflammatory responses. Furthermore, oxidative stress may affect AQP5 stability and trafficking through post-translational modifications[235, 236]. While limited data exists on the relationship between the effect of Elaeagnus genus on AQP5, our findings demonstrated that E. latifolia fruit extract significantly elevated AQP5 expression in t-BHP-induced HSG cells at both gene and protein levels. This finding is in line with previous studies showing the protective role of antioxidant compounds in combating oxidative stress-related damage on AQP5. For instance, cordycepin has been shown to increase AQP5 gene expression in H2O2-induced HSG cells(13) and apigenin could activate AQP5 transcription through estrogen receptor signaling, restoring saliva flow rates in xerostomia models.[237].

Salivary α-amylase, encoded by the AMY1 gene, is essential for human carbohydrate digestion, breaking down starch into simpler sugars. This enzyme, primarily produced in the salivary glands, initiates digestion by catalyzing the hydrolysis of α-1,4 glycosidic bonds in starch, generating maltose and oligosaccharides for further breakdown in the intestine. Efficient salivary amylase activity allows starch digestion to begin before food reaches the stomach, enhancing overall digestive efficiency[238]. Dysfunction in amylase production, such as low AMY1 expression or reduced enzymatic activity, can negatively impact oral health and lead to dry mouth, increasing the risk of dental caries and infections[239].

The relationship between t-BHP and amylase activity remains poorly understood; however, some studies provide relevant insights. For example, research on t-BHP perfusion in isolated rat pancreas models reported no significant effect on pancreatic enzyme levels, including amylase. This suggests that t-BHP may not directly interfere with amylase activity under such conditions[240]. Conversely, t-BHP injection into the bile-pancreatic duct led to significant elevations in serum amylase levels, indicating substantial pancreatic damage[241]. In our study, we observed that t-BHP exposure significantly reduced both amylase expression and activity in HSG cells, reflecting a complex and context-dependent interaction. This aligns with findings from Jaiboonma et al., who reported that oxidative stress induced by H2O2 in HSG cells reduced amylase mRNA expression and activity(13). This consistency suggests that oxidative stress whether induced by t-BHP or H2O2 similarly impacts amylase production in salivary gland cells, contrasting with effects seen in pancreatic tissue. Moreover, post-treatment with cordycepin was shown to enhance both amylase activity and AMY1 expression in HSG cells(13). Similarly, our study revealed that co-treatment with the E. latifolia fruit extract significantly improved AMY1 mRNA expression and amylase activity in t-BHP-induced HSG cells. These findings hint at potential protective or restorative effects of the extract against oxidative stress-induced reductions in amylase levels. The restoration of

amylase activity under oxidative stress by E. latifolia may involve ROS-mediated signaling pathways such as MAPK, Nrf2/Keap1, and NF-KB, known to regulate both antioxidant and pro-oxidant gene expression [242]. This suggests a complex interplay between oxidative stress, cellular signaling, and amylase production. Furthermore, this extract probably promotes effective AQP5 function, which is crucial for regulating salivary fluid secretion[243].

Our findings indicate that the E. latifolia fruit extract holds significant benefits for alleviating a salivary dysfunction and probably managing oral diseases. This potential arises from its antioxidative properties and ability to modulate apoptosis, as oxidative stress is a common underlying factor in numerous oral conditions. The mechanisms by which E. latifolia fruit extract exert its protective effects can be attributed to its interactions with key signaling pathways and cellular function.

For conditions like xerostomia, it commonly referred to as dry mouth, results from reduced salivary production caused by dysfunction or injury to the salivary glands. The mechanisms underlying this condition vary based on the cause, which may include the use of certain medications, systemic illnesses, or exposure to radiation therapy. Xerostomia is often caused by chemotherapy or radiation therapy, which can damage the acinar cells of the salivary glands and reduce their saliva-producing capability. Radiation-induced ROS play a significant role in promoting glandular atrophy and fibrosis[244]. Our studies demonstrated that the E. latifolia fruit extract upregulated AQP5 expression, a crucial element for promoting hydration in glandular tissues, while also minimizing oxidative damage in submandibular gland cells. By supporting proper water transport and lowering ROS levels, this mechanism contributes potential benefits for individuals experiencing xerostomia by aiding in the restoration of salivary gland function and alleviating related symptoms.

In addressing Sjögren's syndrome (SS), an autoimmune disorder characterized by diminished salivary and lacrimal secretion, leading to dryness and inflammation. A

key pathological feature of SS is apoptosis, which plays a significant role in glandular dysfunction and tissue damage. In SS, activated immune cells, including T cells, B cells, and macrophages, infiltrate the salivary and lacrimal glands, producing ROS as a component of the inflammatory response. Moreover, immune cells release pro-inflammatory cytokines such as TNF-α, IFN-γ, and IL-6, which trigger intracellular apoptotic pathways in glandular epithelial cells, ultimately resulting in cell death. Excessive production of ROS damages cellular components, triggering apoptosis through mitochondrial dysfunction. Damaged mitochondrial in epithelial cells results in the release of cytochrome c, which activates caspase-9 and downstream apoptotic cascades, ultimately resulting in finally cell death [245]. E. latifolia fruit extract regulates apoptotic regulators by modulating the Bax/Bcl-2 ratio, restoring balanced apoptosis levels, and strengthening cellular antioxidant defenses. These effects may support improved salivary gland function, ultimately enhancing hydration and alleviating discomfort in patients with xerostomia.

In cases of hyposalivation, often linked to medication side effects or systemic diseases[11, 246] . The extract could reduce oxidative damage caused by excessive ROS production. It also restores the expression of critical mRNAs and proteins, such as AQP5 and AMY1, helping to maintain a balanced oral biochemical environment. While dental caries and periodontitis are closely linked to oxidative stress-induced inflammation[247]. The antioxidant properties of E. latifolia fruit extract provides a dual defensive mechanism by preserving HSG cell integrity through reduced ROS levels and potentially improving salivary function via increased amylase activity and upregulated AMY1 and AQP5 expression. This combined action helps regulate bacterial populations, strengthens innate oral defenses, reducing tissue damage, and supports a healthier oral microbiome, ultimately reducing the risk of these oral diseases.

As summarized in Figure 51, t-BHP exposure triggered excessive ROS production, inducing oxidative stress in HSG cells. This leads to increased p38 MAPK

phosphorylation, subsequently activating apoptosis through upregulation of pro-apoptotic markers such as cleaved caspase-3 and the Bax/Bcl-2 ratio, ultimately results in decreased cell viability and promotes cell death through apoptosis. The *E. latifolia* fruit extract demonstrated high bioactive chemical composition and antioxidant properties, effectively scavenges ROS and reduces oxidative damage in HSG cells. Co-treatment with the *E. latifolia* fruit extract with t-BHP significantly decreased intracellular ROS levels, enhancing HSG cell survival. This protective effect is achieved through modulation of apoptotic pathways and restoration of key proteins like AQP5 and AMY1, thereby enhancing overall salivary gland function.

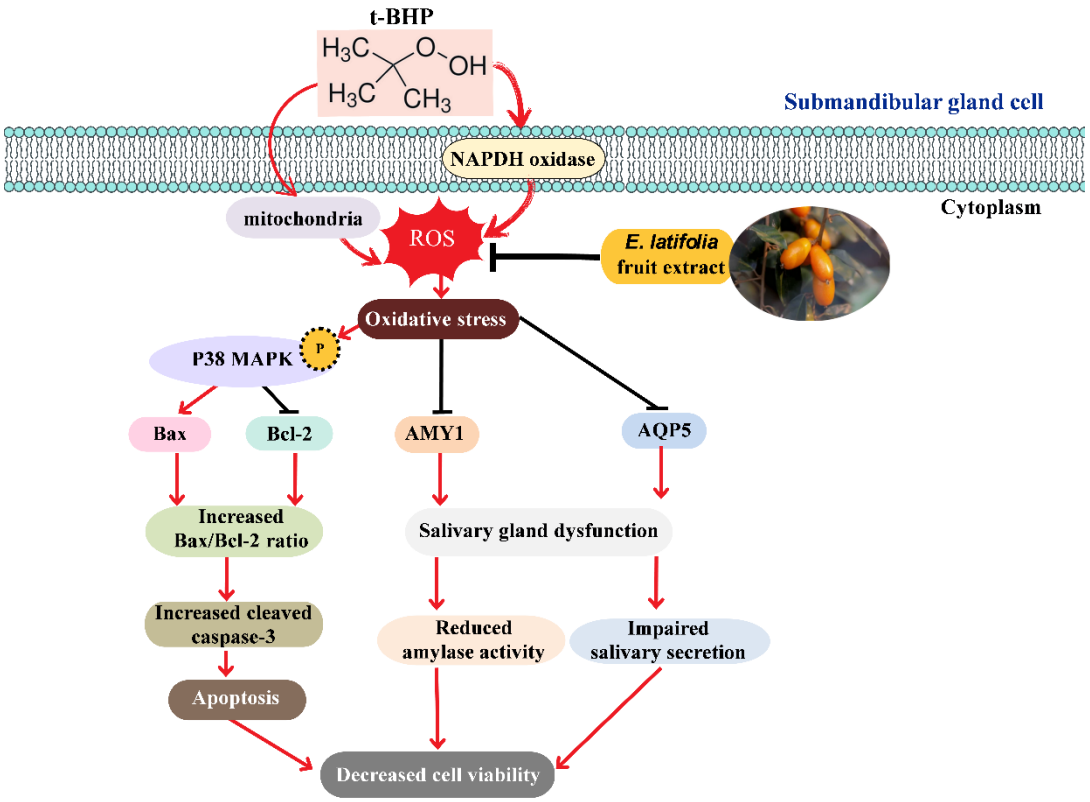

Figure 51 Impact of heated water extract of *E. latifolia* fruits on t-BHP-induced oxidative stress in HSG cells

Limitations

While this study provides valuable insights into the protective effects of the *E. latifolia* fruit extract on HSG cells, several limitations warrant attention in future research such as animal studies are necessary to examine the extract's effects within a physiological context and to explore complex *in vivo* interactions. Future investigations should assess the activity of key bioactive compounds, such as malic acid and GABA, in HSG cells to understand their individual contributions to the observed protective effects. Research should be extended to additional signaling pathways (e.g., AKT, cytochrome C, Nrf-2, HO-1, TNF-α, and AP-1) for a more comprehensive understanding of *E. latifolia* fruit extract 's influence on cellular responses under oxidative stress. Incorporating flow cytometry to quantify apoptotic and necrotic cell populations would provide stronger evidence for the extract's protective role. Examining mechanisms involving NF-kB, mTOR, and COX-2 would yield deeper insights into *E. latifolia* fruit extract's effects on inflammatory responses and salivary gland function. Predicting binding affinities between bioactive compounds and relevant proteins could further elucidate their pharmacodynamics. Systematically assessing the extract's impact on salivary secretion would bridge the gap between research findings and clinical application, further studying *E. latifolia*'s therapeutic potential in managing oxidative damage and salivary dysfunction.

Conclusion

This study demonstrated that *E. latifolia* fruit extract effectively protects human submandibular gland cells from t-BHP-induced oxidative damage. Its potent antioxidant properties enable it to scavenge ROS, thereby alleviating the harmful effects of oxidative stress. Furthermore, the extract demonstrated an anti-apoptotic mechanism by inhibiting apoptosis-related signaling pathways and reducing the expression of these markers such as p38 MAPK, the Bax/Bcl-2 ratio, and caspase-3. Importantly, the extract increased the expression of salivary marker genes and enhanced amylase activity, suggesting its ability to support and maintain salivary gland function. Taken together, *E. latifolia* fruit extract could be a promising phytomedicine for reducing or possibly preventing oxidative stress-related injury to the salivary glands, suggesting its viability as a novel supportive treatment option for managing salivary gland and oral disorders associated with oxidative stress.

REFERENCES

1. Scully C. Oral and maxillofacial medicine: the basis of diagnosis and treatment: Elsevier Health Sciences; 2012.

2. Lobo V, Patil A, Phatak A, Chandra N. Free radicals, antioxidants and functional foods: Impact on human health. Pharmacognosy reviews. 2010;4(8):118.

3. Sharifi-Rad M, Anil Kumar NV, Zucca P, Varoni EM, Dini L, Panzarini E, et al. Lifestyle, oxidative stress, and antioxidants: back and forth in the pathophysiology of chronic diseases. Frontiers in physiology. 2020;11:694.

4. Żukowski P, Maciejczyk M, Waszkiel D. Sources of free radicals and oxidative stress in the oral cavity. Archives of Oral Biology. 2018;92:8-17.

5. Kumar J, Teoh SL, Das S, Mahakknaukrauh P. Oxidative stress in oral diseases: understanding its relation with other systemic diseases. Frontiers in physiology. 2017;8:693.

6. Tóthová Lu, Kamodyova N, Červenka T, Celec P. Salivary markers of oxidative stress in oral diseases. Frontiers in cellular and infection microbiology. 2015;5:73.

7. Huang Y-K, Chang K-C, Li C-Y, Lieu A-S, Lin C-L. AKR1B1 represses glioma cell proliferation through p38 MAPK-mediated Bcl-2/BAX/Caspase-3 apoptotic signaling pathways. Current issues in molecular biology. 2023;45(4):3391-405.

8. Kim B-J, Ryu S-W, Song B-J. JNK-and p38 kinase-mediated phosphorylation of Bax leads to its activation and mitochondrial translocation and to apoptosis of human hepatoma HepG2 cells. Journal of Biological Chemistry. 2006;281(30):21256-65.

9. Delporte C, Bryla A, Perret J. Aquaporins in salivary glands: from basic research to clinical applications. International journal of molecular sciences. 2016;17(2):166.

10. Hosoi K. Physiological role of aquaporin 5 in salivary glands. Pflügers Archiv-European Journal of Physiology. 2016;468(4):519-39.

11. Peyrot des Gachons C, Breslin PA. Salivary amylase: digestion and metabolic syndrome. Current diabetes reports. 2016;16:1-7.

12. Abdulkareem MA, Owolabi BA, Saheed ES, Aromolaran RF, Bashiru RM, Jumah TA, et al. Genetic factors and the role of pancreatic amylase in the pathogenesis of type 2 diabetes. Egyptian Journal of Medical Human Genetics. 2024;25(1):33.

13. Jaiboonma A, Kaokaen P, Chaicharoenaudomrung N, Kunhorm P, Janebodin K, Noisa P, et al. Cordycepin attenuates salivary hypofunction through the prevention of oxidative stress in human submandibular gland cells. International Journal of Medical Sciences. 2020;17(12):1733.

14. Panja S, Chaudhuri D, Ghate NB, Le Minh H, Mandal N. In vitro assessment of phytochemicals, antioxidant and DNA protective potential of wild edible fruit of Elaeagnus latifolia Linn. Fruits. 2014;69(4):303-14.

15. Nazir N, Zahoor M, Nisar M. A review on traditional uses and pharmacological importance of genus Elaeagnus species. The Botanical Review. 2020;86:247-80.

16. Proctor GB. The physiology of salivary secretion. Periodontology 2000. 2016;70(1):11-25.

17. Jensen S, Vissink A, Firth N. Salivary gland disorders and diseases. Contemporary Oral medicine: a comprehensive approach to clinical practice Cham: Springer International Publishing. 2018:1-85.

18. Piraino LR, Benoit DS, DeLouise LA. Salivary gland tissue engineering approaches: state of the art and future directions. Cells. 2021;10(7):1723.

19. Hui ELC, Kim FCC, Kamaruddin NKNB, Thentamil A, Jacob M. Aquaporins in Salivary Gland-The Water Fa (u) cet of an Acini? Journal of Academy of Dental Education. 2018;4(1):12-6.

20. Ghannam MG, Singh P. Anatomy, head and neck, salivary glands. 2019.

21. Bordoni B, Varacallo M. Anatomy, head and neck, sternocleidomastoid muscle. StatPearls [Internet]: StatPearls Publishing; 2022.

22. Maes M, Mihaylova I, Kubera M, Uytterhoeven M, Vrydags N, Bosmans E. Increased 8-hydroxy-deoxyguanosine, a marker of oxidative damage to DNA, in major depression and

myalgic encephalomyelitis/chronic fatigue syndrome. Neuroendocrinology Letters. 2009;30(6):715.

23. Pedersen A, Sørensen C, Proctor G, Carpenter G, Ekström J. Salivary secretion in health and disease. Journal of oral rehabilitation. 2018;45(9):730-46.

24. Iorgulescu G. Saliva between normal and pathological. Important factors in determining systemic and oral health. Journal of medicine and life. 2009;2(3):303.

25. Wang Z, Shen M-M, Liu X-J, Si Y, Yu G-Y. Characteristics of the saliva flow rates of minor salivary glands in healthy people. Archives of oral biology. 2015;60(3):385-92.

26. Pedersen AML, Belstrøm D. The role of natural salivary defences in maintaining a healthy oral microbiota. Journal of dentistry. 2019;80:S3-S12.

27. Irshad S, Iqbal A, Zulqarnain A, Nawaz S, Anjum S. Comparative sequential solvent extraction of phytochemicals from ripe, ripening and unripe Carissa carandas fruit extracts and their antioxidant investigation. Pakistan Journal of Botany. 2021;53.

28. Fisher SZ, Govindasamy L, Tu C, Agbandje-McKenna M, Silverman DN, Rajaniemi HJ, et al. Structure of human salivary α-amylase crystallized in a C-centered monoclinic space group. Acta Crystallographica Section F: Structural Biology and Crystallization Communications. 2006;62(2):88-93.

29. Mandel AL, Peyrot des Gachons C, Plank KL, Alarcon S, Breslin PA. Individual differences in AMY1 gene copy number, salivary α-amylase levels, and the perception of oral starch. PloS one. 2010;5(10):e13352.

30. Ali N, Nater UM. Salivary alpha-amylase as a biomarker of stress in behavioral medicine. International journal of behavioral medicine. 2020;27:337-42.

31. Maciejczyk M, Gerreth P, Zalewska A, Hojan K, Gerreth K. Salivary gland dysfunction in stroke patients is associated with increased protein glycoxidation and nitrosative stress. Oxidative Medicine and Cellular Longevity. 2020;2020(1):6619439.

32. Zalewska A, Kossakowska A, Taranta-Janusz K, Zięba S, Fejfer K, Salamonowicz M, et al. Dysfunction of salivary glands, disturbances in salivary antioxidants and increased

oxidative damage in saliva of overweight and obese adolescents. Journal of Clinical Medicine. 2020;9(2):548.

33. Kołodziej U, Maciejczyk M, Miąsko A, Matczuk J, Knaś M, Żukowski P, et al. Oxidative modification in the salivary glands of high fat-diet induced insulin resistant rats. Frontiers in Physiology. 2017;8:20.

34. Okabayashi K, Narita T, Takahashi Y, Sugiya H. Effect of oxidative stress on secretory function in salivary gland cells. Oxidative Stress-Environmental Induction and Dietary Antioxidants. 2012:189-200.

35. Liu Z, Dong L, Zheng Z, Liu S, Gong S, Meng L, et al. Mechanism, prevention, and treatment of radiation-induced salivary gland injury related to oxidative stress. Antioxidants. 2021;10(11):1666.

36. Wyss T, Boesch M, Roos L, Tschopp C, Frei KM, Annen H, et al. Aerobic fitness level affects cardiovascular and salivary alpha amylase responses to acute psychosocial stress. Sports medicine-open. 2016;2:1-11.

37. Nomura S, Zhao B, Yamagishi K, editors. Evaluation of Human Stress with Salivary Alpha-amylase. Proceedings of the Annual Meeting of the Cognitive Science Society; 2007.

38. Ahari UZ, Falsafi P, Eslami H, Maleki S, Pakdel F. Comparison of salivary alpha amylase and peroxidase levels in women with GDM and non-diabetic pregnant women. Biomedical and Pharmacology Journal. 2016;9(2):499-506.

39. Dodds M, Roland S, Edgar M, Thornhill M. Saliva A review of its role in maintaining oral health and preventing dental disease. Bdj Team. 2015;2:15123.

40. Miranda-Rius J, Brunet-Llobet L, Lahor-Soler E, Farré M. Salivary secretory disorders, inducing drugs, and clinical management. International Journal of Medical Sciences. 2015;12(10):811.

41. Kapoor R. Effect of Antioxidant Gel on Oxidative Stress and Salivary Flow Rate in Xerostomic Patients 2017.

42. Halliwell B, Gutteridge JM. Free radicals in biology and medicine: Oxford university press, USA; 2015.

43. ERICSON D, BRATTHALL D. Simplified method to estimate salivary buffer capacity. European Journal of Oral Sciences. 1989;97(5):405-7.

44. Ercal N, Gurer-Orhan H, Aykin-Burns N. Toxic metals and oxidative stress part I: mechanisms involved in metal-induced oxidative damage. Current topics in medicinal chemistry. 2001;1(6):529-39.

45. Martemucci G, Costagliola C, Mariano M, D'andrea L, Napolitano P, D'Alessandro AG. Free radical properties, source and targets, antioxidant consumption and health. Oxygen. 2022;2(2):48-78.

46. Valko M, Leibfritz D, Moncol J, Cronin MT, Mazur M, Telser J. Free radicals and antioxidants in normal physiological functions and human disease. The international journal of biochemistry & cell biology. 2007;39(1):44-84.

47. Bisht S, Dada R. Oxidative stress: Major executioner in disease pathology, role in sperm DNA damage and preventive strategies. Front Biosci (Schol Ed). 2017;9(3):420-47.

48. Drew J. Redox reduxed: Application of a non-analogous definition for oxidation state. Teaching Science. 2020;66(3):5-15.

49. Phaniendra A, Jestadi DB, Periyasamy L. Free radicals: properties, sources, targets, and their implication in various diseases. Indian journal of clinical biochemistry. 2015;30:11-26.

50. Di Meo S, Venditti P. Evolution of the knowledge of free radicals and other oxidants. Oxidative Medicine and Cellular Longevity. 2020;2020.

51. Milkovic L, Cipak Gasparovic A, Cindric M, Mouthuy P-A, Zarkovic N. Short overview of ROS as cell function regulators and their implications in therapy concepts. Cells. 2019;8(8):793.

52. Sinenko SA, Starkova TY, Kuzmin AA, Tomilin AN. Physiological signaling functions of reactive oxygen species in stem cells: from flies to man. Frontiers in cell and developmental biology. 2021;9:714370.

53. Ojha NK. Voltage-gated sodium channels as non-photonic sensors for membrane-delimited reactive species: Dissertation, Jena, Friedrich-Schiller-Universität Jena, 2018; 2018.

54. Masschelin PM, Cox AR, Chernis N, Hartig SM. The impact of oxidative stress on adipose tissue energy balance. Frontiers in physiology. 2020;10:1638.

55. Davies MJ. Protein oxidation and peroxidation. Biochemical journal. 2016;473(7):805-25.

56. Kehm R, Baldensperger T, Raupbach J, Höhn A. Protein oxidation-formation mechanisms, detection and relevance as biomarkers in human diseases. Redox Biology. 2021;42:101901.

57. Ayala A, Muñoz MF, Argüelles S. Lipid peroxidation: production, metabolism, and signaling mechanisms of malondialdehyde and 4-hydroxy-2-nonenal. Oxidative medicine and cellular longevity. 2014;2014.

58. Zalewska A, Maciejczyk M, Szulimowska J, Imierska M, Błachnio-Zabielska A. High-fat diet affects ceramide content, disturbs mitochondrial redox balance, and induces apoptosis in the submandibular glands of mice. Biomolecules. 2019;9(12):877.

59. Seil M, Fontanils U, Etxebarria IG, Pochet S, Garcia-Marcos M, Marino A, et al. Pharmacological evidence for the stimulation of NADPH oxidase by P2X 7 receptors in mouse submandibular glands. Purinergic Signalling. 2008;4:347-55.

60. Ahmed SF. Comparative Study of Gamma Radiation and Prednisolone Induced Submandibular Salivary Gland Oxidative Damage. Egyptian Journal of Radiation Sciences and Applications. 2019;32(1):13-21.

61. Onopiuk B, Onopiuk P, Dąbrowska Z, Dąbrowska E, Pietruska M, Car H. Effect of metronidazole on the oxidoreductive processes in the submandibular and parotid glands in experimental research. Oxidative Medicine and Cellular Longevity. 2018;2018(1):7083486.

62. Tai Y, Inoue H, Sakurai T, Yamada H, Morito M, Ide F, et al. Protective effect of lecithinized SOD on reactive oxygen species-induced xerostomia. Radiation research. 2009;172(3):331-8.

63. Zhao L, Xu J, Li S, Li B, Jia M, Pang B, et al. Resveratrol alleviates salivary gland dysfunction induced by ovariectomy in rats. Biochemical and Biophysical Research Communications. 2022;630:112-7.

64. Maciejczyk M, Bielas M, Zalewska A, Gerreth K. Salivary biomarkers of oxidative stress and inflammation in stroke patients: from basic research to clinical practice. Oxidative Medicine and Cellular Longevity. 2021;2021:1-22.

65. Tonnus W, Meyer C, Paliege A, Belavgeni A, von Mässenhausen A, Bornstein SR, et al. The pathological features of regulated necrosis. The Journal of pathology. 2019;247(5):697-707.

66. Asensi V, Collazos J, Celada A, Valle-Garay E. Role of Neutrophils Apoptosis in Osteomyelitis Pathogenesis. Clin Microbiol. 2017;6:e139.

67. Jan R. Understanding apoptosis and apoptotic pathways targeted cancer therapeutics. Advanced pharmaceutical bulletin. 2019;9(2):205.

68. Wanner E, Thoppil H, Riabowol K. Senescence and apoptosis: Architects of mammalian development. Frontiers in Cell and Developmental Biology. 2021;8:620089.

69. Whitaker RH, Cook JG. Stress relief techniques: p38 MAPK determines the balance of cell cycle and apoptosis pathways. Biomolecules. 2021;11(10):1444.

70. Jia Y-T, Wei W, Ma B, Xu Y, Liu W-J, Wang Y, et al. Activation of p38 MAPK by reactive oxygen species is essential in a rat model of stress-induced gastric mucosal injury. The Journal of Immunology. 2007;179(11):7808-19.

71. Zhou Y, Wang Q, Evers BM, Chung DH. Oxidative stress-induced intestinal epithelial cell apoptosis is mediated by p38 MAPK. Biochemical and biophysical research communications. 2006;350(4):860-5.

72. Frohwitter G, Zimmermann OL, Kreutzer K, Doll C, Rendenbach CM, Dommisch H, et al. Oxidative and nitrosative stress in oral squamous cell carcinoma. Cells Tissues Organs. 2020;209(2-3):120-7.

73. UTAIPAN T, SATTAYAKHOM A, PRACHONGSAI I, CHARONG N, CHUNGLOK W. Reduction of intracellular-reactive oxygen species and diminished mitogen-activated protein kinases (MAPKs) activation are associated with oral squamous cell carcinoma cell aggressiveness. Walailak Journal of Science and Technology (WJST). 2018;15(2):131-41.

74. So K-Y, Kim S-H, Jung K-T, Lee H-Y, Oh S-H. MAPK/JNK1 activation protects cells against cadmium-induced autophagic cell death via differential regulation of catalase and heme oxygenase-1 in oral cancer cells. Toxicology and applied pharmacology. 2017;332:81-91.

75. Kurata S-i. Selective activation of p38 MAPK cascade and mitotic arrest caused by low level oxidative stress. Journal of Biological Chemistry. 2000;275(31):23413-6.

76. Ma D, Warabi E, Yanagawa T, Kimura S, Harada H, Yamagata K, et al. Peroxiredoxin I plays a protective role against cisplatin cytotoxicity through mitogen activated kinase signals. Oral oncology. 2009;45(12):1037-43.

77. Guillonneau M, Paris F, Dutoit S, Estephan H, Bénéteau E, Huot J, et al. Oxidative stress disassembles the p38/NPM/PP2A complex, which leads to modulation of nucleophosmin-mediated signaling to DNA damage response. The FASEB Journal. 2016;30(8):2899-914.

78. Wang Q, Xu C, Fan Q, Yuan H, Zhang X, Chen B, et al. Positive feedback between ROS and cis-axis of PIASxα/p38α-SUMOylation/MK2 facilitates gastric cancer metastasis. Cell Death & Disease. 2021;12(11):986.

79. Goldar S, Khaniani MS, Derakhshan SM, Baradaran B. Molecular mechanisms of apoptosis and roles in cancer development and treatment. Asian Pacific journal of cancer prevention. 2015;16(6):2129-44.

80. Ant A. Oxidative stress and oral cavity cancer. Cancer: Elsevier; 2021. p. 55-65.

81. Pedro NF, Biselli JM, Maniglia JV, de Santi-Neto D, Pavarino ÉC, Goloni-Bertollo EM, et al. Candidate biomarkers for oral squamous cell carcinoma: differential expression of oxidative stress-related genes. Asian Pacific journal of cancer prevention: APJCP. 2018;19(5):1343.

82. Sardaro N, Della Vella F, Incalza MA, Di Stasio D, Lucchese A, Contaldo M, et al. Oxidative stress and oral mucosal diseases: An overview. in vivo. 2019;33(2):289-96.

83. Le M. Relationship between Oxidative Stress and Several Common Oral Mucosal Diseases: A Review. International Journal of Frontiers in Medicine. 2023;5(2).

84. Saso L, Reza A, Ng E, Nguyen K, Lin S, Zhang P, et al. A comprehensive analysis of the role of oxidative stress in the pathogenesis and chemoprevention of oral submucous fibrosis. Antioxidants. 2022;11(5):868.

85. Nguyen H, Sangha S, Pan M, Shin DH, Park H, Mohammed AI, et al. Oxidative stress and chemoradiation-induced oral mucositis: a scoping review of in vitro, in vivo and clinical studies. International Journal of Molecular Sciences. 2022;23(9):4863.

86. Kale J, Osterlund EJ, Andrews DW. BCL-2 family proteins: changing partners in the dance towards death. Cell Death & Differentiation. 2018;25(1):65-80.

87. Orrù G, Muggironi F, Mameli A, Demontis C, Arcadu B, Scano A, et al. BAX gene overexpression in the tongue could warn of infection risk due to periodontal pathogens. The Open Dentistry Journal. 2018;12(1):1070-8.

88. Teni T, Pawar S, Sanghvi V, Saranath D. Expression of bcl-2 and bax in chewing tobacco-induced oral cancers and oral lesions from India. Pathology Oncology Research. 2002;8:109-14.

89. Azad N, Iyer A, Vallyathan V, Wang L, Castranova V, Stehlik C, et al. Role of oxidative/nitrosative stress-mediated Bcl-2 regulation in apoptosis and malignant transformation. Annals of the New York Academy of Sciences. 2010;1203(1):1-6.

90. Jordan R, Catzavelos G, Barrett A, Speight P. Differential expression of bcl-2 and bax in squamous cell carcinomas of the oral cavity. European Journal of Cancer Part B: Oral Oncology. 1996;32(6):394-400.

91. Chamorro-Petronacci CM, De Mendoza IL-I, Suarez-Peñaranda JM, Padin-Iruegas E, Blanco-Carrion A, Lorenzo-Pouso AI, et al. Immunohistochemical characterization of bcl-2 in oral potentially malignant disorders. Applied Immunohistochemistry & Molecular Morphology. 2021;29(9):706-12.

92. Oshikawa T, Okamoto M, Ahmed SU, Tano T, Sato M. The relationship between gene expression of Bcl-2 and Bax and the therapeutic effect in oral cancer patients. Gan to Kagaku ryoho Cancer & Chemotherapy. 2006;33(12):1723-5.

93. Xiao S, Chen F, Gao C. Antitumor activity of 4-O-Methylhonokiol in human oral cancer cells is mediated via ROS generation, disruption of mitochondrial potential, cell cycle arrest and modulation of Bcl-2/Bax proteins. J BUON. 2017;22(6):1577-81.

94. Nimse SB, Pal D. Free radicals, natural antioxidants, and their reaction mechanisms. RSC advances. 2015;5(35):27986-8006.

95. Wikner S, Söder Pö. Factors associated with salivary buffering capacity in young adults in Stockholm, Sweden. Eur J Oral Sci. 1994;102(1):50-3.

96. Madi M, Babu S, Kumari S, Shetty S, Achalli S, Madiyal A, et al. Status of serum and salivary levels of superoxide dismutase in type 2 diabetes mellitus with oral manifestations: a case control study. Ethiopian journal of health sciences. 2016;26(6):523-32.

97. Nogueira FN, Romero AC, da Silva Pedrosa M, Ibuki FK, Bergamaschi CT. Oxidative stress and the antioxidant system in salivary glands of rats with experimental chronic kidney disease. Archives of Oral Biology. 2020;113:104709.

98. Pandey KB, Rizvi SI. Markers of oxidative stress in erythrocytes and plasma during aging in humans. Oxidative medicine and cellular longevity. 2010;3(1):2-12.

99. Bouayed J, Bohn T. Nutrition, well-being and health: BoD–Books on Demand; 2012.

100. Tsao R. Chemistry and biochemistry of dietary polyphenols. Nutrients. 2010;2(12):1231-46.

101. Maoka T. Carotenoids as natural functional pigments. Journal of natural medicines. 2020;74(1):1-16.

102. Kaźmierczak-Barańska J, Boguszewska K, Adamus-Grabicka A, Karwowski BT. Two faces of vitamin C—antioxidative and pro-oxidative agent. Nutrients. 2020;12(5):1501.

103. Niki E. Lipid oxidation that is, and is not, inhibited by vitamin E: Consideration about physiological functions of vitamin E. Free Radical Biology and Medicine. 2021;176:1-15.

104. Liu C, Zhao L, Yu G. The dominant glutamic acid metabolic flux to produce γ-amino butyric acid over proline in Nicotiana tabacum leaves under water stress relates to its significant role in antioxidant activity. Journal of Integrative Plant Biology. 2011;53(8):608-18.

105. Salah A, Zhan M, Cao C, Han Y, Ling L, Liu Z, et al. γ-Aminobutyric acid promotes chloroplast ultrastructure, antioxidant capacity, and growth of waterlogged maize seedlings. Scientific reports. 2019;9(1):1-19.

106. Ren T, Zheng P, Zhang K, Liao J, Xiong F, Shen Q, et al. Effects of GABA on the polyphenol accumulation and antioxidant activities in tea plants (Camellia sinensis L.) under heat-stress conditions. Plant Physiology and Biochemistry. 2021;159:363-71.

107. Deng Y, Wang W, Yu P, Xi Z, Xu L, Li X, et al. Comparison of taurine, GABA, Glu, and Asp as scavengers of malondialdehyde in vitro and in vivo. Nanoscale research letters. 2013;8:1-9.

108. Meeploy M, Niwaspragrit C, editors. Biological activities and GABA content of Ma-Lod (Elaeagnus latifolia Linn.). IOP Conf Ser Mater Sci Eng 2019: IOP Publishing.

109. Nonkratok K, Kamtuo A, Techawongstein S, Nera S. Study on floral and fruit biology of Ma Lord (Elaeagnus latifolia L.). Kaen Kaset. 2007.

110. Bahukhandi A, Attri DC, Bhatt ID. Assessment of Antioxidant Properties of Elaeagnus latifolia L.: An Important Wild Edible Fruit Species of Western Himalaya. National Academy Science Letters. 2023;46(1):55-9.

111. Patel S. Plant genus Elaeagnus: underutilized lycopene and linoleic acid reserve with permaculture potential. Fruits. 2015;70(4):191-9.

112. Niwaspragrit C, Ratanachamnong P, Munyanont M, Deewatthanawong R, editors. Study on organic acid and anti-oxidant properties of Elaeagnus latifolia LActa Hortic 2020;(1298):551–6.

113. Gómez-Moreno G, Guardia J, Aguilar-Salvatierra A, Cabrera-Ayala M, de-Val JEM-S, Calvo-Guirado JL. Effectiveness of malic acid 1% in patients with xerostomia induced by antihypertensive drugs. Medicina oral, patologia oral y cirugia bucal. 2013;18(1):e49.

114. Bardellini E, Amadori F, Conti G, Veneri F, Majorana A. Effectiveness of a spray containing 1% malic acid in patients with xerostomia induced by graft-versus-host disease. Medicina Oral, Patologia Oral Y Cirugia Bucal. 2019;24(2):e190.

115. Rachmaniah O, Fazriyah LJ, Seftiyani NH, Rachimoellah M, editors. Tailoring properties of acidic types of Natural Deep Eutectics Solvents (NADES): Enhanced solubility of curcuminoids from curcuma zeodaria. MATEC Web of conferences; 2018: EDP Sciences.

116. Dutta I, Gogoi B, Sharma R, Sharma HK. In vitro evaluation of leaves and fruits of Elaeagnus latifolia L. for antioxidant and antimicrobial activities. Asian J Chem. 2018;30(11):2433-6.

117. Singh K, Singh M, Joshi S. Phenolic content and antioxidant activity of some underutilized wild edible fruits of the Sikkim Himalaya. SMU Med J. 2014;2(1).

118. Kedtien P, Joomwong A, editors. Study on total phenolic contents and antioxidant activities in wild olive (Elaeagnus latifolia) fruit. Acta Hortic 2018;(1213):429–32.

119. Dasila K, Singh M. Bioactive compounds and biological activities of Elaegnus latifolia L.: An underutilized fruit of North-East Himalaya, India. S Afr J Bot 2022;145:177-85.

120. Shailasree S, Sampathkumara K, Niranjana S, Prakash H. Bioactive potential of medicinal plants from western ghats region, India. J Herbs Spices Med Plants. 2014;20(3):221-34.

121. Farahbakhsh S, Arbabian S, Emami F, Moghadam BR, Ghoshooni H, Noroozzadeh A, et al. Inhibition of cyclooxygenase type 1 and 2 enzyme by aqueous extract of Elaeagnus angustifolia in mice. Basic Clin Neurosci. 2011;2(2):31-7.

122. Khodakarm-Tafti A, Mehrabani D, Homafar L, Farjanikish G. Healing effects of Elaeagnus angustifolia extract in experimentally induced ulcerative colitis in rats. J Pharmacol Toxicol. 2015;10(1):29-35.

123. Natanzi MM, Pasalar P, Kamalinejad M, Dehpour AR, Tavangar SM, Sharifi R, et al. Effect of aqueous extract of Elaeagnus angustifolia fruit on experimental cutaneous wound healing in rats. Acta Medica Iranica. 2012:589-96.

124. Sun Y, Yao H, Zhang X, Yuan X-X, Xu H-L. Protective effects of Elaeagnus angustifolia L. leaves against H2O2-induced oxidative damage in Rat Schwann Cells (RSC-96) through regulation of PI3K/Akt signaling pathway. Pharmacogn Mag 2021;17(74):315.

125. Okmen G, Turkcan O. A study on antimicrobial, antioxidant and antimutagenic activities of Elaeagnus angustifolia L. leaves. Afr J Tradit Complement Altern Med 2014;11(1):116-20.

126. Taheri JB, Anbari F, Maleki Z, Boostani S, Zarghi A, Pouralibaba F. Efficacy of Elaeagnus angustifolia topical gel in the treatment of symptomatic oral lichen planus. J Dent Res Dent Clin Dent Prospects 2010;4(1):29.

127. Hekmatian E, Shadmehr E, Asghari G. Effect of Elaeagnus angustifolia lozenge on gag reflex in dental patients. J Iran Dent Assoc 2012;24(2):43-7.

128. Gupta M, Gulati M, Kapoor B, Kumar B, Kumar R, Kumar R, et al. Anti-ulcerogenic effect of methanolic extract of Elaeagnus conferta Roxb. seeds in Wistar rats. J Ethnopharmacol. 2021;275:114115.

129. Kupina S, Fields C, Roman MC, Brunelle SL. Determination of total phenolic content using the Folin-C assay: single-laboratory validation, first action 2017.13. Journal of AOAC International. 2018;101(5):1466-72.

130. Shraim AM, Ahmed TA, Rahman MM, Hijji YM. Determination of total flavonoid content by aluminum chloride assay: A critical evaluation. LWT. 2021;150:111932.

131. Shui G, Leong LP. Separation and determination of organic acids and phenolic compounds in fruit juices and drinks by high-performance liquid chromatography. Journal of chromatography A. 2002;977(1):89-96.

132. Chedea VS, Pop RM. Total polyphenols content and antioxidant DPPH assays on biological samples. Polyphenols in plants: Elsevier; 2019. p. 169-83.

133. Bibi Sadeer N, Montesano D, Albrizio S, Zengin G, Mahomoodally MF. The versatility of antioxidant assays in food science and safety—Chemistry, applications, strengths, and limitations. Antioxidants. 2020;9(8):709.

134. Won G, Choi S-I, Park N, Kim J-E, Kang C-H, Kim G-H. In vitro antidiabetic, antioxidant activity, and probiotic activities of Lactiplantibacillus plantarum and Lacticaseibacillus paracasei strains. Current Microbiology. 2021;78(8):3181-91.

135. Adjimani JP, Asare P. Antioxidant and free radical scavenging activity of iron chelators. Toxicology reports. 2015;2:721-8.

136. Benzie IF, Choi S-W. Antioxidants in food: content, measurement, significance, action, cautions, caveats, and research needs. Advances in food and nutrition research. 2014;71:1-53.

137. Osorio E, Londoño J, Bastida J. Low-density lipoprotein (LDL)-antioxidant biflavonoids from Garcinia madruno. Molecules. 2013;18(5):6092-100.

138. Azmi S, Jamal P, Amid A. Xanthine oxidase inhibitory activity from potential Malaysian medicinal plant as remedies for gout. International Food Research Journal. 2012;19(1).

139. Özyürek M, Bektaşoğlu B, Güçlü K, Apak R. Measurement of xanthine oxidase inhibition activity of phenolics and flavonoids with a modified cupric reducing antioxidant capacity (CUPRAC) method. Analytica Chimica Acta. 2009;636(1):42-50.

140. Li X. Solvent effects and improvements in the deoxyribose degradation assay for hydroxyl radical-scavenging. Food chemistry. 2013;141(3):2083-8.

141. Brizzolari A, Campisi GM, Santaniello E, Razzaghi-Asl N, Saso L, Foti MC. Effect of organic co-solvents in the evaluation of the hydroxyl radical scavenging activity by the 2-deoxyribose degradation assay: the paradigmatic case of α-lipoic acid. Biophysical chemistry. 2017;220:1-6.

142. Parul R, Kundu SK, Saha P. In vitro nitric oxide scavenging activity of methanol extracts of three Bangladeshi medicinal plants. The pharma innovation. 2013;1(12, Part A):83.

143. Coneski PN, Schoenfisch MH. Nitric oxide release: part III. Measurement and reporting. Chemical Society Reviews. 2012;41(10):3753-8.

144. Sroka Z, Cisowski W. Hydrogen peroxide scavenging, antioxidant and anti-radical activity of some phenolic acids. Food and Chemical Toxicology. 2003;41(6):753-8.

145. Grosu E-F, Cârjă G, Froidevaux R. Development of horseradish peroxidase/layered double hydroxide hybrid catalysis for phenol degradation. Research on Chemical Intermediates. 2018;44:7731-52.

146. Uzarski JS, DiVito MD, Wertheim JA, Miller WM. Essential design considerations for the resazurin reduction assay to noninvasively quantify cell expansion within perfused extracellular matrix scaffolds. Biomaterials. 2017;129:163-75.

147. Chen X, Zhong Z, Xu Z, Chen L, Wang Y. 2′, 7′-Dichlorodihydrofluorescein as a fluorescent probe for reactive oxygen species measurement: forty years of application and controversy. Free radical research. 2010;44(6):587-604.

148. Atale N, Gupta S, Yadav U, Rani V. Cell-death assessment by fluorescent and nonfluorescent cytosolic and nuclear staining techniques. Journal of microscopy. 2014;255(1):7-19.

149. Chen Y, Zhang S, Qu L. The protective effect of Artemisia Capillaris Thunb. Extract against UVB-induced apoptosis and inflammation through inhibiting the cGAS/STING pathway. Journal of Photochemistry and Photobiology B: Biology. 2024;258:112989.

150. Aramouni K, Assaf R, Shaito A, Fardoun M, Al-Asmakh M, Sahebkar A, et al. Biochemical and cellular basis of oxidative stress: implications for disease onset. J Cell Physiol. 2023;238(9):1951-63.

151. Korczowska-Łącka I, Słowikowski B, Piekut T, Hurła M, Banaszek N, Szymanowicz O, et al. Disorders of endogenous and exogenous antioxidants in neurological diseases. Antioxidants. 2023;12(10):1811.

152. Ashraf MV, Khan S, Misri S, Gaira KS, Rawat S, Rawat B, et al. High-Altitude Medicinal Plants as Promising Source of Phytochemical Antioxidants to Combat Lifestyle-Associated Oxidative Stress-Induced Disorders. Pharmaceuticals. 2024;17(8):975.

153. Giovanoudis I, Athanasiadis V, Chatzimitakos TG, Kalompatsios D, Mantiniotou M, Bozinou E, et al. Antioxidant Capacity in Two Different Cultivars of Ripe and Unripe Peaches Utilizing the Cloud-Point Extraction Method. AgriEngineering. 2023.

154. Turkmen FU, Takci HAM, Sekeroglu N. Total Phenolic and Flavonoid Contents, Antioxidant and Antimicrobial Activities of Traditional Unripe Grape Products. Indian Journal of Pharmaceutical Education and Research. 2017;51.

155. Rye WH, Weon PM, Young CM, editors. Antioxidant Properties of Unripened Apple Extracts2005.

156. Srinivasan R, Aruna A, Manigandan K, Pugazhendhi A, Kim M, Shivakumar MS, et al. Phytochemical, antioxidant, antimicrobial and antiproliferative potential of Elaeagnus indica. Biocatalysis and Agricultural Biotechnology. 2019.

157. Al Bashera M, Mosaddik A, El-Saber Batiha G, Alqarni M, Islam MA, Zouganelis GD, et al. In Vivo and In Vitro Evaluation of Preventive Activity of Inflammation and Free Radical Scavenging Potential of Plant Extracts from Oldenlandia corymbosa L. Applied Sciences. 2021.

158. Ullah N, Haseeb A, Tuzen M. Application of Recently used Green Solvents in Sample Preparation Techniques: A Comprehensive Review of Existing Trends, Challenges, and Future Opportunities. Critical reviews in analytical chemistry. 2023:1-20.

159. Sharma S, Kataria A, Singh B. Effect of thermal processing on the bioactive compounds, antioxidative, antinutritional and functional characteristics of quinoa (Chenopodium quinoa). Lebenson Wiss Technol. 2022;160:113256.

160. Wan F, Feng C-X, Luo K, Cui W, Xia Z, Cheng A. Effect of steam explosion on phenolics and antioxidant activity in plants: A review. Trends Food Sci Technol. 2022;124:13-24.

161. Rahman MJ, Malunga LN, Eskin MNA, Eck PK, Thandapilly SJ, Thiyam-Hollander U. Valorization of Heat-Treated Brewers' Spent Grain Through the Identification of Bioactive Phenolics by UPLC-PDA and Evaluation of Their Antioxidant Activities. Front Nutr 2021;8:634519.

162. Cui W-S, Zhang Q, Zhao X-h. Impact of heat treatment on anti-oxidative and anti-colon cancer activities of the soluble extracts from black mulberry (Morus nigra L.) using water and ethanol–water solvents. RSC Adv. 2020;10:30415 - 27.

163. López-Téllez JM, del Pilar Cañizares-Macías M. Evaluation of Tomato (Lycopersicon esculentum P. Mill.) By-product Extracts Obtained by Different Extraction Methods as Exploitation Strategy of High-Value Polyphenols. Food Bioproc Tech 2024;17(10):3217-35.

164. Liu R, Yang Y, Zhao M, Wang Y, Meng X, Yan T, et al. Effect of heat-treating methods on components, instrumental evaluation of color and taste, and antioxidant properties of sea buckthorn pulp flavonoids. J Food Sci. 2022;87(12):5442 - 54.

165. Coelho MC, Ribeiro TB, Oliveira CM, Batista P, Castro PM, Monforte AR, et al. In Vitro Gastrointestinal Digestion Impact on the Bioaccessibility and Antioxidant Capacity of Bioactive Compounds from Tomato Flours Obtained after Conventional and Ohmic Heating Extraction. Foods. 2021;10(3):554.

166. Chaaban H, Ioannou I, Chebil L, Slimane M, Gérardin C, Paris C, et al. Effect of heat processing on thermal stability and antioxidant activity of six flavonoids. J Food Process Preserv. 2017;41(5):e13203.

167. Rumpf J, Burger R, Schulze M. Statistical evaluation of DPPH, ABTS, FRAP, and Folin-Ciocalteu assays to assess the antioxidant capacity of lignins. International journal of biological macromolecules. 2023:123470.

168. Ahmouda K, Benhaoua B, Laouini SE, Labbi A. Plant extract FRAP effect on cation vacancies formation in greenly synthesized wüstite (FeO) nanoparticles: A new contribution. Sustainable Chemistry and Pharmacy. 2022.

169. Jansová H, Šimůnek T. Cardioprotective Potential of Iron Chelators and Prochelators. Current medicinal chemistry. 2019;26 2:288-301.

170. Sasikumar JM, Joghee DP, Adithya ES, Christabel PH, Shamna R. Antioxidant capacity and phenolic content of Elaeagnus kologa schlecht. an underexploited fruit from India. Free Radicals and Antioxidants. 2012;2:28-35.

171. Zhang J, Xu X, Liu X, Chen M, Bai B, Yang Y, et al. The Separation, Purification, Structure Identification, and Antioxidant Activity of Elaeagnus umbellata Polysaccharides. Molecules. 2023;28.

172. Banerjee S, Kar P, Sarkar I, Chhetri A, Mishra DK, Dutta A, et al. Structural elucidation and chemical characterization of underutilized fruit silverberry (Elaeagnus pyriformis) silver

nanoparticles playing a dual role as anti-cancer agent by promoting apoptosis and inhibiting ABC transporters. South African Journal of Botany. 2021.

173. Munkong N, Ruxsanawet K, Ariyabukalakorn V, Mueangchang W, Sangkham S, Silangirn P, et al. Hepatoprotective effects of Elaeagnus latifolia fruit extract against acetaminophen-induced hepatotoxicity in mice: Mechanistic insights. Journal of Functional Foods. 2024.

174. Goyal AK, Mishra T, Bhattacharya M, Kar P, Sen A. Evaluation of phytochemical constituents and antioxidant activity of selected actinorhizal fruits growing in the forests of Northeast India. Journal of Biosciences. 2013;38:797 - 803.

175. Yıldırım I, Gökçe Z, editors. The Determination of Antioxidant Vitamin Levels, Radical Scavenging Effect of Elaeagnus Angustifolia Methanol Extracts Against to MDA2014.

176. Ishaq S, Rathore HA, Sabir SM, Marouf MS. Antioxidant properties of Elaeagnus umbellata berry solvent extracts against lipid peroxidation in mice brain and liver tissues. Food Science and Biotechnology. 2015;24:673-9.

177. Nazir N, Zahoor M, Nisar M, Khan I, Ullah R, Alotaibi AA. Antioxidants Isolated from Elaeagnus umbellata (Thunb.) Protect against Bacterial Infections and Diabetes in Streptozotocin-Induced Diabetic Rat Model. Molecules. 2021;26.

178. Koriem KMM, Tharwat HAK. Malic Acid Improves Behavioral, Biochemical, and Molecular Disturbances in the Hypothalamus of Stressed Rats. Journal of integrative neuroscience. 2023;22 4:98.

179. Ashraf H, Qamar A, Maheshwari N. Attenuation of hexaconazole induced oxidative stress by folic acid, malic acid and ferrocenecarboxaldehyde in an invertebrate model Bombyxmori. Heliyon. 2022;8.

180. Niklander SE, Fuentes F, Sánchez DC, Araya V, Chiappini G, Martinez R, et al. Impact of 1% malic acid spray on the oral health-related quality of life of patients with xerostomia. Journal of oral science. 2018;60 2:278-84.

181. Battino M, Ferreiro M, Gallardo I, Newman H, Bullon P. The antioxidant capacity of saliva. Journal of Clinical Periodontology: Review article. 2002;29(3):189-94.

182. Choe H, Lee H, Lee J, Kim Y. Protective effect of gamma-aminobutyric acid against oxidative stress by inducing phase II enzymes in C2C12 myoblast cells. Journal of food biochemistry. 2021:e13639.

183. Liang JJ, Guo F, Cao S, Zhao K, Zhao K, Wang H, et al. γ-aminobutyric acid (GABA) alleviated oxidative damage and programmed cell death in fresh-cut pumpkins. Plant physiology and biochemistry : PPB. 2022;180:9-16.

184. Teng J, Yu T, Yan F. GABA attenuates neurotoxicity of zinc oxide nanoparticles due to oxidative stress via DAF-16/FoxO and SKN-1/Nrf2 pathways. The Science of the total environment. 2024:173214.

185. Chen X, Li H, Zhang B, Deng Zy. The synergistic and antagonistic antioxidant interactions of dietary phytochemical combinations. Critical Reviews in Food Science and Nutrition. 2021;62:5658 - 77.

186. Kang KA, Zhang R, Chae S, Lee SJ, Kim J, Kim J, et al. Phloroglucinol (1,3,5-trihydroxybenzene) protects against ionizing radiation-induced cell damage through inhibition of oxidative stress in vitro and in vivo. Chemico-biological interactions. 2010;185 3:215-26.

187. Kuo MT, Chen HH-W, Feun LG, Savaraj N. Targeting the Proline–Glutamine–Asparagine–Arginine Metabolic Axis in Amino Acid Starvation Cancer Therapy. Pharmaceuticals. 2021;14.

188. Wu G. Dietary requirements of synthesizable amino acids by animals: a paradigm shift in protein nutrition. Journal of Animal Science and Biotechnology. 2014;5:34 -

189. Liu Y, Yi L, Ruan C, Yao S, Deng L, Zeng K. Proline Increases Pigment Production to Improve Oxidative Stress Tolerance and Biocontrol Ability of Metschnikowia citriensis. Frontiers in Microbiology. 2019;10.

190. Yoon K-Y, Hong J-y, Shin S-R, editors. Analysis on the Components of the Elaeagnus multiflora Thunb. Leaves2007.

191. Abizov EA, Tolkachev ON, Mal'tsev SD, Abizova EV. Composition of biologically active substances isolated from the fruits of Russian olive (Elaeagnus angustifolia) introduced in the European part of Russia. Pharmaceutical Chemistry Journal. 2008;42:696-8.

192. Gamba G, Donno D, Mellano MG, Riondato I, De Biaggi M, Randriamampionona D, et al. Phytochemical Characterization and Bioactivity Evaluation of Autumn Olive (Elaeagnus umbellata Thunb.) Pseudodrupes as Potential Sources of Health-Promoting Compounds. Applied Sciences. 2020.

193. Cheng T-Y, Lin Y-J, Saburi W, Vieths S, Scheurer S, Schülke S, et al. β-(1⟶4)-Mannobiose Acts as an Immunostimulatory Molecule in Murine Dendritic Cells by Binding the TLR4/MD-2 Complex. Cells. 2021;10.

194. Nan F, Sun Y, Liang H, Zhou J, Ma X, Zhang D. Mannose: A Sweet Option in the Treatment of Cancer and Inflammation. Frontiers in Pharmacology. 2022;13.

195. Chen Q, Chen J, Du H, Li Q, Chen J, Zhang G, et al. Structural Characterization and Antioxidant Activities of Polysaccharides Extracted from the Pulp of Elaeagnus angustifolia L. International Journal of Molecular Sciences. 2014;15:11446 - 55.

196. Theparambil SM, Kopach O, Braga A, Nizari S, Hosford PS, Sági-Kiss V, et al. Adenosine signalling to astrocytes coordinates brain metabolism and function. Nature. 2024;632:139 - 46.

197. Zhang J-X, Feng W, Liu G-C, Ma Q-Q, Li H-L, Gao X-Y, et al. Corosolic Acid Attenuates Hepatic Lipid Accumulation and Inflammatory Response via AMPK/SREBPs and NF-**K**B/MAPK Signaling Pathways. The American journal of Chinese medicine. 2020:1-17.

198. Bergandi L, Apprato G, Silvagno F. Antioxidant and Anti-Inflammatory Activity of Combined Phycocyanin and Palmitoylethanolamide in Human Lung and Prostate Epithelial Cells. Antioxidants. 2022;11.

199. Lin GC, Smajlhodzic M, Bandian A-M, Friedl H-P, Leitgeb T, Oerter S, et al. An In Vitro Barrier Model of the Human Submandibular Salivary Gland Epithelium Based on a Single Cell Clone of Cell Line HTB-41: Establishment and Application for Biomarker Transport Studies. Biomedicines. 2020;8.

200. de Bari L, Scirè A, Minnelli C, Cianfruglia L, Kalapos MP, Armeni T. Interplay among Oxidative Stress, Methylglyoxal Pathway and S-Glutathionylation. Antioxidants. 2020;10.

201. Goffart S, Tikkanen P, Michell CT, Wilson T, Pohjoismäki JLO. The Type and Source of Reactive Oxygen Species Influences the Outcome of Oxidative Stress in Cultured Cells. Cells. 2021;10(5):1075.

202. Chen Y, Guo X, Zeng Y, Mo X, Hong S, He H, et al. Oxidative stress induces mitochondrial iron overload and ferroptotic cell death. Sci Rep. 2023;13(1):15515.

203. Wang J, Tan Q, Chen J, Liu X, Di Z, Xiao Q, et al. Alkyl Hydroperoxide Reductase as a Determinant of Parasite Antiperoxide Response in Toxoplasma gondii. Oxid Med Cell Longev. 2021;2021(1):1675652.

204. Mu M, Walker KL, Sánchez‐Sanz G, Waymouth RM, Trujillo C, Muldoon MJ, et al. Insights into the Palladium(II)-Catalyzed Wacker-Type Oxidation of Styrene with Hydrogen Peroxide and tert-Butyl Hydroperoxide. ACS Catalysis. 2024;14:1567 - 74.

205. Wufuer R, Fan Z, Liu K, Zhang Y. Differential Yet Integral Contributions of Nrf1 and Nrf2 in the Human HepG2 Cells on Antioxidant Cytoprotective Response against Tert-Butylhydroquinone as a Pro-Oxidative Stressor. Antioxidants. 2021;10(10):1610.

206. Lee YH, Kuk MU, So MK, Song ES, Lee H-H, Ahn SK, et al. Targeting Mitochondrial Oxidative Stress as a Strategy to Treat Aging and Age-Related Diseases. Antioxidants. 2023;12(4).

207. Abbasi A, Pakravan N, Hassan ZM. Hyaluronic acid optimises therapeutic effects of hydrogen peroxide‐induced oxidative stress on breast cancer. J Cell Physiol. 2020;236:1494 - 514.

208. He MT, Park CH, Shin YS, Kim JH, Cho EJ. Carthamus tinctorius L. Seed and Taraxacum coreanum Attenuate Oxidative Stress Induced by Hydrogen Peroxide in SH-SY5Y Cells. Foods. 2023;12(19).

209. Raghunandan S, Ramachandran S, Ke E, Miao Y, Lal R, Chen ZB, et al. Heme Oxygenase-1 at the Nexus of Endothelial Cell Fate Decision Under Oxidative Stress. Front Cell Dev Biol. 2021;9:702974.

210. Zhao W, Feng H, Sun W, Liu K, Lu J-j, Chen X. Tert-butyl hydroperoxide (t-BHP) induced apoptosis and necroptosis in endothelial cells: Roles of NOX4 and mitochondrion. Redox Biology. 2017;11:524 - 34.

211. Kučera O, Endlicher R, Roušar T, Lotková H, Garnol T, Drahota Z, et al. The Effect of tert-Butyl Hydroperoxide-Induced Oxidative Stress on Lean and Steatotic Rat Hepatocytes In Vitro. Oxidative Medicine and Cellular Longevity. 2014;2014.

212. Jiang J, Dong C, Zhai L, Lou J, Jin J, Cheng S, et al. Paeoniflorin suppresses TBHP-induced oxidative stress and apoptosis in human umbilical vein endothelial cells via the Nrf2/HO-1 signaling pathway and improves skin flap survival. Frontiers in Pharmacology. 2021;12:735530.

213. Sayadi MH, Fahoul N, Kharkan J, Khairieh M. Investigating the protective effects of Elaeagnus angustifolia fruit extract on hematological parameters and damage of different tissues of male mice exposed to graphene oxide nanoparticles. Nano Select. 2023.

214. Lu J, Wang Z, Cao J, Chen Y, Dong Y. A novel and compact review on the role of oxidative stress in female reproduction. Reproductive Biology and Endocrinology : RB&E. 2018;16.

215. Iannuzzi AM, Giacomelli C, De Leo M, Pietrobono D, Camangi F, de Tommasi N, et al. Antioxidant Activity of Compounds Isolated from Elaeagnus umbellata Promotes Human Gingival Fibroblast Well-Being. Journal of Natural Products. 2020;83:626 - 37.

216. Wang C-Y, Lin C-S, Hua C-H, Jou Y-J, Liao C-R, Chang Y-S, et al. Cis-3-O-p-hydroxycinnamoyl Ursolic Acid Induced ROS-Dependent p53-Mediated Mitochondrial Apoptosis in Oral Cancer Cells. Biomolecules & Therapeutics. 2018;27:54 - 62.

217. Elmore SA. Apoptosis: A Review of Programmed Cell Death. Toxicologic Pathology. 2007;35:495 - 516.

218. Ebadollahi S, Pouramir M, Zabihi E, Golpour M, Aghajanpour-Mir M. The Effect of Arbutin on The Expression of Tumor Suppressor P53, BAX/BCL-2 Ratio and Oxidative Stress Induced by Tert-Butyl Hydroperoxide in Fibroblast and LNcap Cell Lines. Cell Journal (Yakhteh). 2020;22:532 - 41.

219. Kim HJ, Lee EK, Park MH, Ha YM, Jung KJ, Kim M-S, et al. Ferulate Protects the Epithelial Barrier by Maintaining Tight Junction Protein Expression and Preventing Apoptosis in Tert-Butyl Hydroperoxide-Induced Caco-2 Cells. Phytotherapy Research. 2013;27.

220. Kanupriya, Prasad DN, Sai Ram M, Sawhney RC, Ilavazhagan G, Banerjee PK. Mechanism of tert-butylhydroperoxide induced cytotoxicity in U-937 macrophages by alteration of mitochondrial function and generation of ROS. Toxicology in vitro : an international journal published in association with BIBRA. 2007;21 5:846-54.

221. Leitl KD, Sperl LE, Hagn F. Preferred inhibition of pro-apoptotic Bak by BclxL via a two-step mechanism. Cell reports. 2024;43 8:114526.

222. Lei K, Davis RJ. JNK phosphorylation of Bim-related members of the Bcl2 family induces Bax-dependent apoptosis. Proceedings of the National Academy of Sciences of the United States of America. 2003;100:2432 - 7.

223. Taha SHN, Zaghloul HS, Ali AA, Rashed LA, Sabry RM, Gaballah IF. Molecular and hormonal changes caused by long-term use of high dose pregabalin on testicular tissue: the role of p38 MAPK, oxidative stress and apoptosis. Molecular Biology Reports. 2020;47:8523 - 33.

224. Cánovas B, Nebreda AR. Diversity and versatility of p38 kinase signalling in health and disease. Nature Reviews Molecular Cell Biology. 2021;22:346 - 66.

225. Ganguly P, Macleod T, Wong C, Harland M, Mcgonagle D. Revisiting p38 Mitogen-Activated Protein Kinases (MAPK) in Inflammatory Arthritis: A Narrative of the Emergence of MAPK-Activated Protein Kinase Inhibitors (MK2i). Pharmaceuticals. 2023;16.

226. Alvarado-Kristensson M, Melander F, Leandersson K, Rönnstrand L, Wernstedt C, Andersson T. p38-MAPK Signals Survival by Phosphorylation of Caspase-8 and Caspase-3 in Human Neutrophils. The Journal of Experimental Medicine. 2004;199:449 - 58.

227. Kim J-S, Oh D, Yim M-J, Park J-J, Kang K-R, Cho I-A, et al. Berberine induces FasL-related apoptosis through p38 activation in KB human oral cancer cells. Oncology Reports. 2015;33:1775 - 82.

228. Fu J, Shi H, Cao N, Wu S, Zhan T, Xie L, et al. Toll-like receptor 9 signaling promotes autophagy and apoptosis via divergent functions of the p38/JNK pathway in human salivary gland cells. Experimental Cell Research. 2019;375:51–9.

229. Tao SC, Yuan T, Rui B-y, Zhu Z, Guo S-C, Zhang C-Q. Exosomes derived from human platelet-rich plasma prevent apoptosis induced by glucocorticoid-associated endoplasmic reticulum stress in rat osteonecrosis of the femoral head via the Akt/Bad/Bcl-2 signal pathway. Theranostics. 2017;7:733 - 50.

230. Zhu C, Fan F, Li C-Y, Xiong Y, Liu X. Caspase-3 promotes oncogene-induced malignant transformation via EndoG-dependent Src-STAT3 phosphorylation. Cell Death & Disease. 2024;15.

231. Lim H-S, Sohn E-W, Kim YJ, Kim B-Y, Kim JH, Jeong S-J. Ethanol Extract of Elaeagnus glabra f. oxyphylla Branches Alleviates the Inflammatory Response Through Suppression of Cyclin D3/Cyclin-Dependent Kinase 11p58 Coupled to Lipopolysaccharide-Activated BV-2 Microglia. Natural Product Communications. 2022;17.

232. Jabeen A, Sharma A, Gupta I, Kheraldine H, Vranić S, Al Moustafa A-E, et al. Elaeagnus angustifolia Plant Extract Inhibits Epithelial-Mesenchymal Transition and Induces Apoptosis via HER2 Inactivation and JNK Pathway in HER2-Positive Breast Cancer Cells. Molecules. 2020;25.

233. King LS, Kozono DE, Agre P. From structure to disease: the evolving tale of aquaporin biology. Nature Reviews Molecular Cell Biology. 2004;5:687-98.

234. Chivasso C, D'Agostino C, Parisis D, Soyfoo MS, Delporte C. Involvement of aquaporin 5 in Sjögren's syndrome. Autoimmunity reviews. 2023:103268.

235. D'Agostino C, Parisis D, Chivasso C, Hajiabbas M, Soyfoo MS, Delporte C. Aquaporin-5 Dynamic Regulation. International Journal of Molecular Sciences. 2023;24.

236. Jung HJ, Park J-Y, Jeon HS, Kwon T-H. Aquaporin-5: A Marker Protein for Proliferation and Migration of Human Breast Cancer Cells. PLoS ONE. 2011;6.

237. Wei W, Cao T-t, Pathak JL, Liu X, Mao T, Watanabe N, et al. Apigenin, a Single Active Component of Herbal Extract, Alleviates Xerostomia via ERα-Mediated Upregulation of AQP5 Activation. Frontiers in Pharmacology. 2022;13.

238. Perry GH, Dominy NJ, Claw KG, Lee AS, Fiegler H, Redon R, et al. Diet and the evolution of human amylase gene copy number variation. Nature Genetics. 2007;39:1256-60.

239. Villa A, Connell CL, Abati S. Diagnosis and management of xerostomia and hyposalivation. Therapeutics and Clinical Risk Management. 2014;11:45 - 51.

240. Mantke R, Rocken C, Schubert D, Pross M, Sokolowski A, Halangk W, et al. Enzymatic and histological alterations in the isolated perfused rat pancreas under conditions of oxidative stress. Langenbeck's Archives of Surgery. 2002;387:170-6.

241. Ławiński M, Śledziński Z, Kubasik-Juraniec J, Spodnik JH, Wozniak M, Bogusławski W. Does Resveratrol Prevent Free Radical-induced Acute Pancreatitis? Pancreas. 2005;31:43-7.

242. Jomová K, Raptová R, Alomar SY, Alwasel SH, Nepovimova E, Kuča K, et al. Reactive oxygen species, toxicity, oxidative stress, and antioxidants: chronic diseases and aging. Archives of Toxicology. 2023;97:2499 - 574.

243. Carmen Martínez-Ballesta M, Bou G, Carvajal M. Aquaporins as targets of pharmacological plant-derived compounds. Phytochemistry Reviews. 2014;13:573-86.

244. Thelin W, Brennan MT, Lockhart PB, Singh ML, Fox PC, Papas A, et al. The oral mucosa as a therapeutic target for xerostomia. Oral diseases. 2008;14 8:683-9.

245. Szodoray P, Jellestad S, Alex P, Zhou T, Wilson PC, Centola M, et al. Programmed Cell Death of Peripheral Blood B Cells Determined by Laser Scanning Cytometry in Sjögren's Syndrome with a Special Emphasis on BAFF. Journal of Clinical Immunology. 2004;24:600-11.

246. Huang Y, Shi X, Mao Q, Zhang Y, Cong X, Zhang X, et al. Aquaporin 5 is degraded by autophagy in diabetic submandibular gland. Science China Life Sciences. 2018;61:1049 - 59.

247. López-Valverde N, López-Valverde A, Montero J, Rodríguez C, Macedo de Sousa B, Aragoneses JM. Antioxidant, anti-inflammatory and antimicrobial activity of natural products in periodontal disease: a comprehensive review. Frontiers in Bioengineering and Biotechnology. 2023;11.

APPENDIX

1. Plant harvest and extraction

2. Reagents for in vitro studies

2.1 Preparation of Standard Solutions

2.1.1 Gallic acid (2 mg/mL)

- Gallic acid 20 mg

Add methanol to 10 mL

Quercetin (2mg/mL)

- Quercetin 20 mg

Add methanol to 10 mL

Malic acid (1mg/mL)

- Malic acid 10 mg

Add dH_2O to 10 mL

GABA (0.1mg/mL)

- GABA 100 mg

Add dH_2O to 10 mL

Ascorbic acid (1 mg/mL)

- Ascorbic acid 10 mg

Add dH_2O to 10 mL

Trolox (2 mg/mL)

- Trolox 20 mg

Add dH_2O to 10 mL

EDTA (1mg/mL)

- EDTA 10 mg

Add dH_2O to 10 mL

2.2 Preparation of Auxiliary solution

2.2.1 TPC assay

- Saturated Na_2CO_3 solution

- Na_2CO_3 25 g

Add ddH_2O to100 let stand for 24 hours, filter through Whatman No. 1, and adjust with ddH_2O to125 mL.

2.2.2 TFC assay

- Potassium acetate 1 M

- CH_3COOK 9.814 g

Add ddH_2O to 100 mL

- Aluminum chloride (10%)

- $AlCl_3$ 10 g

Add ddH_2O to 100 mL

2.2.3 Determination of malic acid content

- Potassium dihydrogen phosphate 25mM

- KH_2PO_4 3.61 g

Add dH_2O to 1000 mL (adjusted with NaOH to pH=10.0)

2.2.4 Determination of GABA content

- Borate buffer 0.4M

- Boric Acid (H_3BO_3) 24.73 g

Add dH_2O to 1000 mL (adjusted with NaOH to pH=10.0)

- Citrate buffer 5mM

- Sodium Citrate ($C_6H_5Na_3O_7 \cdot 2H_2O$) 3.83 g

Add dH_2O to 1000 mL (adjusted with citric acid to pH=8.5)

2.2.5 DPPH assay

- DPPH solution
  - DPPH 1 g

Add methanol to 50 mL adjusted absorbance to 1.0-1.2

2.2.6 ABTS assay

- 7mM ABTS solution
  - ABTS 0.234 g
  - Potassium persulfate ($K_2S_2O_8$) 2.45mM 0.061 g

Using 1:0.5 ratio of ABTS to potassium persulfate, adjusted with 50 mL methanol, and adjusted absorbance to 0.8±0.02

2.2.7 FIC assay

- Ferrous Sulfate 2 mM
  - $FeSO_4 \cdot 7H_2O$ 0.0554 g

Add dH_2O to 100 mL

- Ferrozine 5 mM
  - Ferrozine 0.0197 g

Add dH_2O to 100 mL

2.2.8 FRAP assay

- Acetate buffer 300 mM
  - Sodium acetate 2.46 g

Add dH_2O 100mL (adjusted with acetic acid to pH=3.6)

- TPTZ 10 mM

- TPTZ 24.1 mg

Add dH_2O 10mL

- $FeCl_3 \cdot 6H_2O$ 10 mM
- $FeCl_3 \cdot 6H_2O$ 27.0 mg

Add dH_2O 10mL

To prepare working solution, mix 100 mL of 300 mM acetate buffer, 10 mL of 10 mM TPTZ, and 10 mL of 10 mM $FeCl_3 \cdot 6H_2O$

2.2.9 lipid peroxidation inhibition assay

- LDL 300 µg/mL
- LDL stock solution 300 µg

Add 1 mL of nuclease free water

- Copper sulfate ($CuSO_4$) 55 µM
- $CuSO_4$ 11.9 mg

Add dH_2O 200mL

- EDTA 1%
- EDTA 0.1 g

Add dH_2O to 10 mL

- TCA-TBA Stock Solution (20% w/v)
- Trichloroacetic Acid (TCA) 2 g
- Thiobarbituric Acid (TBA) 2 g

Add dH_2O to 10 mL

Superoxide radical scavenging activity assay

- Sodium Phosphate Buffer 50 mM,
- Sodium phosphate dibasic ($Na_2HPO_4 \cdot 7H_2O$) 1.42 g
- Sodium phosphate monobasic ($NaH_2PO_4 \cdot H_2O$) 0.83 g

Add ddH_2O to 100 mL (adjust with HCl or NaOH to pH=7.5)

- Xanthine Oxidase (XO) solution
- XO 0.2 units/mL
- Sodium phosphate dibasic ($Na_2HPO_4 \cdot 7H_2O$) 1.42 g
- Sodium phosphate monobasic ($NaH_2PO_4 \cdot H_2O$) 0.83 g

Add ddH_2O to 100 mL (adjust with HCl or NaOH to pH=7.0)

- Xanthine 0.15mM
- Xanthine 0.234 g

Add ddH_2O to 100 mL

- HCl 0.5M
- Glacial HCl 1.53 mL

Add ddH_2O to 100 mL

2.2.11 Hydroxyl radical scavenging activity assay

- 2-deoxyribose 10mM
- 2-deoxyribose 2 mg

Add ddH_2O to 1 mL

- Ferric Chloride ($FeCl_3$)10mM
- $FeCl_3 \cdot 6H_2O$ 0.0165 g

Add ddH_2O to 10 mL

- Hydrogen peroxide (H_2O_2) 10mM

- H_2O_2 30% solution 1.16mL

Add ddH_2O to 100 mL

- EDTA 1mM
- EDTA 19 mg

Add ddH_2O to 10 mL

- Ascorbic acid 1mM
- Ascorbic acid 17.6 mg

Add ddH_2O to 10 mL

- TCA 2.8% w/v
- TCA 2.8 mg

Add ddH_2O to 100 mL

- TBA 1% w/v
- TBA 0.5 g

Add 50 mM NaOH 50 mL

2.2.12 Nitric oxide radical scavenging activity assay

- Sodium nitroprusside (SNP) 10 mM
- SNP 0.26 g

Add phosphate buffer 100 mL (adjust with HCl or NaOH to pH=7.4)

- Sulfanilamide 1%
- Sulfanilamide 1 g

Add 2% H_3PO_4 to 100 mL

- N-(1-naphthyl) ethylenediamine dihydrochloride (NED) 0.1%

- NED 0.1 g

Add ddH_2O to 100 mL

2.2.13 Hydrogen peroxide scavenging activity assay

- Phenol red 0.2 mg/mL

- Phenol red 2 mg

Add ddH_2O to 10 mL

- Horseradish Peroxidase (HRP) 0.1 mg/mL

- HRP 1 mg

Add ddH_2O to 10 mL

3. Reagents for in vitro cell-based studies

3.1 Cell culture media

- DMEM 13.4 g

- Sodium bicarbonate 3.7 g

Add dH_2O to 1000mL

To prepare working solution;

- 10% FBS 50 mL

- 1% non-essential amino acid 5 mL

Add DMEM solution to 500mL

4. Hoechst staining assay

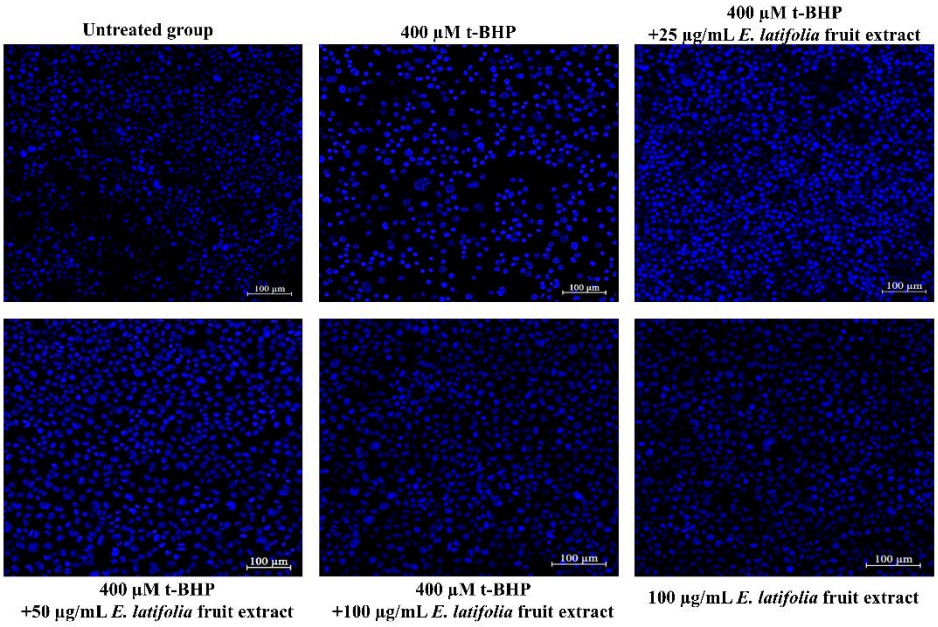

Figure 52 Nuclear alterations stained with Hoechst 33342 visualized using confocal laser scanning microscope (scale bar: 100 µm; Zeiss, Germany).

5. AO/EB staining assay

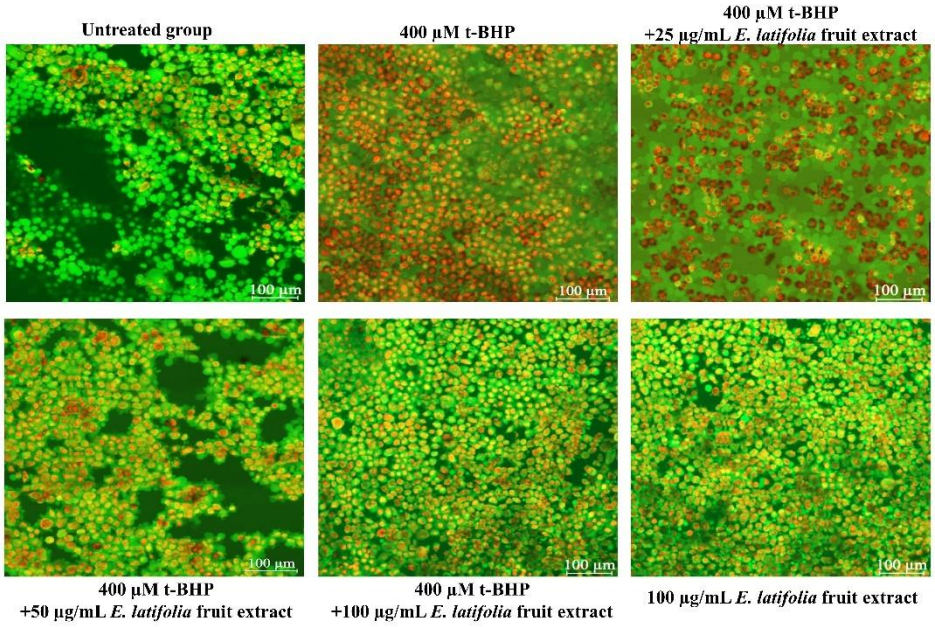

Figure 53 Apoptotic morphology detection by AO/EB staining of HSG cells visualized using confocal laser scanning microscope (scale bar: 100 µm; Zeiss, Germany).

6. Preparation and reagents for Western Blot analysis

6.1 Gel preparation

Lower gel preparation

- Monomer:

  Acrylamide 60g

  Bis-acrylamide 1.6g

Add dH_2O 200 mL

- 4x running gel buffer:

  1.5 M Tris-HCl 36.3 g

Add ddH_2O 200 mL (adjusted with HCl to pH=8.8) stored at 4°C

- 10% SDS:

  SDS 10g

Add ddH_2O 100 mL stored at room temperature

- 10% Ammonium persulfate (APS)

  APS 1g

Add dH_2O 1 mL stored at -20°C

- TEMED stored at 4°C
- Ponceau staining:

  Ponceau 100 mg

dissolved with 5% acetic acid (5mL in ddH_2O 95 mL)

Upper gel preparation

- 4x stacking gel buffer

  0.5M tris-HCl 12.11 g

Add ddH_2O 200mL (adjusted with HCl to pH=6.8) stored at 4°C

14% gel preparation

Lower gel:

- monomer 9.4 mL
- 4x running gel buffer 5 mL
- 10%SDS 200 µL
- ddH_2O 5.4mL
- 10%APS 130µL
- TEMED 10µL

Upper gel:

- Monomer 880 µL
- 4x stacking gel buffer 1.66mL
- 10%SDS 60 µL
- ddH_2O 4.06 mL
- 10%APS 50µL
- TEMED 6µL

15%gel preparation

Lower gel:

- Monomer 10 mL
- 4x running gel buffer 5 mL
- 10%SDS 200 µL
- ddH_2O 4.8mL
- 10%APS 130µL
- TEMED 10µL

Upper gel:

- monomer 880 µL
- 4x stacking gel buffer 1.66mL
- 10%SDS 60 µL

- ddH_2O 4.06 mL
- 10%APS 50µL
- TEMED 6µL

6.2 Buffer preparation

Running buffer or tank buffer (10x)

:

- 0.25M Tris-base 30.3g
- 1.924M Glycine 144.13g
- SDS 10g

Add ddH_2O 1000mL

running buffer (1x):

- 10x running buffer 100mL

Add ddH_2O 900mL

Transfer buffer (10x):

- 25mM tris-base 30.30g
- 192mM Glycine 144.2g

Add ddH_2O 1000mL

transfer buffer (1x):

- 10x transfer buffer 80 mL
- Methanol 200mL

Add ddH_2O 720mL

Wash buffer:

- 1M tris-HCl 157.6g

Add ddH_2O 1000mL (adjusted with NaOH to pH=7.4)

- 3M NaCl 175.32 g

Add ddH_2O 1000mL

TBST wash buffer preparation:

Add ddH_2O 2250mL mixed with 1Mtris-HCl 125mL and 3NaCl 125 mL

6.3 Other reagents

6x loading dye (1 tube):

- 0.5M tris HCl pH=6.8 700 µL
- 10%SDS 0.1g
- Glycerol 300 µL
- DTT 0.093g
- Bromophenol blue 0.0012g

2% BSA:

- BSA 10g
- TBST 500mL

Mild stripping

- Glycine 15g
- SDS 1g
- Tween-20 10mL

Add ddH_2O 1000mL (adjusted with HCl to pH=2.2)

7. Quantification of protein concentration for western blot analysis using a standard BSA calibration curve with the Bradford assay

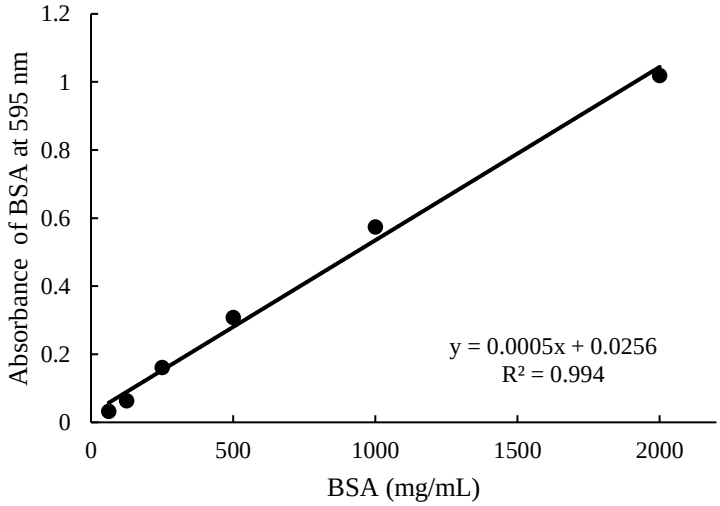

Figure 54 Calibration curve for protein quantification using BSA standard via Bradford Assay

8. Nitrophenol calibration curve for each time point at Tfinal

A

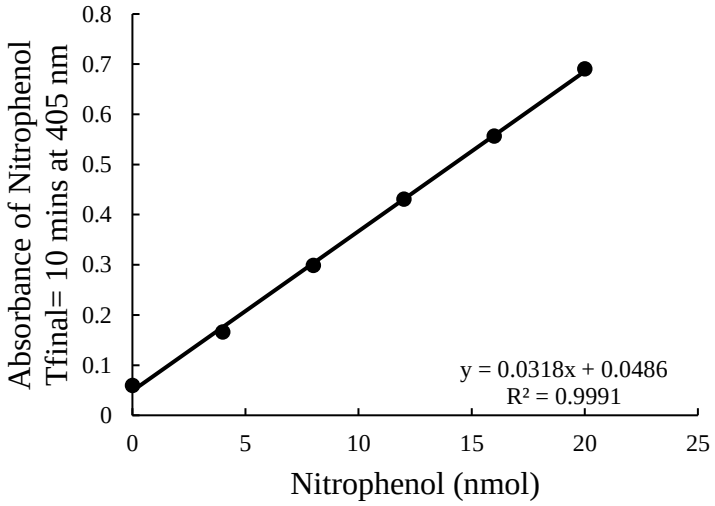

B

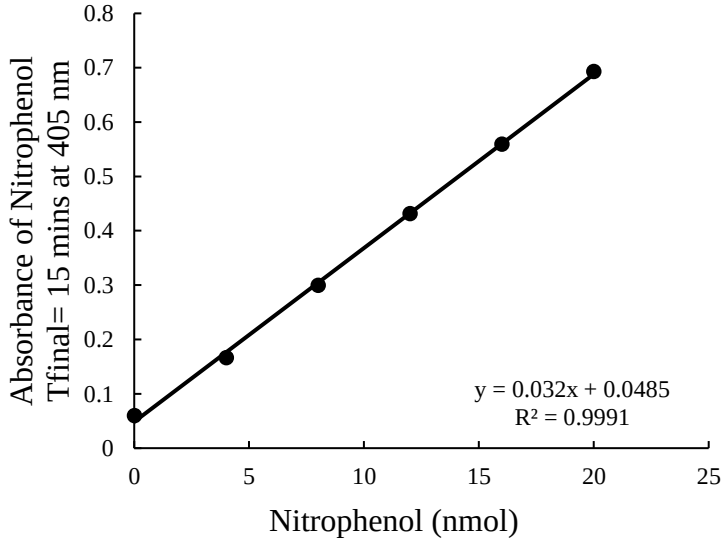

C

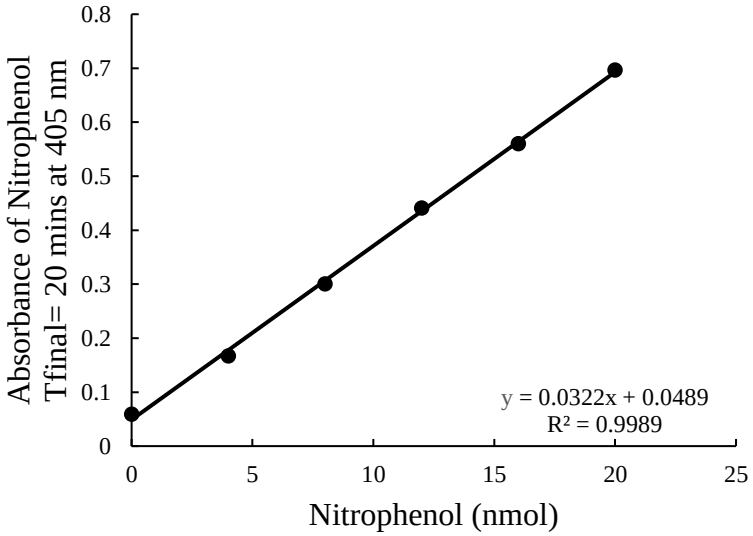
Absorbance of Nitrophenol
Tfinal= 20 mins at 405 nm
0.8
0.7
0.6
0.5
0.4
0.3
0.2
0.1
0
0
5
10
15
20
25
Nitrophenol (nmol)
y = 0.0322x + 0.0489
R² = 0.9989

D

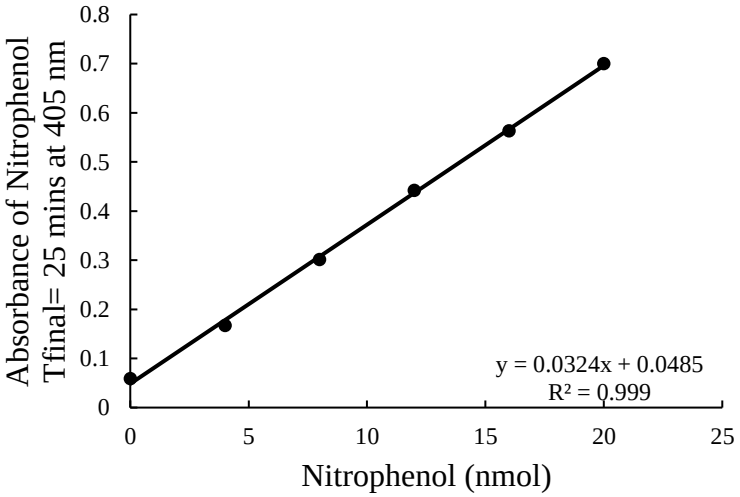
Absorbance of Nitrophenol
Tfinal= 25 mins at 405 nm
0.8
0.7
0.6
0.5
0.4
0.3
0.2
0.1
0
0
5
10
15
20
25
Nitrophenol (nmol)
y = 0.0324x + 0.0485
R² = 0.999

E

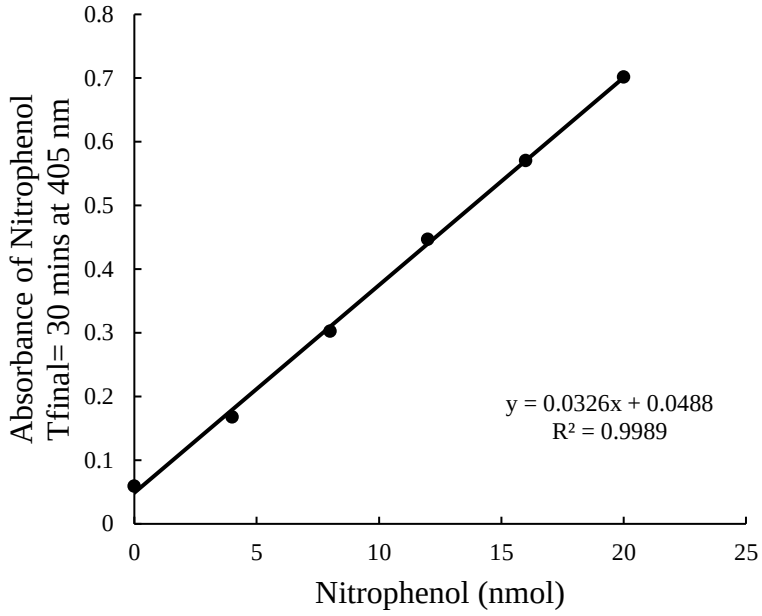
Absorbance of Nitrophenol
Tfinal= 30 mins at 405 nm
0.8
0.7
0.6
0.5
0.4
0.3
0.2
0.1
0
0
5
10
15
20
25
Nitrophenol (nmol)
y = 0.0326x + 0.0488
R² = 0.9989

F

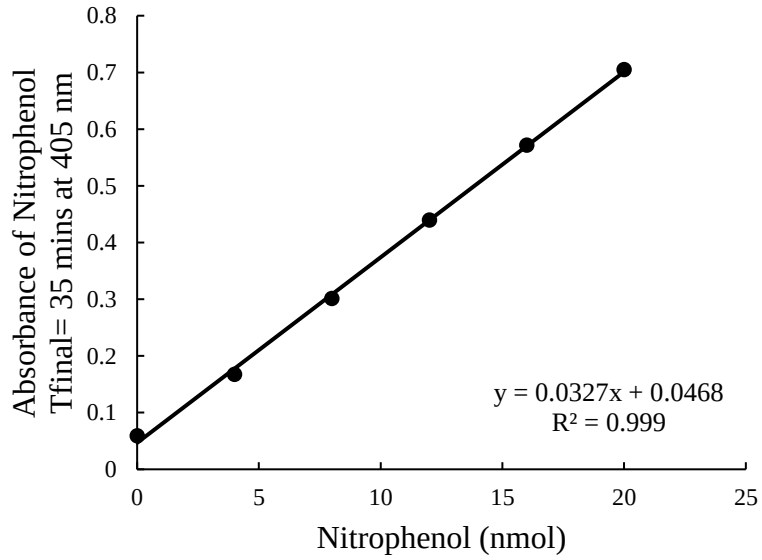
Absorbance of Nitrophenol
Tfinal= 35 mins at 405 nm
0.8
0.7
0.6
0.5
0.4
0.3
0.2
0.1
0
0
5
10
15
20
25
Nitrophenol (nmol)
y = 0.0327x + 0.0468
R² = 0.999

G

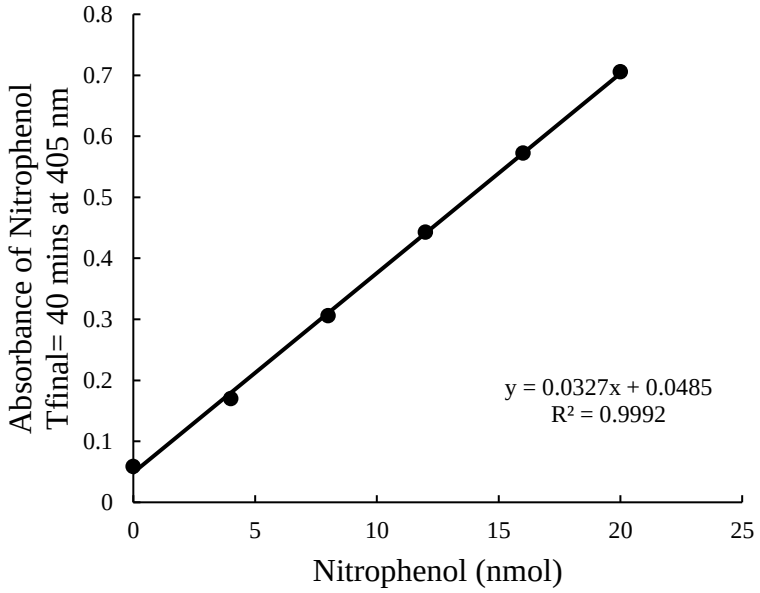

Figure 55 Comprehensive calibration curves of Nitrophenol for amylase activity measurement at various final time points (T_{final}).

VITA